Raman spectroscopy of minerals and mineral pigments in archaeometry

Journal of RAMAN SPECTROSCOPY

Raman spectroscopy of minerals and mineral pigments in archaeometry

Journal:	*Journal of Raman Spectroscopy*
Manuscript ID	JRS-15-0347.R1
Wiley - Manuscript type:	Review
Date Submitted by the Author:	n/a
Complete List of Authors:	Bersani, Danilo; University of Parma, Physics and Earth Sciences; Lottici, Pier Paolo; University, Physics;
Keywords:	Raman spectroscopy, minerals, archaeometry, pigments, ceramics

Raman spectroscopy of minerals and mineral pigments in archaeometry

D. Bersani and P.P. Lottici

Department of Physics and Earth Sciences, University of Parma, Parco Area delle Scienze 7/A, 43124 Parma, Italy.

Keywords: Raman spectroscopy, minerals, archaeometry, pigments, ceramics, gems

Abstract

Minerals, as raw structural materials or pigments, play a fundamental role in archaeometry, for the understanding of nature, structure and status of an artefact or object of interest for Cultural Heritage. . A detailed knowledge of the mineral phases is crucial to solve archaeological problems: Raman spectroscopy is a powerful investigation technique and has been applied extensively in the last 30 years on mineral identification and on pigment degradation. Here we report an updated review, covering the last decade, of the applications of Raman techniques to issues in which raw minerals, including mineral pigments, are involved. Particular attention is devoted to cases where the Raman analysis of minerals is deeper than a simple identification of the phases present in an archaeological or artistic object.

Introduction

The use of Raman spectroscopy for archaeometry applications has quickly grown in the last years, in both micro-Raman and mobile Raman versions of the technique, thanks to the main advantages as the small time required for the measurements, the possibility to study untreated raw material and, especially, the non-invasivity. This tendency is indicated by the increasing number of dedicated conferences, as the International Conference in Application of Raman Spectroscopy in Art and Archaeology (RAA), now arrived at the 8th edition: many examples of interesting applications are reported in the RAA conference special issues [1–3]. Some good review articles show the progression in the recent years of the state-of-the art of the use of Raman spectroscopy in different fields of archaeometry. We would like to cite only the most relevant for this work: Smith and Clark [4], Smith [5], Smith [6], Fotakis et al. [7], Vandenabeele et al. [8], Bersani and Lottici [9], Clark [10], Colomban [11], Capel Ferron et al. [12], Vandenabeele et al. [13], Madariaga [14].

The possibility to study many different kind of materials, from crystalline to amorphous, organic and inorganic, even when largely heterogeneous, thanks to its micrometric space resolution, made Raman spectroscopy an unique tool for the study of archaeological materials. The complexity of the archaeological findings and the extremely wide range of substances they contain, make a complete analysis very difficult, especially when only non-destructive techniques can be used. For this reason, in many cases the identification of the different organic and inorganic phases is limited to a “raw” identification. In the case of

mineral phases, often the identification is at the level of the group (e.g. “feldspar” or “garnet”) or series (e.g. “nephrite”), because of the difficulty to obtain more detailed identification which is not seen as a priority. In this paper we would like to show the importance to have a detailed knowledge of the mineral phases encountered in some archaeological problems, how that knowledge is helpful for archaeometry and how it can be obtained by Raman spectroscopy.

The development of Raman spectroscopy followed two main directions, both useful for applications in mineralogy and archaeometry: the increase in performance of the micro-Raman systems, especially in sensitivity, leading to fast Raman mapping machines, and the realization of affordable mobile spectrometers. Recently, Vandenabeele et al. [13] published a complete review about the mobile Raman instrumentation for applications in the field of archaeometry (and not only). From this overview, it appears that most mobile tools use as excitation the 785 nm line of a laser diode, considered one of the best compromises between efficiency and low fluorescence. Some of the instruments use instead the 532 nm line of a doubled Nd:YAG laser, allowing more efficiency and giving the possibility to explore the high wavenumber range of Raman spectrum (up to 4000 cm^{-1}, including the OH stretching region). Only few models of mobile Raman spectrometers are up to now exploiting the new InGaAs detectors allowing using the 1064 nm line of the Nd:YAG laser as excitation. This solution allows to have an IR excitation and virtually no fluorescence, but with a very low scattering efficiency, due to the high wavelength. Works based on mobile or micro-Raman instrumentation are considered in this paper.

This review, far from being a review of “Raman spectroscopy and pigments in Art and Archaeometry”, aims to provide a synopsis of recent Raman studies which escaped or which have appeared since the various last more general reviews carried out on the use of Raman spectroscopy for Art and Archaeometry. In addition, see the cumulative annual reviewing papers (I to VIII) appeared on Journal of Raman Spectroscopy or, in particular, the summaries of the works presented at the eight Raman in Art and Archaeometry (RAA) Congresses (or Conferences) up to that in 2013 in Ljubljana (see ref. [3] and references therein). Roughly, the last decade will be covered in this work, with some less recent but important or specific references.

Ceramics and lapidary

Raman spectroscopy is largely used in the study of ceramics in their various components: body, paintings and decorations, ingobes and glazes [15–41]. The number of scientific papers about Raman spectroscopy and pottery is still increasing: a quick survey on Google Scholar shows that in the latest years nearly 300 papers per year on Raman spetroscopy and archaeological ceramics were published; this number was nearly one half seven years ago, and nearly one sixth fifteen years ago. In the very last years, some good review articles appeared, dedicated to the multi-technique characterization of the ceramics materials and more specifically to the Raman study of enamelled and glazed ceramics[42] [43]. Ancient pottery is a heterogeneous material from the mineralogical and chemical points of view. The minerals present in the body of pottery can be subdivided in primary phases, present in the raw material or added as tempers, new phases formed during the firing process, and secondary phases, formed later during the use of ceramics or their burial. While primary minerals are mostly used to identify the provenance of raw materials, new formed phases bring information on the firing technology. Finally, secondary minerals are related to the life of the object and the geological and chemical conditions during the burial. Due to the strong heterogeneity of the material, Raman spectroscopy is not the best technique to obtain the average composition of a ceramic, because it’s mostly a “point” technique, analysing very small amount of material in each measurement and because of the large difference in scattering efficiency of the different minerals [16]. Nevertheless, especially when used in combination with different, more averaged, “volume” techniques, such as X-Ray diffraction (XRD) or neutron diffraction (ND) [24,25,31,35,40,41,44], Raman spectroscopy can give interesting results, especially on the minor phases, hardly detected with other techniques, in a non-invasive way. For that reason, the coupling of Raman spectroscopy with optical or electron microscopy and a diffraction technique is the most typical combination in publications involving Raman study of ceramics. Very often, Fourier-transform infrared absorption (FTIR) [26,27,45–48] and elemental techniques such as scanning electron microscope coupled with energy dispersive X spectroscopy (SEM-EDXS) [40,41,49] or X-ray fluorescence (XRF)[24,50,51] are also present. Sometimes other techniques are present, as LIBS, PIXE, XAS, AAS and ICP-OES.

We notice also the use of combined machines, with different techniques measuring the same spot, as in the case of the study of ceramics by a Raman/SEM-EDS apparatus [25].

Iron oxides

Between the "minor" mineral phases present in ceramic bodies and decorations, iron oxides are probably the most studied, being responsible of most red-black colorations [41,52,53] and largely used to discriminate between annealing in oxidizing or reducing atmosphere. Iron oxides features appear often in pottery Raman spectra, thanks to their strong signal, in particular hematite. The main debated point is about the fact that the spectrum of hematite (α-Fe_2O_3) in archaeological samples is often accompanied by a band at ~670 cm^{-1}, not present in the Raman spectrum of pure hematite [54]. In various papers, this band was used as a marker of the presence of magnetite (Fe_3O_4), because it's very similar to magnetite main Raman band [17,55]. From a technological point of view, the correct identification of the iron oxide phase is very relevant: the red hematite means oxidizing environment while the black magnetite is obtained under reducing conditions. Different authors [53,56] showed that the band at ~670 cm^{-1} could be present in disordered or impure hematite. If the 670 cm^{-1} band is always present together with other hematite bands and never alone, the presence of magnetite should be considered doubtful [35,57]. Only when it is found alone and at slightly lower wavenumbers (~660 cm^{-1}) the attribution to magnetite can be considered as certain [41]. We have also to take into account that the presence in the magnetite structure of different metals (as chromium) usually leads to an increase of the wavenumber of its main band [58]. The constant presence of hematite in red ceramics and its strong Raman signal make it a good probe to investigate the thermal and mineralogical history of the ceramic bodies. The shifts, relative amplitudes and broadening of its Raman peaks were studied to differentiate natural hematite from that obtained by heating goethite (α-FeOOH) [59], to estimate the presence of Al in the hematite structure [40], to evaluate purity, disorder and degree of crystallinity [26,36] or also finite-size effects in nano-crystalline hematite [17] and to relate them with raw materials provenance and firing conditions of ceramics. The main Raman band of hematite, at 287 cm^{-1}, was used to obtain Raman maps in *terra sigillata*, to evidence the slip/body border [33]. Raman micro-maps were also obtained using the position and the width of the main Raman band of hematite, relating these parameters to hematite formation temperature. This made it possible to obtain the firing temperature of the different layers of Athenian pottery replicas [20]; the results indicated a very complex procedure in the manufacture of the red-black vessels, with two separate firings, each composed by two or three different steps. Different iron oxide phases were also identified in ceramic bodies. In particular, the detection of maghemite (γ-Fe_2O_3), which could be seen as an iron-deficient form of magnetite, is helpful to understand the transformation hematite-magnetite in ceramics [36,40,57,60]. Rarely, even ε-Fe_2O_3 was detected [40].

Titanium oxides and thermometry

Titanium oxides (anatase, rutile and brookite) are detected by Raman spectroscopy in a very large number of studies on archaeological pottery [24,26,31,48,55,61,62], even when present in small amount, due to their huge Raman signal and their diffusion in many geological environments. This fact gave rise to some debated cases: the Raman spectra obtained on white decorations in many ceramics, coming from different areas and with very different ages [25,48,63,64] showed as main Raman feature the strong spectrum of anatase, like it was painted by "titanium white", which was synthesized only at the beginning of 20th c. Elemental analyses revealed in all the cases that the white material was just a Ti-containing clay (Ti content usually lower than 2%). The Raman efficiency of anatase is so large to completely hide the Raman features of the clay minerals. A good review of these and other cases involving interesting white ceramic decorations are reported by Buzgar [15]. The couple anatase/rutile (the low-T and high-T polymorphs of TiO_2, respectively) is often used as a thermometer to evaluate the firing temperature of the ceramics, because the anatase-to-rutile transition temperature is commonly considered to be nearly 650 °C [35,57]. Actually, this couple of minerals should be used very carefully as thermometers: some recent works [55] [65] [18] [66] have shown that the transformation temperature is largely influenced by many factors, such as chemical environment, association with different mineral phases, size and purity of the starting oxides. We report the case of synthetic undoped anatase which is not transformed into rutile after annealing over 950 °C [67]. The presence in potteries of an unusual large amount of brookite, the rarest TiO_2 polymorph, is sometimes seen

as an indication of incomplete anatase-to-rutile transformation [57] [68], being considered an intermediate product. Actually, this cannot be taken as a rule: sometimes brookite is largely present in the raw material. In addition, the sequence of TiO_2 phases during thermal transformations depends on many different parameters, including crystal size. In particular, the presence of alkali ions as Na^+ and Ca^{2+} stabilizes the brookite phase [69–71]. Raman analysis could however identify other minerals useful for thermometry [57]. Wollastonite, often detected by Raman spectroscopy and present as a new formed phase, can be used as thermometer [57]. Diopside-anorthite-quartz were also used [33]: the presence of the feldspar anorthite, formed starting from near 950 °C, of the pyroxene diopside, formed over 850 °C, and of α-quartz, stable up to 1000 °C, defines a range of annealing temperature between 850 and 1000 °C in French sigillata wares. In a similar way, the couple quartz-crystobalite is used to asses the temperatures in an higher range[22]. Calcite, easily detected by Raman spectroscopy, indicates a low firing temperature, as it starts to decompose into CaO and CO_2 around 650 °C and it disappears completely at about 900 °C [26] [31]. Many minerals, easily identified by Raman spectroscopy, including dolomite, diopside, wollastonite and titanium dioxides were used to define the firing temperature in Lancaster delftware [69]. In the same work, an extensive Raman study of the local rocks allowed to identify the provenance of the raw materials. Shoval et al. [72] applied second-derivative and curve-fitting techniques to distinguish between meta-smectite and meta-kaolinite in calcareous Iron-Age pottery, estimating the firing temperature. The best definition of the firing temperature was however obtained by a multi-technique approach, combining the phases detected by Raman spectroscopy with other phases revealed by complementary techniques [41].

Feldspars

A family of minerals largely present in ceramic bodies are feldspars. These tectosilicates are widespread in many rocks and geological environments [73] and are present in ceramics as part of the raw materials, or intentionally introduced as flux or also produced during the firing as neo-formation phases [74]. Despite the complexity of the feldspar family, where the members are distinguished not only by the composition but also by the order degree, different important Raman spectroscopy studies on feldspars are present in literature [75,76]. Many investigators used Raman spectroscopy to characterize feldspar in ceramics [25,69,77] because the correct identification of the right term could allow one to recognize the provenance of the raw materials or to better understand the firing conditions of the pottery. An important point to consider is that the correct phase identification (and, in turn, the possible geological origin) depends not only from the composition, but also from the structural order. This means that the width of the Raman bands is important as well as their positions [76]. The sub-micrometric heterogeneity and the usual strong fluorescence of archaeological ceramics often results in very noisy Raman spectra, not clean enough to have a precise identification of the feldspar species; frequently a generic mixed phase (as bitownite) is indicated. It is noteworthy that different results are obtained in the identification of feldspars when analysing the same ceramic with different techniques. This is due to an incomplete miscibility between the different members of the feldspar family, especially considering the most ordered (low-T) terms, leading to micrometric patterns of finely intergrown laminae with different compositions[73,78–80]. Because of this small-scale heterogeneity, techniques with different space resolution will give different results. In addition, the dependence on the composition of the position of the Raman peaks is not perfectly reproduced by the changes in the cell parameters. As an example, when analysing a K-rich albite with diffraction techniques (ND or XRD), cell parameters typical of plagioclases are obtained, and the feldspar is identified as albite or anorthite, while by Raman spectroscopy a signature very similar to K-feldspar is obtained, even at low potassium content (few percent) [25,75]. For this reason, for the identification of feldspar in ceramics, the use of multiple techniques is recommended; the Raman spectroscopy results should carefully compared with literature, avoiding the simple comparison with automated or generic databases.

Lofrumento et al. [33] studied the distribution of feldspars in the body, and in particular around the body-coating boundary, by means of Raman imaging. Even if the spectral resolution was too low to discriminate between different feldspars, a strong decrease of feldspars content moving from body to coating was evidenced.

Rare minerals in bodies

The ability of Raman, especially micro-Raman, spectroscopy to spot and identify minor and rare mineral phases during point-to-point measurements or mappings leads to a detailed knowledge, even if not quantitative, of mineralogy of ceramics. Up to 25 different crystalline phases were found by Raman spectroscopy on ancient ceramics from Macedonia [36] including titanite, $CaTiSiO_5$; hornblende, $Ca_2(Mg,Fe,Al)_5(Al,Si)_8O_{22}(OH)_2$; phlogopite, $(Mg,Fe,Mn)_3Si_3AlO_{10}(F,OH)_2$; epidote, $Ca_2Al_2(Fe^{3+}Al)(SiO_4)(Si_2O_7)O(OH)$; barite, $BaSO_4$; augite, $(Ca,Mg,Fe)SiO_3$; olivine, $(Mg,Fe)_2SiO_4$; fayalite, Fe_2SiO_4; sphalerite, (Zn,Fe)S; spessartine, $Mn_3Al_2(SiO_4)_3$; diopside, $MgCaSi_2O_6$; siderite, $FeCO_3$ and dolomite, $CaMg(CO_3)_2$ (Fig.1).

FIGURE 1

The local origin of raw materials was inferred by the 17 minerals found by Raman spectroscopy in bronze-age ceramics by Medeghini et al. [32]. In particular, the presence of mineral phases such as zircon and apatite suggests a contribution of granitic-metamorphic rocks while sulphate minerals, such as barite and gypsum, originate from evaporates and olivine from surrounding basic and ultrabasic rocks. The different kinds of porcelain (soft- and hard-paste ceramics) were identified by the peak intensity of the most characteristic minerals [29][81]: beta-wollastonite ($CaSiO_3$) and/or tricalcium phosphate [beta-$Ca_3(PO_4)_2$] have strong Raman signals in in soft pastes, whereas mullite ($3Al_2O_3{\cdot}2SiO_2$) or mullite-like glassy-phase prevail in hard-paste porcelains.

Pigments and decorations in ceramics

Decorations in ceramics revealed, under Raman investigation, a surprising rich mineralogy in terms of pigments, opacifiers and other crystalline compounds. Not all the crystalline phases found should be called "minerals" *sensu stricto*, due to the lack of the equivalent natural phase. As an example, the purple pigment $BaCuSi_2O_6$, a new silicate structure type with isolated four-ring tetrahedral and square-planar Cu, synthesized in 1988, was found in ceramics produced 1845 years ago [33]. Other unusual minerals detected by Raman as pigments were covellite (CuS), used in decoration of lacquer wares in China during the West Han Dynasty (206 BC–8 AD)[82], ilmenite [57] and lapis lazuli, historically used as pigment for paintings, jewels or decorative stones, but not considered as typical pigment for ceramics. Lapis lazuli was found underglaze on an ancient ewer (Iran, 13th c.) belonging to the Lajvardina blue glazed ceramics, confirming the ancient use of Lajvard (lapis lazuli) as reported in an old alchemist's treatise of 14th c. [83]. Lapis lazuli was also found in 13th - 14th c. ceramics from Apulia (Southern Italy) [49] and in 12th-13th c. enamels coming from Frederick II Castle in Melfi (Southern Italy)[84]. Caggiani et al. [85] investigated, by means of temperature-dependent Raman measurements and Raman mappings, the enamels from Melfi and natural lazurite and haüyne crystals, in order to evaluate the use as pigment of heated haüyne, a silicate of sodalite group as lazurite, easy to find in the volcanic rocks surrounding Melfi. The use of Raman micro-mapping was fundamental for the understanding of the distribution of S^- blue chromophores in the crystals. The use of true lapis lazuli, composed of lazurite, and not of local haüyne was confirmed.

Among the white pigments used in ceramics, alumina Al_2O_3 was one of the most common. In addition to the weak Raman bands of corundum, located at 379, 417, 644 and 750 cm^{-1} [86], alumina is often identified, when using the 632.8 nm excitation, by the strong doublet appearing at 1367 and 1397 cm^{-1} [48,52]. It is important to note that this is not a real "Raman identification" because these are very strong photoluminescence bands of Cr^{3+} ions, always present in the alumina crystals. Another very common pigment, especially in non-glazed pottery, is carbon black: apart from the many attempts to differentiate the origin of carbon by the D and G carbon bands in the Raman spectra [87 - 89], the presence of the phosphate Raman band (around 960 cm^{-1}) typical of apatite helps to distinguish between "bone black" and other kind of carbonaceous materials [48,90]. However, this method should be applied very carefully, because the strong and broad carbon bands could hide the peak of a minor phosphate phase. Caggiani and Colomban [91] reported a complete discussion on the identification of black ceramic pigments by Raman spectroscopy.

Crystalline phases in glazes

The ceramic glaze is a silica glassy layer and was successfully characterized by Raman spectroscopy in terms of silica network using the deconvolution method proposed by Colomban's group [29,92–98] to obtain a polymerization index, an estimation of the fictive temperature and the amount of modifiers and to distinguish between different kinds of glasses. In addition, many crystalline phases are present in the glazes, as devitrification of recrystallization products, as residues of the raw materials, or migrating from the bulk. Many other crystalline phases were intentionally added in the glaze or underglaze as pigments or opacifiers. The use of minerals and rocks as pigments for glazes and their Raman detection was recently discussed [99].

Raškovska et al. [36] found many different crystalline phases in Macedonian ceramic glazes, depending on their color: quartz, feldspars and anatase were found in the white parts while hematite, magnetite, maghemite, rutile, augite and CrO^4-based compounds in the brown parts. Colomban [99] found many chromophores in porcelain glazes, some of them very unusual: uvarovite, sphene, $PbUO_4$. The resonant Raman spectra obtained with suitable excitation wavelength was useful to detect chromophores present in very low amount.

Miao [100] found Pb,Sn and Sb antimonates in porcelain glazes and enamels. Even if they could not be considered all as true minerals (lacking of a natural equivalent), the correct identification of these crystalline phases by their Raman spectra is fundamental to our understanding of the production technology and the chemical reactions involved. The lead antimonite "Naples Yellow" was found in 12th-13th c. Byzantine pottery glazes, together with many other compounds, by Kirmizi et al. [101]. Vieria Ferreira [102] [103] found many rare minerals in 16th c. portuguese ceramics glazes: e.g. kentrolite ($Pb_2Mn^{3+}{}_2O_2(Si_2O_7)$), melanotekite ($Pb_2Fe^{3+}{}_2O_2Si_2O_7$), malayaite ($CaSnO(SiO_4)$), hausmannite ($Mn^{2+}Mn^{3+}{}_2O_4$). Malayaite and rammelsbergite $NiAs_2$, were identified in the glazes of Lancaster delftware [69].

Mobile Raman and data treatment

Pottery and ceramic fragments are easier to move than other archaeological findings or artworks, as paintings or statues; for this reason, mobile Raman equipments have up to now not been extensively used in studies on ceramics. However, their use is increasing and also in the ceramic field some works are appearing. In addition to the glass signal on the glazes, through portable systems Colomban et al. [61,62,92,93,104] were able to detect many minerals phases, useful to distinguish technology and provenance, in ceramic bodies and decorations: quartz, chromite spinels, hematite, calcium phosphate, mullite, dysthene and fluorite. As an example, in Chinese ceramics, the frequent presence in the Raman spectrum of a small peak at around 322 cm^{-1}, confirmed that the fluorite use as opacifier dates back to the Tang dynasty. Mobile Raman was also used to differentiate between genuine artefacts and copies of Limoges enamels [105].

Data treatment is an important part of the experimental procedures. In the analysis of Raman spectra, especially when dealing with identification of well-defined crystalline phases, the use of statistical methods, as principal component analysis, is not frequent. Rarely, multivariate analysis can be used to distinguish minerals in ceramics or to group and classify ceramics from the identified mineral phases [106]. In particular, to discriminate Raman signals of the different ceramic components in case of high fluorescence background, BTEM (Band-target entropy minimization), a self-modeling curve resolution technique, was proposed [107]. The resulting pure component spectra show an excellent signal-to-noise ratio.

Pietra Ollare

Common use dishes and pots were not only made of true ceramics, sometimes they were made of stones. Raman spectroscopy, coupled with other techniques, was used to characterize archaeological stone objects [108]. For wide historical periods, stoneware made of the so called *pietra ollare (soapstone)* was widely diffuse. Pietra ollare is a generic term referring to a metamorphic rock mostly composed of low-hardness silicates with high chemical, thermal and weathering resistance [109]. Pietra ollare can be classified in four main groups: chlorite-schists, talc-schists, serpentine-schists and ultrabasites. Provenance studies on pietra ollare pots and millstones [110,111] are usually based on standard petrological techniques as thin sections, XRD and SEM-EDS, so involving sampling and invasive techniques. Raman spectroscopy was proven to be effective in the identification of minerals phases (chlorite, chloritoid, talc, garnets, olivine, etc), useful to

assess the provenance of the raw materials and the consequent trade routes [112]. In the case of chlorite-schists, the study of the composition of included garnets, made using the Miragem software [113], allowed to compare their zonation with that reported in literature for the historical quarry of St. Marcel (Aosta Valley, Italy), identified as provenance locality [114]. In the case of medieval talc-schists pot fragments, the combination between mobile Raman apparatus and laboratory micro-Raman allowed the direct comparison between the archaeological findings (studied in laboratory) and the stones present in the quarry identified as possible source (examined *in-situ* by mobile spectrometer)[112]. The Raman spectra showed the presence of the same minerals (mostly talc, chlorite, calcite, magnesite and iron oxides). In addition, it was possible to precisely identify the olivine phase as a prevalent forsterite in both cases, thanks to the Mg/Fe ratio obtained by the separation of the characteristic doublet present in the Raman spectrum [115]. This match between the olivine phases was a strong element supporting the provenance hypothesis of the archaeological fragments. The orientational texture of chlorite was also mapped by using the micro-Raman apparatus (Fig.2).

FIGURE 2.

Gems and gemstones

The use of Raman spectroscopy for the analysis of minerals, including gemstones, started with the origin of the technique. Raman spectrometers appeared in few gemological laboratories nearly 35 years ago, especially in France [116–119]. Only after the advent of compact micro-Raman instruments, and even more with the uptake of mobile Raman systems, the use of Raman spectroscopy became common in the analysis of gemologic material. In the last 15 years, few works tried to point out the main aspects of the applications of Raman spectroscopy to gemology [120]. In particular, some extensive review papers on Raman and gemology appeared few years ago [9,121] even related to forensic aspects [122]. A particular review, centered on mineralogical studies of archaeological gems by means of many techniques, including Raman spectroscopy, appeared few years ago [123].

In this work we would like to update the last reviews, giving a quick overview of the most recent literature on Raman gem analysis, with particular attention to the works related to cultural heritage and archaeology. Despite the diffusion of the use of Raman spectroscopy both in mineralogy and in archaeometry, the number of papers dealing with Raman study of gems related with art or archaeological did not increase as much as in other fields (e.g. study of ceramics). Actually, most of the Raman analysis of gems is now carried out in laboratories for routine investigations, and only few of them are part of research projects.

Historical and archaeological gems

Examples of the use of a particular setup of a micro-Raman instrument are given by Karampelas et al. [124,125], investigating the gems mounted in the important artworks (chalices and ciborium) present in the Benedictine Abbey of Einsiedeln, and by Jeršek and Kramar [126] analysing the huge amount of gems (465) embedded in a baroque chalice, including 24 diamonds, 93 rubies, 4 sapphires, 152 emeralds. UV-visible fluorescence was used to complement Raman spectroscopy for the identification of synthetic gems used to substitute original ones: the very strong red fluorescence characteristic of Verneuil type of synthetic rubies [127] was detected in some red gems. The majority of recently published investigations on archaeological gems were performed using mobile equipment, thanks to the diffusion of powerful portable Raman systems, with sufficient spectral resolution and decreasing costs. This kind of *in-situ* investigation was very rare up to ten years ago [128]. To characterize not only the gems, but even the noble metals in the sceptre of the Faculty of Science of Charles University in Prague, Petrovà et al. [129] combined handheld Raman with handheld XRF instruments, obtaining a complete in-situ analysis. A large series of mounted gems was characterized, and in some cases re-attributed, by the sole use of mobile (handheld and portable) Raman apparatus in the regional museums of Messina [130] and Siracusa (Italy) [131] (Fig.3).

FIGURE 3.

The use of multiple laser lines allowed to evidence the higher number of identifications obtained by a laser diode at 785 nm, due to a lower fluorescence background, with respect to the other typical line used in

mobile Raman instruments, the 532 nm emission of the doubled Nd:YAG lasers. The latter is however useful when studying Cr^{3+} containing gems, as corundum and beryls, in order to avoid the chromium photoluminescence [86,132]. The 785 nm line was however successfully used with a mobile spectrometer to clearly identify minerals of the group of beryls (aquamarine, goshenite and heliodor) during the characterization of gemstone beads of the Han Dynasties in Guangxi Province (China) [133]. The combined use of portable Raman and portable energy-dispersive X-ray fluorescence spectrometer (pXRF) allowed to obtain important information on provenance and trade of the gemstones, non-destructively and directly *in-situ.*

Silica gemstones

Most of the ancient jewelry is not based on very precious gems, according to a modern point of view; most of the cameos, pendants and small objects were made on various silica-based materials, from siliceous stones (as jaspers), to the micro- and crypto-crystalline varieties of silica (chalcedony), to the chromatic varieties of quartz (amethyst, citrine, etc.). When investigated in-situ [131,134], in a non-destructive way, the careful observation of texture and colours, possibly with the help of a microscope, should complement Raman analysis in the description of the material, because Raman spectrum will be very similar in most of the cases, showing mainly the features of quartz. In chalcedony (including agate and carnelian) the presence of minor moganite is expected. Moganite is the monoclinic silica polymorph approved as a new mineral by the IMA in 1999 and identified by its main band at 501 cm^{-1} [135–137]. In some rare case, objects carved in opal CT (cristobalite–tridymite) can be identified by the cristobalite band at 410 cm^{-1} [121,137]. The presence of hematite bands is also expected in some agates and carnelians. A rare use of hematite in gemology, as dyeing agent in the intermediate layer of a triplet simulating a red stone, was also signaled [138]. This simulant, as well as enhancement treatments performed on the gems in historic times, were detected by Raman and FTIR spectroscopies in the collections preserved in V&A museum in London. Provenance studies on silica gemstones, largely diffuse and lacking of characterizing elements, are very difficult. Raman spectroscopy was used by Gliozzo et al. [139] to complement synchrotron radiation X-ray diffraction (SR-XRD) and proton-induced X-ray emission spectroscopy (PIXE) to obtain a complete non-destructive characterization of the gemstones of the collection from Vigna Barberini (Rome, Italy), including 20 chalcedonies. Capel Ferrón et al. [140] published very recently a detailed combined Raman and Rietveld study on a set of prehistoric lithic tools from Spain. In particular they developed, from the Raman spectra of the archaeological objects, after a calibration procedure, a method to obtain the moganite to quartz ratio in a fast and non-destructive way.

Gemstones: nature, genesis and provenance

The majority of the works that have appeared recently, especially on measurements obtained with laboratory micro-Raman instruments, are not strictly related to archaeological objects, but mostly devoted to the study of specific gemstones or family of gemstones: sapphires [86], tourmalines [141], emeralds [132,142–144], aquamarine [145] and pezzottaite [146], the new Cs-rich red gemstone related to beryls [147,148].

In addition to the simple mineralogical identification of the gems, in jewellery the recognition of fakes (simulants or synthetic gems) and the identification of provenance are the most required information to the analysts [149]. Taking advantage of the confocality of the micro-Raman apparatus, it is possible to identify fluid or solid, organic and inorganic inclusions. This is one of the main tools for the study of provenance and to identify synthetic materials [9]. A study of organic inclusions in beautiful “watermelon” elbaite tourmalines from Nuristan was recently reported [141]. The diffuse presence of hydrogen sulphide (main band at 2610 cm^{-1}), methane (2912 cm^{-1}), ethane (2950 cm^{-1}), propane (2895 cm^{-1}) ad carbonaceous matter (~1340 and ~1600 cm^{-1}) was evidenced by the Raman spectra. This kind of inclusions is typical of natural materials and explained by a model of the graphitization process. The study of mineral inclusions by micro-Raman spectroscopy was recently extended to many different families of minerals used in gemmology. Important examples are yellow scapolites [150], demantoid and topazolite garnets from Madagascar [151], orange spinels [152], tourmalines, peridot and garnets from Vietnam [153], tanzanite [154] and chrysoprase from Turkey [155]: Raman spectroscopy has become a standard, routinary technique for provenance studies. In addition, genetic information can be gathered from the Raman study of inclusions in

gemstones, as in the case of topaz from the miarolitic pegmatites from Ukraina, where the identified inclusions (including beryl, orthoclase, lepidolite, zinnwaldite and monazite) suggest a post-magmatic genesis [156]. Going in deeper detail, Noguchi et al. [157] used the well-known pressure dependence of Cr^{3+} fluorescence in corundum to realize combined micro-Raman and photoluminescence micro-maps to visualize the internal stress fields in an Australian sapphire gemstone around a zircon inclusion. Crystallization pressure and temperature of the host sapphire can be deduced from the internal stress field, helping in the identification of the origin of the gemstone.

Organic gemmological material, as amber, can be fruitfully analysed by Raman spectroscopy, despite frequent fluorescence problems, thanks to the richness of the spectra [9]. Over 100 amber jewellery objects from Poland, dated to Iron Age, were studied by Raman spectroscopy complemented by positron annihilation spectroscopy (PAS) [158]. In addition to the classical estimation of the geological age from the polymerization degree, obtained by the intensity ratio between the peaks at 1645 and 1449 cm^{-1} [159–161], the spectral region between 700 and 750 cm^{-1} was used to distinguish between Baltic amber (succinite) from Moravian amber (valchovite). In addition, Rao et al. [162] from the presence of a Raman peak at 1589 cm^{-1}, attributed to an unsaturated resin acid, differentiated colophony from amber and copal. Even the most poor (but very diffuse) gemmological material, as quartz, can be characterized in terms of naturalness and provenance by Raman spectroscopy: Zu et al. [163] proposed a method to discriminate between synthetic and natural quartz crystals, based on the linewidth of the main Raman band. Micro-Raman and optical microscopy were used to study mineral inclusions in prehistoric rock-crystal (quartz) artefacts from Lower Silesia (Poland)][164]. Anatase, kaolinite, chlorite, hematite and goethite were found allowing to recognize the provenance rocks of the quartz used as raw material.

When analyzing gems with a mobile equipment, the study of inclusions is usually impossible, with the only possible exception of TiO_2: in a quartz or sapphire crystal full of rutile needles, the rutile main bands may appear even with a millimeter-sized laser spot. Due to the low space resolution of portable systems, it is often very difficult to gather information more than the simple gem identification from in situ measurements. One of the best possibilities to get deeper in the Raman study of the gems, even with mobile equipment, is offered by water. This requires, of course, a suitable wide spectral range, rarely obtained on portable systems, and only with the 532 nm line as excitation. In gems containing water or OH groups, the OH stretching region of the Raman spectra is usually very sensitive to the local environment of hydroxyls, i.e. the presence of different ions and impurities, order and geometry. The analysis of this region is very helpful to obtain information on the genesis of water containing minerals, as beryls, to identify synthetic ones and to made hypothesis on their provenance [132,142–144] (Fig.4).

FIGURE 4.

Treatments

The identification of enhancement treatments on the gems, in order to distinguish between “allowed” and “non-allowed” ones, is of great interest in gemmology, because the commercial value of a gem strongly depends on its “naturalness”[120] [122] [9]. From the beginning of its application to gemmology, Raman spectroscopy was required to help in the identification of gemstone treatments [165]. The fight between new treatments and their detection requires a continuous research and use of updated technique. In a recent overview [166], the use of Raman spectroscopy is reported for the detection of treatments in heated black diamonds [167], impregnated turquoise [168], chalcedony simulating opals [169] and spinel. In fact, heat treatments in spinels can be detected by Raman spectroscopy, measuring the width of the band at 405 cm^{-1} [152]. The peak broadening, from 10 to 30 cm^{-1} after the heating process, is related to the increase of inversion in the spinel structure [170]. Recently, the identification by FTIR and Raman spectroscopies of heat-treatments in aquamarine, affecting the 682, 1070 and 3604 cm^{-1} bands of beryl, was proposed [145].

Raman Maps

Raman systems able to perform micro-maps, with a large number of points in a very short time, are becoming largely available. The application in the field of gems, and generally in the mineralogical world,

can cover a variety of subjects of great interest [171]. However, in the last years the number of publications including Raman maps in gems was very limited, usually related to the study of residual stress, as in the previously cited work of Noguchi et al. [157] (Fig.5).

FIGURE 5.

Pink diamonds are among the rarest and most valuable gems, yet, the origin of the pink colour is still not fully understood. High spatial resolution Raman and FTIR mapping were used to study defects and remaining strain in the diamond structure. Raman spectroscopy allowed identifying and characterizing the defective zones, with many photo-luminescent defects, where the strain is mostly localized. These regions are related to the presence of winnings, used by diamonds to accommodate a large amount of stress in mantle conditions [172].

Stones used in jewellery: jades

The term jade refers to many different hard green translucent materials used in jewellery. Usually only jadeitic jades, made by the pyroxene jadeite, and nephritic jades, made by nephrite, a generic term of the amphibole series tremolite-actinolite, are considered "true" jades [173]. But, from commercial and archaeological point of view, many other rocks or minerals have been sometimes classified as "jades". Wang et al. [174] performed an extended Raman study on ancient and modern Chinese jades of many different kinds, comparing classical amphibole jades with serpentine jades, turquoise jades and cryptocrystalline quartz jades. Great attention was put on the OH stretching region of the Raman spectra, between 3000 and 4000 cm^{-1}, very sensitive to small compositional or structural variations, in all the investigated mineral families. In fact, even in the oldest works related to jades, the OH stretching was used to obtain detailed compositional information. In nephritic jades, the number and relative intensities of the OH stretching peaks, related to the $Fe^{2+}/(Fe^{2+}+Mg)$ ratio, proved to be an effective method to identify the composition of a nephrite in the tremolite (Mg-rich term)-actinolite(Fe-rich term) series [175,176]. Even in the serpentine family the position of the OH bands allow to distinguish between the different polymorphs, obtaining their distribution on micrometric scale by means of Raman mapping of the different OH bands [177]. Provenance of serpentine jades was non-destructively studied by the Raman identification of the inclusions [178]: actinolite, chlorite, quartz, magnetite and goethite, typical of metamorphism of ultramafic rocks, were found. In addition, jade quality was evaluated from the ratio of the Raman bands of serpentine (antigorite) and inclusions. A handheld Raman spectrometer was used, in a multi-technique campaign, to study in-situ jade (greenstone) objects in the Mayan site of Palenque, Mexico [179]. In addition to prevalent jadeite objects, many other green minerals were found: omphacite, amazonite, albite, muscovite and quartz.

Mineral pigments

Colour is extremely important when studying art and archaeological objects. Traces of pigments have been found in coloured prehistoric figures found in caves and rock shelters and in coloured objects in archaeological layers, dating at least in the Palaeolithic period. The colour palette used on art objects, paintings, tools and objects of daily life has been extended from natural (mainly mineral) pigments to synthetic colours. The identification of the nature of the pigments in archaeological artefacts (or "archaeomaterials") allows to gain insight into the provenance, manufacture, use, exchange, alterations and to solve problems due the alteration of the colours over time, conservation and restoration. It is fundamental also to allow the reconstruction of ancient objects and paints as they would have appeared in their original state and can be useful to uncover forgeries.

Minerals have played a major role in the use of pigments. Most natural organic molecules cannot be used as colorants in artworks because of weathering: they fade with light, react with other chemicals (oil, resins, substrates, etc.) of the artwork itself or pollutants. Mineral pigments are usually more stable and are therefore preferred for artistic techniques, whether it is in mural paintings, oil paintings, or polychromatic pottery, etc. Natural coloured minerals are known from prehistoric times (red and yellow ochres, black manganese oxides). Carbon black may also be included when of fossil origin. The chronological use of most

pigments has been assessed and certain pigments may be used as a dating criterion for coloured (painted) artworks.

Inorganic (mainly mineral) pigments include hundreds of different types. Often the mineral pigments are embedded in a matrix. Each pigment is characterized by a particular composition, proportion of mineral phases and combination of different elements. Minor phases, inclusions, trace elements and specific graininess (particle morphology), allow in many cases a precise identification of the geographical provenance (sources) and give information on the manufacturing of particular pigments and on the pigment trading.

Prehistoric painters used earth pigments, soot and charcoal. Ferric oxide monohydrate $Fe_2O_3.H_2O$ or FeOOH (goethite), mixed with silica and clay, is responsible for the yellow colour (yellow ochre). Red ochre may be produced by heating the yellow ochre to anhydrous ferric oxide Fe_2O_3 (hematite) but occurs also naturally. Blues and greens were not available to prehistoric painters. Malachite and azurite mineral pigments, both copper carbonates, were used by Egyptians from the Fourth Dynasty. The Egyptians introduced also from about 4000 BC a synthetic calcium copper silicate, Egyptian blue, whose corresponding (rare) mineral is cuprorivaite ($CaCuSi_4O_{10}$) and the Chinese made the barium based Chinese Blue ($BaCuSi_2O_{10}$) and Purple ($BaCuSi_2O_6$).

Orpiment, yellow arsenic sulphide (As_2S_3), was used for bright yellow or gold, and realgar, red arsenic sulphide (As_4S_4), for bright reds. Their colours are not permanent and fade on exposure to light. Jarosite, potassium ferric sulphate hydroxide $KFe_3(SO_4)_2(OH)_6$, was used to produce a pale yellow. The Chinese developed the red vermilion pigment 2000 years before the Romans by crushing, washing and heating the mineral cinnabar, or mercuric sulphide HgS. A synthetic route was also developed. Greeks created the white lead pigment (idrocerussite $(2Pb(CO_3)_2 . Pb(OH)_2)$ from metallic lead in vinegar. White lead and cerussite (lead carbonate $PbCO_3$) remained the most used white pigments until the 19th c. Greeks used also red lead (Pb_3O_4), found naturally as the mineral minium or synthesized by heating mineral litharge (PbO) in air. The Romans made use of the pigments developed by the Egyptians and Greeks and of cinnabar mined in Spain. It was extensively used in wall decorations in the houses (as those found in Pompeii) and it was still being used in the 19th c. Maya Blue, a hybrid organic-inorganic pigment, was invented by pre-Columbian Mesoamericans.

Other mineral pigments were used in medieval and renaissance periods as umbers (earth pigments containing iron oxides and manganese oxides) and green earths. In addition to azurite, the most important blue in the Middle Ages (but used from Aegyptian times) was ultramarine, made by grinding the semi-precious mineral lapis lazuli, a rock containing the mineral lazurite, $Na_3Ca(Al_3Si_3O_{12})S$, an aluminosilicate zeolite with the sodalite structure, imported mainly from Afghanistan. Ultramarine was an extremely expensive pigment until a synthetic ultramarine was invented in 1826 by Guimet. Malachite and verdigris (synthetic copper acetate) were used as greens, orpiment and ochres continued to be used for yellow, together with various forms of synthetic lead containing yellow pigments, known from the antiquity. Smalt, a blue pigment comprising ground glass containing cobalt, was discovered before the 16th c. and was made by heating quartz, potassium carbonate and cobalt chloride. It was replaced in the 19th c. by cobalt blue, developed in 1802 by Thenard. For much of recorded history, up to the 17-18th c., the pigments were mainly the minerals and the synthetic compounds described above [180] [181]. Then, large amounts of chemically synthesised pigments were introduced starting from 19th c. [182].

Raman spectroscopy technique is a most elegant method for pigment analysis of relevant artistic and archaeological materials. Pigment investigation is one of the most active research areas in cultural heritage (archaeometry and analysis of artefacts) using Raman spectroscopy. Many natural mineral pigments can be distinguished from their synthetic forms by their morphology or by the impurities. The original mineral components of the colour may be mixed with alteration products that have formed over time. In archaeometric investigations or on ancient artworks, pure minerals used as pigments, even for short periods, are continuously suggested: this work aims to review the micro-Raman spectroscopy contributions, mostly of the last years, both off and on-site, on the identification of mineral pigments, taking into account, when necessary, related aspects as photo-chemical degradations.

This review is primarily targeted at pigments of mineral origin of interest for art, cultural heritage and archaeometry. In particular, it is devoted to how the micro-Raman spectroscopy studies have helped in understanding the use of mineral pigments in art history. Some mention has to be made to degradation products, which often provide other "natural pigments ". From the review are almost totally excluded works done exclusively on pigments of certain synthetic origin, those on modern pigments or dyes of organic nature (unless involved with minerals in hybrids like indigo in Maya Blue) and those that characterize the colour in ceramics, glass and mosaics, coloured gems or minerals inside gems, which are the subject of the first part of this review. Therefore, SERS application are excluded.

Always in the scheme of a review on Raman spectroscopy “and” mineral pigments, the emphasis is put on reported unusual or rare pigments and on the open issues relating to the difficult discrimination between intentionally used mineral pigments – intentionally used synthetic mineral pigments - mineral pigments of degradation origin. Some common mineral pigments will be excluded, in particular the white pigments and the well-known “anatase” issue.

In the following, we list some recent applications of Raman spectroscopy to identify the pigments, when pigments of mineral origin are involved, even marginally, on different artworks. If any, the comments report particular results or issues.

Prehistoric pigments

Palaeolithic rock art paintings are often found in excellent condition. Palaeolithic artists used mainly red, yellow, and black colours. The most common mineral pigments found in rock art are earths (red-yellow ochres) or manganese oxyhydroxides (black pigments). Ochre is coloured earth, composed of a mixture of clays, quartz, and iron oxides or oxy-hydroxides, such as hematite or goethite. Hematite is a widespread red pigment for rock paintings, in natural or synthetic form, when obtained from goethite by firing. Raman spectroscopy seems not effective in distinguishing between natural hematite and hematite produced by heating goethite.

A large number (~30) of different mineralogical varieties of black manganese oxides/hydroxides exist and their identification through Raman spectroscopy is difficult and thermal laser induced transformations are possible.

The prehistoric rock paintings have attracted a large amount of Raman investigations. Here we report only on some of the most recent works, starting from year 2008. The first Raman spectroscopic study of San rock art in the Ukhahlamba Drakensberg Park, South Africa, was reported by Prinsloo et al. [183]. According to a study by Hernanz et al. [184], hematite, α-Fe_2O_3, with different granularities, was the pigment generally used in the pictographs from open-air rock shelters at the Sierra de las Cuerdas (Cuenca, Spain). Calcined bones and a mineral cement with alpha quartz, anatase, muscovite and illite have been found in the white pigment. Charcoal particles suggested a previous sketch of the pictograph. Similar conclusions were reported by Hernanz et al. [185] on Prehistoric rock paintings from the Hoz de Vicente, Minglanilla, Cuenca, Spain.

Darchuk et al. [186] investigated on pigment samples from the Carriqueo rock shelter (Rio Negro Province, Argentina) by SEM-EDX, FTIR and Raman spectroscopy. The basic components were determined as yellow or red ochres. A green-grey pigment was recognized as celadonite, through FTIR and elemental SEM/EDS analysis. Gialanella et al. [187] explored red-ochre samples from the Palaeolithic site of Riparo Dalmeri, a rock-shelter in northeastern Italy, dated to 13 000 cal BP. According to the authors, a low level of chemical impurities can be inferred by the low intensity of the “disorder induced” hematite band at about 660 cm^{-1} [54]. The hematite pigment was probably obtained from the thermal treatment of goethite, available in the neighborhood of the site.

In situ non-destructive analysis on prehistoric drawings with portable instruments was made on rock paintings in the Rouffignac-Saint-Cernin and Villars caves (Dordogne, France) by Lahlil et al. [188] and Beck et al. [189], confirming the use of mixtures of manganese oxides (romanechite and pyrolusite). De Faria et al. [190] experimented Raman spectroscopy on rock art paintings from Abrigo do Janelão (Minas Gerais, Brazil) and identified white pigment as calcite ($CaCO_3$), charcoal as black and goethite (α-FeOOH) in yellow and

hematite (α-Fe_2O_3) in red ochres. Whewellite ($CaC_2O_4.H_2O$) and weddelite ($CaC_2O_4.2H_2O$) were detected, common degradation products of microbiological activity.

Tournié et al. [191] reported new in situ results on San rock art in South Africa, whereas Lofrumento et al. [192] analysed Ethiopian prehistoric rock paintings, revealing celadonite as green pigment. Darchuk et al. [193] found red and yellow ochres in rock-painting pigments from Egypt (Gilf Kebia area) and claimed also the presence of rutile. Jezequel et al. [194] investigated by Raman, X-ray diffraction, ICP/MS and analytical TEM some paintings from the Magdalenian age in the Grottes de la Garenne (Saint-Marcel, Indre, France) and objects found on the floor, that could have been used as "crayons". Hematite, clays, carbon matter and carbonates were found in the red pigments and in some crayons. Black pigment was obtained by cryptomelane, pyrolusite, clays, carbonates and carbon matter: an allochtonous origin is suggested.

Erdogu and Ulubey [195] studied the red ochre (mainly hematite) and its symbolic use in Chalcolithic West Mound at Çatalhöyük (Turkey). Bonneau et al. [196] made a detailed investigation of the painting layers in a painted rock shelter in the Drakensberg Mountains of the Eastern Cape Province, South Africa, evidencing, on a complex substrate, carbon black and mixtures of red ochres with very fine texture. In a further work, Bonneau et al. [197] found gypsum, calcite and white clay for white paints in four rock art sites in the Phuthiatsana Valley in Lesotho. Martin-Sanchez et al. [198] attempted by SERS the study of black stains in Lascaux Cave, France, identifying their organic origin, while Hernanz et al. [199] [200] applied Raman spectroscopy to palaeolithic rock paintings from the Tito Bustillo and El Buxu Caves in Asturias, Spain, and in other sites, reporting the main contribution of hematite and revealing hydroxyapatite and wustite (by a Raman peak at 643 cm^{-1}) (Fig.6).

FIGURE 6.

Other research groups experimented Raman spectroscopy on the nature of the ochres and the presence of binders in the rock-shelter paintings at world-heritage site of Bhimbetka (India) [201], in the Minateda rock shelters (Albacete) and other post-palaeolithic drawings of the Mediterranean Basin in Spain [202], in the palaeolithic rock paintings in the La Pena cave in Asturias, Spain [203] and in the post-Palaeolithic blackish pictographs of Los Chaparros site (Albalate del Arzobispo, Teruel Province, Spain) [204]. A detailed analysis on the nature and production techniques of the red ochres was made by Gomes et al. [205] in a study of the Pego da Rainha and Lapa dos Coelhos rock-shelters in Portugal and in La Calderita in Badajoz and Frizo del Terror (Monfrague National Park) in Cáceres, Spain. Dayet et al. [206], using also Raman data, performed an extensive study of ochre procurement, processing and use over a long sequence related to Middle Stone Age site of Diepkloof Rock Shelter (Western Cape Province, South Africa). The same group [207] carried out a detailed multi-technique analysis of pigment use and their provenance in three Châtelperronian sites Roc-de-Combe (Lot), Le Basté and Bidart (Pyrénées Atlantiques).

Iriarte et al. [208] investigated pictographs, including an unusual bichrome figure, discovered in the Abrigo Remacha (Villaseca, Segovia, Spain). They found hematite as the most abundant component in the samples of red pigment and asserted that a bluish black pigment was made with amorphous carbon from charcoal or soot and paracoquimbite $Fe_2(SO_4)_3.9H_2O$ (characterized by a very strong Raman band at 1027 cm^{-1}). This iron sulphate was also identified in fresco paintings on the walls of a Pompeian house [209]: a decaying process of hematite caused by atmospheric SO_2 pollutant seems plausible (Fig.7).

FIGURE 7.

Gomes et al. [210] analysed painting materials from the Gode Roriso rock shelter, Ethiopia. They hypothesize white beeswax as white "pigment" and carbon black without phosphates. The spectra of a red pigment suggest a mixture of hematite and magnetite, through the debated Raman band at about 660 cm^{-1} [54]. A thermal origin for hematite is claimed, contrary to Gialanella et al. [187] hypothesis.

López-Montalvo et al. [211] identified carbon-based black pigments in the Cova Remigia shelters in the Valltorta-Gassulla area (Castellon, Spain), example of Spanish Levantine Rock Art, opening the possibility of radiocarbon dating, whereas Bonjean et al. [212] reported in Scladina Cave (Andenne, Belgium) for the first time a type of black pigment collected by Neandertals around 40.000-37.000 BP that is not a manganese oxide, but carbonaceous material.

Darchuk et al. [213] reported on prehistoric pigments from excavations and on coloured child bones from North Patagonia, Argentina. Excavated pigments show red or yellow ochres (containing minerals as α- and γ-FeOOH, hematite, erdite and haapalaite sulfosalts, and jarosite), probably used for burial ceremonies. Pigments covering human bones were identified as hematite and magnetite. Rogerio-Candelera et al. [214] investigated on red pigments spread over a single inhumation in a monumental Megalithic tomb surrounding Valencina de la Concepción, a Copper Age settlement. Cinnabar, mixed with small amounts of iron oxides was diffusely found: its provenance and use for funerary purposes are discussed.

The ochre associated with the human burial of Magdalenian age in El Mirón Cave (Ramales de la Victoria, Cantabria, Spain) was analysed by Seva Román et al. [215] and found to be a special ochre with unique features (deep red colour, brightness and particle size distribution), identified as hematite with idiomorphic crystallinity.

Perforated and pigment-stained marine shells from two sites of the Iberian Neandertal-associated Middle Palaeolithic, dated approximately 50.000 years ago, were analysed by Zilhão et al. [216]. Raman spectroscopy helped to identify the most important pigments as iron compounds (lepidocrocite γ-FeOOH, goethite, hematite and pyrite). On the other hand, Henshilwood et al. [217] investigated a liquefied ochre-rich mixture, stored in two Haliotis midae (abalone) shells dating back to 100.000 years ago, found during excavations at Blombos Cave, South Africa: they hypothesized a particular production process for this pigment.

Villa et al. [218] recently reported on a case of a paint, preserved as a mineral and organic residue on the working edge of a stone flake from a Middle Stone Age (MSA) layer of Sibudu (South Africa), dated 49.000 years ago. Gas chromatography/mass spectrometry (GC/MS), proteomic and SEM/EDS analyses indicate a mixture of ochre and casein from bovid milk. The powdered pigment mixed with milk is a paint medium that could have been applied to a surface or to human skin.

Rousaki et al. [219] investigated 30 samples of different nature (rock art fragments, grinding tools, shells, raw pigment material, as well as painted ceramics and beads) from the archaeological excavation of two hunter–gatherer regions in Northern Patagonia (Traful Lake and Manso River areas). Micro-Raman analyses revealed mostly the use of red ochre (as always, not pure hematite (Fe_2O_3)). A comprehensive discussion on the origin of hematite (natural or by heating goethite) and on iron oxide phases is given: carbon black, anatase, Mn_3O_4 is observed in some samples. Di Lernia et al. [220] analysed pigments and coloured residues from the Early-Middle Holocene site of Takarkori (SW Libya) and found jarosite and kaolinite, in addition to hematite and goethite. A recent work by Huntley et al. [221] on "mulberry rock art" reports at least two distinct mineral mulberry pigments, jarosite $KFe_3(OH)_6(SO_4)_2$ and hematite, on the basis of elemental analysis (SEM-EDXA and pXRF). No Raman analysis has yet been reported.

Manuscripts

The first application of the micro-Raman spectroscopy to cultural heritage material was on manuscripts [222] [223]. Extensive reviews on the application of Raman spectroscopy on pigments in manuscripts were published by Brown et al. [224] and Clarke [225], on Anglo-Saxon illuminated manuscripts, and by Clark [226] and recently by Clarke [227]. Vandenabeele et al. [8] also detailed a review on the applications on manuscripts up to 2006. We give only the most important references, starting from 2005/2006, with some comments.

A survey on the investigation on illuminated manuscripts appeared in 2012 by Pessanha et al. [228] and in 2013 by Orna [229]. Chaplin et al. [230], after the study on Gutenberg Bibles [231], analysed astronomical and cartographic folios from an Islamic 13th c. book and found orpiment. A study of medieval illuminated manuscripts by means of portable Raman equipment was performed by Bersani et al. [232]; a 9th c. Italian manuscript containing the Homilies on the Gospels of Gregory the Great, now in Vercelli, was studied by Aceto et al. [233] and the Book of Kells by Bioletti et al. [234]. In all cases typical pigments were detected.

Worth of mention are several other investigations using additional techniques [235-239].

Iron oxides in admixture with azurite were revealed on Medieval and Renaissance Italian Manuscript Cuttings by Burgio et al. [240]. Daniilia and Andrikopoulos [241] investigated two full-page Byzantine miniatures and found lapis lazuli, cinnabar, orpiment, yellow ochre, hematite, green earth, carbon black

and lead white. A deliberate use of pyrite and of black metallic bismuth as pigment is reported by Burgio et al. [242] in a study of Bourdichon miniatures.

Duran et al. [243] detected a forgery on an Arabic illuminated manuscript while Deneckere et al. [244] tried to identify the pigments in the 12th c. manuscript Liber Floridus or in three full-page miniatures from the Arnold of Egmond Breviary [245]. Two Byzantine 6th c. manuscripts known as Vienna Dioskurides and Vienna Genesis, held in the Austrian National Library at Vienna, were analysed by Aceto et al. [246]. The palettes are very rich: in addition to vergaut (indigo+orpiment), ultramarine blue is detected at least three centuries before its use in Western manuscripts.

Medieval Cistercian 12–13th c. manuscripts in Santa Maria de Alcobaça, Portugal, were explored by Muralha et al. [247]. The same group [248] identified the pigments on 16–17th c. Persian manuscripts: lazurite, red lead, vermilion, orpiment, a carbon-based black, lead white, malachite, hematite, indigo, carmine and pararealgar and mixtures of indigo and orpiment and indigo and vermilion.

Aceto et al. [249] proposed in 2012 an analytical protocol for miniature paintings. Rasmussen et al. [250] examined the constituents of the ink from a Qumran inkwell to get insight into the ink on the Dead Sea Scrolls and El Bakkali et al. [251] proposed a multi-technical non-invasive approach for the typology of inks, dyes and pigments in two 19th c. ancient Moroccan manuscripts. The Nastova's group in Macedonia investigated medieval old-Slavonic [252] [253], Byzantine and post-Byzantine manuscripts [254] and Islamic illuminated manuscripts (16–18th c.) [255], where a rich palette was identified: vermilion, red lead, lazurite, realgar/pararealgar, orpiment, malachite and its degradation products, atacamite and brochantite. In the illuminated mediaeval manuscript De Civitate Dei, Lauwers et al. [256] identified mosaic gold (i.e. tin(IV) sulphide SnS_2): in mediaeval manuscripts the use of mosaic gold is rather rare.

Recently the list was increased by: an illuminated Manueline foral charter (LeGac et [257]), a 16th c. printed Book "Osorio" with colourful fore-edge Miniatures (Lukačević, et al. [258]), the Manueline foral charter of Sintra (Manso et al. [259]), a rare Old Slavic manuscript (Kostadinovska et al. [260]), a royal 15th c. illuminated parchment (Duran et al. [261]), a 15th c. manuscript (Zoleo et al. [262]), the Manuscript of The Gospel of Jesus's Wife (Yardley and Hagadorn [263]) and the pre-Hispanic Maya "Madrid Codex" (Buti et al. [264]).

Paintings

As recalled before, different reviews, including the comments to the RAA Conferences up to 2013 (see Ref. [3] and references therein) describe the application of Raman spectroscopy to artworks. Paintings, icons, miniatures, polychromies, coffins, mummies etc. have been largely investigated.

Pigments from dynastic Egyptian funerary artefacts were considered by Edwards et al. [265]. A Raman spectroscopic study on a crucifix (15th c.) now in the National Museum in Gdansk, Poland, was performed by Kaminska et al. [266]; Correia et al. [267] [268] explored accurately 23 paintings by Henrique Pousao, a 19th c. Portuguese painter, belonging to the collection of Museo Nacional Soares dos Reis, Porto, Portugal. The Brécy Tondo, supposed an artwork by Raphael, was analysed by Edwards and Benoy [269] and a complete investigation on the technique of El Greco was reported by Daniilia et al. [270].

Other artworks examined include a 16th c. painting Portrait of a Youth (Lau et al. [271]), a 13th c. panel painting (Van der Werf et al. [272]) and South-Asian Shaman paintings (Vandenabeele et al. [273]). The Raman analyses helped to identify bassanite and anhydrite as degradation products in 16th c. Portuguese oil paintings (Benquerenca et al. [274]) and Egyptian blue in a painting by Giovanni Battista Benvenuto from 1524 (Bredal-Jørgensen et al. [275]).

The pigments were identified in a 5th c. Chinese lacquer painting screen (Tao Li et [276]), in 16th c. Chinese folding screens (Pessanha et al. [277]), on a folding screen of the Momoyama period (Pessanha et al. [278]), in Murillo's paintings (Duran et al. [279]) and in 17th c. Indian miniatures by Ravindran et al. [280]. Odlyha et al. [281] described the alteration of selected pigments in paintings, Marchettini et al. [282] studied the pigments palette of 'Adorazione dei Magi', a wooden panel painted by Bartolo di Fredi of the second half of 14th c. Mancini et al. [283] analysed six French miniature portraits on ivory and paper and demonstrated that the pigments could be identified without removing the glass protection.

Raman was experimented also on a portrait and a paint box of a Turkish artist (Akyuz et al. [284]), on the ground layer of "St. Anthony from Padua" 19th c. oil painting (Vančo et al. [285]) and on 17th c. panel painting 'Servilius Appius' by Isaac van den Blocke (Pięta et al. [286]).

Gutiérrez-Neira et al. [287] made a careful investigation on Diego Velázquez paintings and found a reduced set of pigments. They supposed a laser induced transformation from hematite to magnetite (the debated well known Raman peak at ~660 cm^{-1}) and distinguished between cerussite $PbCO_3$ and hydrocerussite $PbCO_3.Pb(OH)_2$ by the hydrocerussite weak band at 828 cm^{-1}.

Van de Voorde et al. [288] reported on a study of "Mad Meg" by Pieter Bruegel the Elder and evidenced an "economic" smalt pigment (SiO_2+K_2O+CoO+Al_2O_3) for the blue colour. A painting of the colonial art in the church of San Pedro Telmo in Buenos Aires was examined by Marte et al. [289].

Other recent investigations on paintings include: a 17th c. Japanese painting (Quattrini et al. [290]), altarpieces and painting workshops of 15th and 16th centuries from Viseu, Coimbra, Lisboa, and Évora (Antunes et al. [291]). Edwards et al. [292] found chrome yellow, synthesized in 1809, in limited zones of ''The Malatesta'' painting, most probably due to a 19th c. retouching.

17th c. gilded miniature portraits on copper were investigated by Veiga et al. [293]. Zmuda-Trzebiatowska et al. [294] reported a study of the yellow and ochre paints of J. Matejko. Two world-famous 17th c. panel paintings of the Gdansk School of Panting were examined by Pieta et al. [286] [295] and a characterization of a canvas painting by the Serbian artist Milo Milunović was presented by Damjanović et al. [296].

Icons

As concern the icons, several investigations appeared on Byzantine or post-Byzantine icons (Andrikopoulos et al. [297], Kouloumpi et al. [298]), coptic (Abdel-Ghani et al. [299], Abdel-Ghani et al. [300] , Iordanidis et al. [301]), greek (Sotiropoulou and Daniilia [302], Karapanagiotis and Dimitrios [303]), Melkite (Lahlil and Martin [304]). Abdel-Ghani et al. [305] examined a Coptic-Byzantine icon dated to the 13th c. from St. Mercurius Church, Old Cairo: hydromagnesite $Mg_5(CO_3)_4(OH)_2{\cdot}4H_2O$ was found and considered as an intentional white pigment. Abdel-Ghani [306] studied the pigment palette of an icon located in Saint Abanoub church in Samanoud, in Egyptian Delta. Two Serbian icons painted on canvas in the Museum of the Serbian Orthodox Church in Belgrade were investigated by Damjanović et al. [307].

Daveri et al. [308] examined gilding techniques of a 13th c. icon and evidenced mosaic gold SnS_2. One of the first evidences of mosaic gold was given in 2000 by Edwards et al. [309] in a 13th c. polychrome statue. A review on gilding materials and techniques on ancient 'gilded' art-objects (9th–19th centuries) from the European cultural heritage was published by Sandu et al. [310]

Polychromies and various artefacts

The pigments of the polychrome limestone sculpture "Las tres generaciones" (Cathedral's Museum of Santiago de Compostela, Spain) were characterized by Prieto et al. [311]. Edwards et al. [312] reported a study on pigments on stone samples from an Augustinian friary. He et al. [313] performed a multi-analytical study of the polychromy in the Guangyuan Thousand-Buddha Grotto, "the museum of painted stone sculpture": the complex analysis suggests atacamite and malachite as true green pigments. The white colour was ascribed to anglesite and gypsum. Some arsenic-containing pigments were detected in the green samples.

Moolooite (copper oxalate, $CuC_2O_4.nH_2O$), a very rare natural mineral, was found as degradation product on *gypsum alabaster* polychrome sculptures by Castro et al [314]. The pigments after modern restorations on statues of Feixiange Cliff in China were identified by Jin et al. [315]. Wang et al. [316] reported on an accurate study of clay-based polychrome sculptures in Jizo Hall of Chongqing Temple, Shanxi Province of China. The mineral pigment used in a green layer was identified as atacamite ($Cu_2Cl(OH)_3$).

Baraldi et al. [317] carried out an analysis on a polychrome wood mask from Papua New Guinea and identified hematite, pyrolusite, magnetite, graphite, goethite and hausmannite together with carbon black. The black colour of the mask's background was obtained with pyrolusite and hausmannite.

A Hindu papier–mâché statue, Kali Walking on Siva, was examined by Edwards et al. [318]. Wooden sculptures were examined by Aliatis et al. [319], Franquelo et al. [320], Lo Monaco et al. [321] and Kuckova et al. [322].

De Santis et al. [323] discussed on the laser induced degradation of the pigments on a 'Cembalo' model musical instrument (A.D. 1650). A micro-Raman spectroscopy study of a multi-coloured tile shard from the Citadel of Algiers was made by Kock and DeWaal [324]. Red pigments from seven Egyptian mummies of the Roman-period (red-shroud mummies) were identified by Walton and Trentelman [325] as red lead Pb_3O_4 with a minor lead tin oxide phase, due to high temperature treatment: the technology and trade between Spain and Aegypt is discussed. An Egyptian wood coffin was investigated by Bonizzoni et al. [326] using different techniques (EDXRF, micro FTIR, FT Raman, GC-MS, XRD and SEM-EDX. Only a few pigments (egyptian blue, cinnabar, probably orpiment) were identified.

One should mention also the studies on pigments from different artworks of Southern Spain Cultural Heritage (Franquelo et al. [327]); on black powders contained in bronze vessels found in Pompeii houses (Canevali et al. [328]); on raw pigments and painted ceramics excavated at Szombathely-Oladi Plató, Hungary (Tóth et al. [329]); on painted pottery figurines from two tombs in Luoyang, China (Liu et al. 2013 [330]); on different artworks and from archaeological sites in Chile (Vallette Campos and Aguayo [331]); on funeral figurines, found in two Hellenistic and two Roman tombs in Thessaloniki, Greece (Fostiridou et al. [332]).

Košařová et al. [333] performed a Raman investigation at different wavelengths of reference samples of natural clay pigments (white clay minerals, green earths and red earths) and samples from historical paintings, looking for the best conditions for the identification of the minerals in the earth pigments. Oujja et al. [334] examined the laser irradiation effects on vermilion, lead chromate and malachite pigments using different wavelengths and pulse duration. Navas et al. [335] applied PCA analysis on first-derivative Raman spectra to investigate historical tempera paint model samples. Using Raman data on the pigments, Siotto et al. [336] tried a virtual reconstruction of the ancient polychromy on a digital 3D model of the sarcophagus dedicated to Ulpia Domnina (National Roman Museum in Rome). Several examples of non-destructive analysis of painted layers on sculptures and plasters using micro-SORS (Spatially-Offset Raman Spectroscopy) have been presented by Conti et al. [337](Fig.8).

FIGURE 8.

Wall paintings

As concerns mineral pigments, ancient wall paintings are a major source of information. Here we report only recent works (roughly the past decade) with a few comments or significant references on mineral pigments.

The list of investigations on mural paintings in which the Raman spectroscopy played a role in the last decade is indeed gigantic: samples of plasters and pictorial layers taken from a fresco of Acireale cathedral (Barilaro et al. [338]); mural paintings by the Italian miniaturist Napoleone Verga (Rosi et al. [339]); polychromy of the decoration of the façade of the Palace of King Pedro I, Seville, Spain (López-Cruz et al. [340]); Roman Plasters of the 'Domus Farini' in Modena (Baraldi et al. [341]); Korean wall paintings (Mazzeo et al. [342]); pigments in the Cemetery of Tutugi, Galera, Granada, Spain and in the Settlement Convento 2, Montemayor, Córdoba, Spain (Parras-Guijarro et al. [343]); pigments extracted from mural paintings in the Notre-Dame Cathedral of Tournai, Belgium (Lepot et al. [344]) or in a medieval monastery of Karaach-Teke, Varna, Bulgary (Zorba et al. [345]); roman wall paintings found in Verona (Mazzocchin et al. [346]); Byzantine wall painting complex in the Protaton Church on Mount Athos, Greece (Daniilia et al. [347]) and Roman plasters in Reggio Emilia (Baraldi et al. [348]).

Pigments in painted mural decorations in a monastery temple from the 15th c. in Lo Manthang, Nepal, have been examined by Mazzeo et al. [349]. They found azurite for the blue colours, sometimes in combination with lazurite particles and malachite: brochantite, a copper sulfate hydrate,(see in the following) was found as alteration product of malachite. The fading of red lead pigment in wall paintings was investigated by Aze et al. [350]. Pérez-Alonso et al. [351] and [352] identified pigments and degradation processes and products (oxalates) in wall paintings in different regions in Spain. Anhydrite was considered an unexplained

degradation product of gypsum. Mazzocchin et al. [353] analized different white pigments in Roman wall paintings of the VIII(a) Regio, Aemilia, and X(a) Regio, Venetia et Histria, identifying calcite, aragonite, dolomite, huntite.

Specific pigments on wall paintings were identified by Raman spectroscopy in further works: samples from three buildings at the Maya site of Copan, Honduras (Goodall et al. [354]); Etruscan polychromes on architectural terracotta panels (Bordignon et al. [355]); St Stephen's wall paintings at Meteora, Greece (Daniilia et al. [356]); the fresco 'Trapasso della Vergine' in the Church of St. John the Baptist in Paterno Calabro, southern Italy (Castriota et al. [357]); frescoes of the Longobard temple in Cividale del Friuli, Italy, and of the 8th c. crypt of San Salvatore in Brescia, Italy (Zucchiatti [358]); 15th c. mural paintings and frescos of the Little Christopher chamber in the Main Town Hall of Gdan´ sk, Poland (Sawczak et al. [359]); the wall paintings from two Romano-British urban centres of Colchester and Lincoln (Edwards et al. [360]).

The first systematic Raman study of the pigments used in medieval wall painting in the churches of Republic of Macedonia has been reported by Minceva-Sukarova et al. [361]. Sodo et al. [362] investigated the mural painting, realized "a fresco", of the Tomba dell'Orco, in the Etruscan necropolis of Tarquinia, Italy. Red ochre (α-Fe_2O_3), cinnabar, orpiment, yellow ochre and egyptian blue were easily identified. The nature of a green pigment was not determined.

Nevin et al. [363] performed an analysis of paint samples from a 16th c. wall painting in the church of Agios Sozomenos in Galata, Cyprus, and found hydrated copper oxalate, analogous to the naturally occurring blue-green mineral moolooite. The 16th c. external wall paintings (fresco technique) of St. Dumitru's Church in Suceava (Romania) were analysed by Hernanz et al. [364], evidencing a degradation due to nitrogenous organic materials.

Boselli et al. [365] reported, in La Verna Sanctuary frescoes, on a white pigment made by a complex mixture of zinc white, lithopone, a minor component of anatase and an unidentified organic material. The paintings in the tomb of Menna (TT69), Theban Necropolis, Egypt, were studied in situ by Vandenabeele et al. [366] but Raman spectroscopy was strongly hampered by fluorescence from paraloid B72 resin used in a previous conservation treatment. Wall painting fragments from Kaiping Diaolou (Qing Dynasty) were investigated by Zeng et al. [367]: lazurite and goethite were the main pigments. They found syngenite $K_2CaSO_4.H_2O$ of undetermined origin in the plaster.

In 2010/2011 a lot of Raman studies dealing with mineral pigments were published: the complex gilt stucco surfaces of different monuments in Lombardia (Sansonetti et al. [368]); Pompeian wall paintings using EDS and HR-SRPD and micro Raman (Duran et al. [369]); pigments in 15th c. mediaeval and 16th c. renaissance vault paintings in the Our Lady's Cathedral in Antwerp, Belgium (Deneckere et al. [370]); mural paintings from the Pyrenean Church of Saint Eulàlia of Unha (Clark et al. [371]); the wall painting "Historia de Concepcion" by Gregorio De La Fuente in Concepcion, Chile (Aguayo et al. [372]); wall painting by Romans and Arabs (Garofano et al. [373]); fresco fragments at the Coriglia, Castel Viscardo, Orvieto, excavation site (Donais et al. [374]); wall paintings by Masolino da Panicale in the Baptistery of Castiglione Olona, Italy (Comelli et al. [375]); pigments from the Mortuary Temple Of Seti I, El - Qurna at Luxor, Egypt (Mahmoud [376]); Roman and Arabic wall paintings in the Patio de Banderas of Reales Alcazares' Palace (Duran et al. [377]); the ceiling of the Gilded Vault of the Domus Aurea in Rome (Clementi et al. [378]).

Raman spectroscopy was used as a diagnostic tool in Marcus Lucretius House, Pompeii, to investigate the nature of deterioration on wall paintings exposed to different environments by Maguregui et al. [209]. Raman mapping allowed to identify oxalates, whewellite and weddellite, which are commonly observed on the surfaces of ancient monuments. They may result from the associated action of microorganisms and environmental conditions. A thermodynamic and spectroscopic investigation on the blackening of hematite into magnetite, attributed to SO_2 attack, in Marcus Lucretius House was performed by Maguregui et al. [379].

Romero-Pastor et al. [380] explored the crystallinity and micro-textural characteristics of the pigments on paintings in the 14th c. Islamic University—Madrasah Yusufiyya— in Granada (Spain) – and discussed about the origin, manufacture and alteration processes of the pigments. Gil et al. [381] reported on an accurate study of the blue pigments from Portuguese 15th to 18th c. churches. Smalt and, in a minor extent, azurite

were found. Smalt pigment seems to be the most affected by conservation problems due to lixiviation. Azurite shows an extraordinary chemical and chromatic stability, probably due to its coarse grains. Iordanidis et al. [382] performed a characterization of Byzantine wall paintings from Kastoria, Northern Greece. Green colour is attributed to admixtures of Fe-rich minerals and lime and not to the commonly used green earths.

The contribution of Raman spectroscopy in 2012/2013 to the pigment identification and on conservation issues has been equally significant: pigments and plasters from the Roman settlement of Thamusida (Rabat, Morocco) (Gliozzo et al. [383]); the tomb of Djehutyemhab (tt194), Elqurna necropolis, Upper Egypt (Mahmoud [384]); pigments from five Medieval Gotland churches in Sweden (Nord and Tronner [385]); the painted vaulted ceiling of the Sant Joan Del Mercat Church, Valencia, Spain (Doménech-Carbó et al. [386]); 16th c. wall paintings in the Saint Andrew Church, Biañez, Biscay, and Saint John the Baptist Church, Axpe, Biscay (Irazola et al. [387]); Sala delle Maschere of the Domus Aurea in Rome (Paradisi et al. [388]); pigments from the 4th to the 3rd c. BC in the Iberian cemetery of Tutugi, Galera, Granada, Spain (Sánchez et al. [389]); Roman plasters applied over Pharaonic walls at Luxor temple, Upper Egypt (Mahmoud et al. [390]); chromatic alterations of Roman Heritage in Aosta (Conz et al. [391]) ; Roman mural paintings (Toschi et al. [392]); the fresco 'The Good and the Bad Judge' located at the medieval village of Monsaraz in southern Portugal (Gil et al. [393]); multi-pigmented surface from the wall decorations of the Theban tomb (TT277), Luxor, Egypt (Mahmoud [394]).

Aceto et al. [395] on mural paintings in Ala di Stura hypothesized the use of pyrite mixed with smalt to reproduce a chromatic effect similar to lapis lazuli, where pyrite is a common accessory mineral. For example, Bersani et al. [396] identified pyrite in the 'Madonna col Bambino e S. Giovannino' by Botticelli. An intentional addition of pyrite to lapis lazuli cannot however be excluded.

Maguregui et al. [397] studied the conservation state of walls and wall paintings in Pompeii, Italy. They confirmed that a severe decay is not observed when the rooms are covered by roofs. In Marcus Lucretius House, Pompeii, Maguregui et al. [398] investigated the nature and distribution of carotenoids in brown patinas from a deteriorated wall painting. Raman mapping also allowed to identify whewellite and weddellite. Oxalate film formation is a pathology that frequently occurs in mural paintings, because of the action of microorganisms and environmental conditions.

Zoppi et al. [399] report a spectroscopic study on some fragments of wall paintings of the Minoan art of Phaistos (Crete) from the Archaeological National Museum in Florence: hematite, goethite, calcite, Egyptian blue, carbon and a green earth (celadonite) were identified.

A rich palette of pigments, both natural/mineral and synthetic ones, was identified by micro-Raman spectroscopy by Cukovska et al. [400] in wall paintings of the 19th c. iconographer Dicho Zograph, in churches from Republic of Macedonia.

De Benedetto et al. [401] claim that in the oldest pictorial cycle in the 12th c. monastery Santa Maria delle Cerrate there is the first known example of smalt and lapis lazuli in South Italy. Zhu et al. [402] analysed wall paintings from the Cizhong Catholic Church of Yunnan Province, China and described a peculiar degradation of emerald green (synthetic) into cornwallite (mineral).

In the last period 2014/2015 we can cite further relevant studies on: wall paintings of two Greek Byzantine Churches from Kastoria, northern Greece (Iordanidis et al. [403]); pigments in the wall paintings at Jokhang Monastery in Lhasa, Tibet, China (Li et al. [404]); a wall painting attributed to Ambrogio Lorenzetti in the St. Augustine Church in Siena, Italy (Damiani et al. [405]); the pigments in dome wall paintings by Correggio in Parma cathedral (Bersani et al. [406]); 17th c. mural paintings, Dominican Convent of Nossa Senhora da Saudacao, Montemor, Portugal (Gil et al. [407]); medieval Nubia wall-paintings from Saras, Old Dongola and Banganarti archaeological sites (Syta et al. [408]); wall paintings in Pompeii (Madariaga et al. [409]); wall paintings from Qasr El-Ghuieta Temple, Kharga Oasis, Egypt (Mahmoud [410]); the wall paintings from the Baños de Doña Maria de Padilla in The Alcazar of Seville (Perez-Rodriguez et al. [411]); binder compositions in Pompeian wall paintings from Insula Occidentalis (Gelzo et al. [412]); gilded plasterwork in the Hall of the Kings in the Alhambra complex, Granada, Spain (de la Torre-López et al. [413]); wall paintings in the San

Francisco Church, Santiago, Chile (Araya et al. [414]); the wall paintings in the Churches of Panagia and Theotokos built in the settlements of Patsos and Meronas at Amari Rethymno, Crete (Cheilakou et al. [415]); wall painting fragments from Roman villas of the Sabina area, Rome (Paladini et al. [416]); the wall paintings from the Hellenistic hypogeum of Apaforte-Licata, Agrigento, Sicily (Aquilia et al. [417]); wall paintings in the Villa of the Papyri in Herculaneum (Amadori et al. [418]); decorative fragments from the hypocaustum in the Roman villa of El Ruedo, Almedinilla, southern Spain (Mateos et al. [419]).

Salvadó et al. [420] made a multi-technique microanalysis of the blue paints in different altarpieces in Catalonia and Crown of Aragon from the 15th c., identifying lapis lazuli, azurite and indigo. Veneranda et al. [421] [422] identified the compounds constituting a mural painting in the Assumption's church of Alaiza in Basque Country, Spain, and investigated the degradation induced by agricultural activities. Maguregui et al. [423] reported on accelerated weathering experiments on wall painting samples from Pompeii, confirming the reduction of hematite into magnetite and the formation of gypsum on calcite plaster. They assessed that high concentrations of SO_2 can cause the sulphation of hematite into paracoquimbite/coquimbite $Fe_2(SO_4)_3.9H_2O$.

Kakoullli et al. [424] provided direct evidence for the earliest use of asbestiform fibres, in Byzantine wall paintings in Cyprus: chrysotile $Mg_3Si_2O_5(OH)_4$ was found in $CaCO_3$-rich finish coatings, just beneath the cinnabar paint layer, providing a very compact and smooth layer with mirror-like surface appearance.

Piovesan et al. [425] described a polychrome sinopia, where cinnabar was also used, under the Lod Mosaic, Israel. Gill et al. [426] analysed the extraordinary palette of pigments on Buddhist wall paintings and sculptures, dating to the 12-13th c., in the interiors of the temple complex at Sumda Chun, Ladakh: azurite, orpiment, vermilion and minium were identified.

Yong and Wang [427] in the wall paintings in Xialu Temple, Tibet Autonomous Region, China, found a large use of orpiment even mixed with cinnabar to produce a reddish orange and determined the sequence of interventions. Schmidt et al. [428] analysed a sample from a wall painting in a Buddhist cave along the northern Silk Road and reported atacamite between the mineral pigments. Gutman et al. [429] investigated mortar layers and pigments of wall paintings from the Roman town of Emona (Ljubljana, Slovenia) and found common earth pigments. Crupi et al. [430] studied the painted surface of plasters withdrawn from different areas of Villa dei Quintili (Rome, Italy) but, due to fluorescence problems, the in-situ Raman spectra, apart calcite, confirmed only the presence of cinnabar.

Blue pigments

In the antiquity, the availability of natural coloured substances was a problem. Earth colours were readily available and were used in cave paintings (rock art) where no blue colour is found. In general, mineral sources for stable blue pigments are exceptionally rare. The first truly stable blue mineral pigment was most likely lapis lazuli. A blue pigment was also the more abundant mineral azurite, a basic copper carbonate. Then, blue-coloured glazes and glasses were prepared by the use of cobalt minerals or by lapis lazuli and methods to produce stable blue materials were developed: Egyptian Blue ($CaCuSi_4O_{10}$) and Maya Blue, a hybrid organic-inorganic. Synthetic blue pigments were developed in China: Chinese Blue and Chinese Purple, also known as Han Blue and Han Purple ($BaCuSi_4O_{10}$ and $BaCuSi_2O_6$). Berke [431] published an excellent historical and scientific survey of the "Invention of blue and purple pigments in ancient times" including Maya Blue.

Azurite

Azurite is one of the two basic copper(II) carbonate minerals, the other being green malachite. The first work on the application of micro Raman spectroscopy to cultural heritage was published in 1984 by Guineau [222] [223] on the identification of azurite and malachite in a 15th c. French manuscript. Then azurite was identified in a large amount of artworks. Unfortunately, this pigment suffers from chemical and/or thermal alterations: discoloration from blue to green due to the degradation of azurite into malachite or into basic copper chlorides (one of the supposed isomers like atacamite, paratacamite, clinoatacamite and botallackite). The conversion into black compounds as copper sulfide (covellite, CuS) or copper oxide (tenorite, CuO) occurs less frequently and is rarely investigated. Conversion of azurite into black tenorite

(CuO) can be due to two different causes: alkaline environment and heat. Mattei et al. [432] explored the conditions for the degradation of azurite into tenorite. They studied also laser-induced degradation of azurite as a function of the grain size. The degradation temperature decreases as the size increases. The conversion of azurite into moolooite has been recently reported by Daniel et al. [433] in a study of the paintings on the 'Royal Portal' of Bordeaux Cathedral. Azurite, being a secondary mineral that forms in the oxidised zones of copper deposits by the interaction of carbonated solutions with primary copper minerals, contains many different impurities. Aru et al. [434] analysed the mineral impurities in azurite pigments using several samples of azurite chosen from historical collections of minerals. They tried to get some hint to ascertain the provenance of an individual azurite-containing pigment.

Maya Blue

Maya Blue, a synthetic pigment produced by the ancient Mayas in pre-Columbian America, is the combination of a fibrous clay (palygorskite-sepiolite) and an organic blue dye (indigo). Indigo was extracted from *Indigofera suffruticosa* plants. Palygorskite is a fibrous clay common in Yucatan. The indigo-palygorskite mixture acquires a considerable stability when a moderate thermal treatment is applied, constituting an artificial mineralization and the first example of a "hybrid" organic-inorganic pigment. The main features of the structure of Maya Blue are known: indigo seem to lie within the palygorskite channels partially substituting the zeolitic water (Chiari et al. [435], Giustetto et al. [436], Giustetto et al. [437]) but the structure of Maya Blue and the nature of its interactions with the clay framework are still investigated. The first Raman spectroscopic examination of a whole set of pigments from archaeological Maya wall painting fragments was made by Vandenabeele et al. [438]. Sánchez del Río et al. [439] performed a Raman study of different preparations of Maya blue and other mixtures of indigo with other inorganic materials. They report that the indigo vibrational spectrum does not change during the thermal treatment and with different clays like sepiolite or montmorillonite. Manciu et al. [440] carried out a Raman and IR study of synthetic Maya pigments as a function of heating time and dye concentration. Synthetic materials demonstrate chemical stability similar to that of the ancient Maya blue samples. The spectroscopic data show the disappearance of the indigo N–H bonding, as the organic molecules incorporate into palygorskite material.

Goodall et al. [354] reported on micro Raman analysis of stucco samples from the buildings of Maya Classic Copan. Wiedemann et al. [441] claimed that original Maya Blue was used to illuminate a fragment of the "Codex Huamantla", but the conclusion was questioned by del Rio and Montes [442]. Moreno et al. [443] studied Maya blue–green pigments found in Calakmul, Mexico, whereas Manciu et al. [444] considered the chemical bonding occurring between thioindigo and inorganic palygorskite, synthesizing a pigment similar to Maya Blue. A review of the Raman results on Maya Blue is given by Doménech et al. [445]. They also considered Maya Blue samples and models obtained by the binding of indigo to phyllosilicate clays, such as palygorskite and sepiolite, using chemometric analysis. A detailed vibrational study of synthetic indigo-paligorskite Maya-Blue was reported by Tsiantos et al. [446].

Indigo@silicalite hybrid pigments are currently investigated for stable pigment (Dejoie et al. [447], Zhang et al. [448]).

Lapis lazuli

Blue-hued minerals have played an important role in the cultural history of mankind. The oldest precious stone of this kind is lapis lazuli, which was already in use in the Sumerian civilisation about 5500 years ago. It was introduced in Europe from Afghanistan and was extensively used in the Middle Ages and during the Renaissance. Lapis lazuli (natural ultramarine blue) takes its coulor to lazurite, which is a sodium aluminosilicate mineral, $(Na,Ca)_8(Al_6Si_6O_{24})(SO_4,Cl,S)_2$. It took until 1806 for the first reliable analysis, suggesting that sulfur species were the colour centres. The earliest syntheses of blue ultramarines were performed in 1826 by J. B. Guimet and C. G. Gmelin, and in 1834 C. Leverkus founded the first plant manufacturing ultramarine in Germany. The colour of the ultramarine blue is due to polysulfur radical anions, S_3^- and S_2^-, chromophores embedded into sodalite cages. The ratio S_3^-/S_2^- determines the hue of the pigment. A tutorial review on the trisulfur radical anion S_3^- has recently appeared (Chivers and Elder [449]). The first evidence of the sulfur chromophore in lapis lazuli by Raman spectroscopy was given by Clark et al.

[450]. The Raman band observed at 547 cm^{-1} is ascribed to the S_3^- symmetric stretching mode, whereas that at 258 cm^{-1} corresponds to the bending vibration of the S_3^- ion: this molecular moiety is responsible for the blue colour. The S_2^- anion (responsible for yellow colour) gives rise to the green tones associated with some ultramarine pigments. Because of its very low concentration in the blue, the corresponding symmetric stretching S_2^- signal appears as a shoulder at about 580 cm^{-1} with very weak intensity. Gobeltz et al. [451] found out that in blue ultramarine, different shades of blue pigments depend on the relative concentration of the two chromophores S_2^- S_3^-, as determined by Raman spectroscopy. Bicchieri et al. [452] characterized azurite and lazurite based pigments. Ostroumov et al. [453], observed also the presence of SO_4^- groups in the Raman spectra of lazurite from Pamir and Siberia. Gobeltz-Hautecoeur et al. [454] studied the occupancy of the sodalite cages, Desnica et al. [455] and Del Federico et al. [456] explored the application of Raman spectroscopy for the discrimination between different ultramarine pigments.

Due to the strong electronic absorption at about 600 nm, resonance Raman effects are evident: Raman spectra show multiphonon processes as overtones and combination bands of the fundamental vibrational modes of S_3^- and S_2^- radical anions (Ballirano and Maras [457]). The 514 nm line excites into the broad absorption band of S_3^- but not into the absorption of S_2^- (at ca. 400 nm), thus resonance effects are observable only for the former species. Ali and Edwards [458] discussed on the discrimination between genuine and fake specimens of lapis lazuli using portable Raman spectrometers and different excitation lines, changing the resonance conditions for the dominant spectral feature arising from the S–S stretching mode of the S_3^- radical anion chromophore. High-pressure resonance Raman spectroscopic study of ultramarine blue pigment has been performed by Barsan et al. [459] indicating weak interactions of the chromophores with the sodalite lattice.

Colomban [42] [99] gave a comprehesive rewiew of the colours in glazed ceramic and enammeled glasses with particular reference to the use of lapis lazuli in ceramics. A first evidence of the use of lapis lazuli as pigment in ceramics was given by Clark et al. [460] [461] on glazed pottery fragments from Castel Fiorentino Castle, Torremaggiore (Foggia, Southern Italy). Blue glazed plates containing lapis lazuli excavated from Siponto (Manfredonia, Apulia) were investigated by Catalano et al. [49]. A Raman and optical/electronic microscopy study of a 13th c. Lajvardina ewer confirmed the use of lapis lazuli grains as glaze pigment (Colomban [83] [462]). In the ewer, glaze cobalt was also detected, demonstrating the use of alternative technologies in the same artefact. Use of lapis lazuli was revealed in glazed Böttger porcelain, the earliest hard-paste "China" porcelain produced in Europe at the Meissen Saxon Court Factory at the beginning of 18th c. (Colomban and Milande [93]).

Greiff and Shuster [463] analysed four fragments of the famous Lübsow glass beaker, with enamelled decorations depicting mythological scenes, found in a 2nd c. tomb in the North of Poland, and the signal of S_3^- chromophore was detected in the blue enamel. Calcite and diopside ($CaMgSi_2O_6$) were also revealed, considered a signature of natural lapis lazuli rock, probably from Afghanistan.

Blue faience artefacts found at Pompeii and assigned to the Ptolemaic–Roman Egyptian production (1st c. BC–1st c. AD) were found coloured by lapis lazuli by Mangone et al. [464]. New evidences on the lapis lazuli use were reported by the Colomban group in some trade blue beads found at Mapungubwe hill, the main archaeological site in South Africa (Tournié et al. [465] and Prinsloo et al. [466])(Fig.9).

FIGURE 9.

The resonance Raman spectrum of the vibrations associated to the lazurite chromophores S_3^- and S_2^- ions under green laser excitation demonstrated the presence of ultramarine in Mamluk enamelled precious objects (Colomban et al. [467]). According to Sendova et al. [468], the chromophores evidenced by Raman spectroscopy in some 'Della Robbia' blue glazes, arose from the thermal treatment of the used raw materials from Co-containing sulphide ores and not from lapis lazuli incorporation. The unicity of this finding has been questioned by Colomban [99].

Derrick et al. [469] by a FTIR study, found a "typical" IR absorption band for lapis lazuli (natural ultramarine) from Afghanistan at about 2340 cm^{-1}, tentatively assigned to S_6^+ species and it was considered distinctive of natural Afghan lapis lazuli. Miliani et al. [470], investigating ultramarine blue pigments by FTIR, interpreted

the absorption band at 2340 cm^{-1} as due to the entrapment of carbon dioxide CO_2 in the sodalite beta-cages of the natural pigment from Afghanistan. Bacci et al. [471] attributed, using also DFT calculations, the same absorption band at 2340 cm^{-1} to the S-H stretching of HS_3^- species in Afghan lapis lazuli, claiming the absence of the band in other lapis lazuli and in the synthetic ultramarine pigments. The result could help in describing the geochemical origin of lapis lazuli. According to Favaro et al. [472] this absorption band, however, is not an indication of genuine Afghan lapis lazuli pigment as it occurs in the spectra of all natural pigments, despite being weaker, for example in the spectra of the Siberian and Chilean pigments. They suggested than it can only be used as a genuine discriminating marker for natural pigments as opposed to synthetic ones.

Osticioli et al. [473] [474] proposed an analytical protocol for the differentiation between natural lapis lazuli and artificial ultramarine blue pigments, as calcite inclusions seem present only in the samples of natural origin. According to Schmidt et al. [475], who considered different natural and synthetic ultramarine samples, the Raman spectra of the natural samples contains non-lazurite features attributed to diopside that could help in provenance studies. These features may be indicative of natural lapis lazuli from Afghanistan. De Torres et al. [476] tried to quantify the Raman spectral differences up to about 2000 cm^{-1} among the synthetic ultramarine blue and three lazurites corresponding to three lapis lazulis from different geographical sources (Chile, Afghanistan, Siberia).

Dominguez-Vidal et al. [477] studied the decorated plasterworks in the seven vaults of the Hall of the Kings of the Palace of the Lions in the Alhambra (Granada, Spain). They found lapis lazuli and a strong luminescence background together with several bands, the most intense located at 1306 and 1508 cm^{-1}, which have been attributed to luminescence of diopside, a mineral commonly associated with lapis lazuli in nature.

Covellite – Mineral pigment or degradation product ?

Jin et al. [82] claimed that the faint blue covellite (CuS), identified by micro-Raman spectroscopy by a characteristic peak at 474.5 cm^{-1} on a Chinese funerary lacquer ware of West Han Dynasty, was used as an intentional pigment (Fig.10).

FIGURE 10.

According to Correia et al. [268] the covellite found in paintings by the Portuguese artist Henrique Pousao (1859–1884) originated from a degradation reaction between a copper-containing pigment and one with sulfur, in the same painted area. Veiga et al. [478], investigating Portuguese portrait miniatures of 17th and 18th centuries, found bluish-black covellite, a pigment rarely found in oil paintings, and supported the hypothesis of an intentional use of the natural mineral species.

Aerinite

Aerinite is a blue fibrous aluminium and calcium hydrate silicate-carbonate with ideal formula $(Ca,Na)_6(Fe^{3+},Fe^{2+},Mg,Al)_4(Al,Mg)_6[Si_{12}O_{36}(OH)_{12}](CO_3)\cdot 12H_2O$. This mineral was the blue pigment commonly used in most Catalan romanic paintings between the XI-XV centuries and in the Pyrenean region (Casas and Llopis [479]) and was extracted in the southern Pyrenees. Aerinite was identified by Raman spectroscopy by Clark et al. [371] in the wall paintings, dating from the Romanesque period to the 16th c., in the church of Santa Eulalia of Unha in the Val d'Aran. Aerinite was also identified in the south-west of France (Daniel et al. [480] [481]) in paintings of the vault of the old abbey home of Moissac (12th C., Tarn-et-Garonne), and in those of the church Saint-Nicolas of Nogaro (end 11th c., Gers). Aerinite was also reported in the Voronet Monastery (Romania) by Buzgar et al. [482]. An accurate micro-characterization of aerinite pigment is reported by Peréz-Aranteguia et al. [483].

Veszelyite

Garcia Moreno et al. [484] [443] investigated the blue-green chromatic palette in early Classic and Late Classic periods in Calakmul (300–850 A.D.), including Maya Blue and Maya Green. In addition to copper based pigments like malachite or pseudomalatiche, they identified veszelyite as a green pigment in blue-green mosaic, polychrome masks and funerary offerings from the royal tombs. Veszelyite is a rare secondary Cu-Zn mineral (hydrated copper-zinc phosphate, $(Cu,Zn)_2ZnPO_4(OH)_3\cdot 2(H_2O)$, and this poses serious questions

about its origin. It is found together with malachite, pseudomalachite and even chrysocolla and it could be a degradation product of malachite.

Vivianite

Vivianite, hydrated ferrous phosphate, $Fe_3(PO_4)_2 \cdot 8H_2O$, has been rarely used as a blue pigment and in mixtures with yellow to produce greens (Scott and Eggert [485]). Mined in areas north of the Alps, vivianite has been identified in about 70 works of art of the European medieval times. It can discoulor to yellowish brown, by oxidation to Fe^{3+} containing species. A comprehensive review and discussion on vivianite has been made by Čermáková et al. [486] [487]. Magnesian vivianite seems to have been identified in a Roman camp near Fort Vechten, Utrecht, The Netherlands, by Kloprogge et al. [488].

Glaucophane – riebeckite

Riebeckite and/or glaucophane, a blue mineral (composed of sodium magnesium (or iron) aluminum hydrosilicate) was used by the Greeks as a blue pigment as early as the 17th c. BC. Riebeckite $Na_2Fe^{2+}{}_3Fe^{3+}{}_2Si_8O_{22}(OH)_2$ is a hydrous silicate mineral of the amphibole group and forms a solid solution with glaucophane $Na_2Mg_3Al_2Si_8O_{22}(OH)_2$. The colour depends on the relative concentration of iron/magnesium. Riebeckite may occur as a fibrous asbestiform mineral (crocidolite or blue asbestos) and is no longer used, being one of the most hazardous asbestiform minerals. Riebeckite (or Mg-riebeckite) was first identified as a blue pigment in the context of studies on Bronze Age wall paintings by Filippakis et al. [489]. Riebeckite is suggested as a pigment in a fresco painted plaster of Bronze Age from Thebes, Greece, by Brysbaert [490]. Westlake et al. [491] carried out a very accurate investigation on 49 wall painting samples from Minoan, Roman and Early Byzantine periods to determine the evolution of the painting materials and reported the presence of blue riebeckite. A study on blue glaucophane-riebeckite pigment on the Akrotiri is reported by Vlachopoulos and Sotiropoulou [492] and by Sotiropoulou et al. [493], but no Raman analysis was performed.

Green pigments

Malachite

Roman artists had a wide knowledge of green pigments, including verdigris, malachite and green earths. Malachite, a copper carbonate hydroxide mineral $Cu_2CO_3(OH)_2$, is identified in many of the previously cited works on paintings and manuscripts. A particular result was reported by Castro et al. [494]: the formation of a copper oxalate (moolooite) in the degradation processes of malachite. Useful for the Raman investigation of malachite and its degradation products is a study of Yu et al. [495] on the characteristics of the Raman spectra of archaeological malachites (not pigments) compared with natural malachites from different mines.

Green Earths

The minerals responsible for the colour of green earths are types of clay micas, glauconite and celadonite. Also smectite, chlorite, serpentines and pyroxenes can be responsible for this colour. The most famous deposits of green earths can be found near Verona, Italy, as well as in Tyrol, Bohemia, Saxony, Poland, Hungary, France, Cyprus and England. Verona earth is made by celadonite found in basaltic rocks. However, the presence of glauconite cannot be excluded from a green earth pigment because it can be found in sandstone levels as a result of mixing between extrusive tertiary products with Eocene sediments (Aliatis et al. [496]). Celadonite and glauconite are minerals with a complex chemical structure, with large variations in composition, crystalline order and morphology. In particular, celadonite $K(Al,Fe^{3+})(Fe^{2+},Mg)(AlSi_3,Si_4)O_{10}(OH)_2$ presents a crystalline structure with a blue nuance whereas glauconite $(K,Na)(Fe^{3+},Al,Mg)_2(Si,Al)_4O_{10}(OH)_2$ has a structure less crystalline than celadonite and its colour is characterised by a yellow component, according to the Fe oxidation state (see Moretto et al. [497]). The similarity in the structure and composition of glauconite and celadonite makes the analytical distinction difficult (Genestar and Pons [498]). Sodium is present just in glauconite, characteristic that could, in principle, be exploited for its identification.

In a detailed Raman study of Byzantine overpainted icons of the 16th c., Daniilia et al. [499] identified green earth but the actual mineral was not specified. Goodall et al. [500], investigating the multiple layered wall paintings from the Rosalila temple, Copan, Honduras, identified the green pigment as a celadonite-based green earth. Ospitali et al. [501] compared the Raman spectra of green earths from commercial sources and from some fragments of Roman frescoes from two archaeological sites in central Italy at Suasa (Ancona) and Pisaurum (Pesaro-Urbino). They showed that the Raman peaks in the range 260–280 cm^{-1} are helpful to discriminate between celadonite (272–279 cm^{-1}) and glauconite (263–266 cm^{-1}). Green coloured samples on wall paintings and green powder from a pigment pot found in Pompeii area were investigated by Aliatis et al. [496]: here the mineralogical identification of the green earths was attempted through the comparison of the vibrational features which, in the low wavenumber region, help in discriminating between the two species. The more ordered structure of celadonite gives sharper features than those of glauconite. The green earth found in the Pompeii wall paintings fragments shows Raman spectra compatible with celadonite, even if the presence of glauconite cannot be excluded.

Cristini et al. [502] studied the alterations of green earths from wall paintings in three different European sites (France, Rome and Greece) of the Roman Empire, dated in the 1st and 2nd c. AD. Samples from mural paintings from archaeological sites from North-East of Italy were investigated by Moretto et al. [497] by a multitechnique approach, by comparison with celadonite and glauconite standards. Interpretative uncertainties, however, excluded FT-Raman technique as a source of reliable information when celadonite and glauconite are mixed. The green pigments in Roman mural paintings, from the Patio de Banderas excavation in Seville Alcazar, explored by Perez Rodriguez et al. [503], showed a complex situation: celadonite and glauconite are found, mixed together and with Egyptian Blue and Egyptian green. Chlorite and chromium oxide could also be responsible for the green colour.

Gebremariam et al. [504] analysed wall paintings from the Petros and Paulos Church in Ethiopia. Talc, a chlorite mineral and dolomite were identified as the main components of the preparatory layer. Green earth like glauconite or clinochlore were suggested for the green colours. Pelosi et al. [505], in a study on the wall paintings on the rock-hewn Church of the Forty Martyrs at Şahinefendi in Cappadocia (Turkey), detected green earths showing a Raman spectrum similar to that of celadonite (Ospitali et al. [501]).

Copper based pigments or degradation products?

The copper secondary minerals sulphates, chlorides, arsenates, carbonates are ubiquitous in the Raman spectra taken on green painted artworks. These “pigments“ could be alteration products of a copper mineral such as malachite, azurite or of Verdigris but also original pigments derived from a natural mineral or artificial products of corrosion of brass or another copper alloy in acid conditions. The Raman investigations on these green mineral pigments faces usually with (Scott [506]): copper trihydroxychlorides (found as atacamite, paratacamite, clinoatacamite, and botallackite polymorphs), copper sulphates (brochantite, posnjajite, antlerite), copper arsenates (conichalcite, cornwallite, olivenite), copper/zinc carbonates (aurichalcite, rosasite).

Atacamite $Cu_2Cl(OH)_3$ is a rare mineral that forms as alteration product of copper minerals in arid climates. This compound has been commonly identified as a degradation product of copper pigments or of metallic objects containing copper, but it is considered often as an intentional pigment. Atacamite as a pigment seems mentioned in old treatises such as the De Diversis Artibus from the monk Theophilus [507] but there is yet no agreement on the use of copper chlorides as raw materials. Gilbert et al. [508] performed a detailed Raman investigation of green copper pigments in illuminated manuscripts (15th and 16th centuries from north-Europe and Italy) identifying several similar phases and in particular posnjakite $CuSO_4 \cdot 3Cu(OH)_2 \cdot H_2O$ as pigments. A careful investigation on mineral greens of a decorative wallpaper and the detection of antlerite is described by Castro et al. [509]. A discrimination between copper trihydroxychlorides is reported by Bertolotti et al. [510]. Eremin et al. [511] in the Japanese masterpiece The Tale of Genji, an album with 54 illustrations, found the hydrated copper chlorides, atacamite and botallackite, maybe alteration products of original malachite and chrysocolla, a natural copper silicate.

Lepot et al. [344] in a study of mural paintings of the Tournai Cathedral (Belgium) identified atacamite and posnjakite as pigments (intentionally used and not due to degradation processes). Bidaud et al. [512]

identified clinoatacamite as a pigment by SEM-EDS and XRD in the 13th c. wall painting in the city castle in Krems, Lower Austria. Castro et al. [509] studied a bleu coloured map from the 17th c. and discussed about the presence of atacamite as pigment or as a degradation product: a molar relationship between copper and chlorine (1:1) suggested atacamite as a raw material.

The use of atacamite as a green pigment seems not only limited to mural paintings. Through micro-Raman spectroscopy, Burgio et al. [513] and Muralha et al. [248] identified the pigments in Islamic religion manuscripts of the 16th-18th c., held at the Victoria and Albert Museum, and explicitly mentioned atacamite as an intentional pigment.

Campos-Sunol et al. [514], on a polychromy on an exterior sculpted stone, identified a green pigment based on copper chlorides. Wei et al. [515] found atacamite in the wall paintings of a Ming Dinasty Dazhao Temple in Hohhot, Inner Mongolia of China. Tomasini et al. [516] recognized atacamite as a natural pigment in a South American colonial polychrome sculpture from the late 16th c. On mural paintings of Ala di Stura (Piedmont, Italy), Aceto et al. [395] evidenced the degradation of azurite to copper oxychlorides (atacamite or paratacamite) and reported green colours obtained by green earths (celadonite) and arsenic-containing green pigments (probably a misture of olivenite $Cu_2(AsO_4)(OH)$, cornwallite $Cu_5(AsO_4)_2(OH)_4$ or conichalcite $CaCu(AsO_4)(OH)$ (Fig.11).

FIGURE 11.

Yong [517] proposed, by the analysis of pigments in the Forbidden City (Beijing) and some architectural pigments in Gansu, Northwest China, that the most popular green pigment for wall painting and architecture might be copper trihydroxychloride, rather than malachite, in the period from North Dynasty (386–581 CE) until late Qing Dynasty (1840–1911 CE). A mixed use of malachite and atacamite has been revealed in three green samples of a sculptural polychromy in the Zhongshan Grottoes, China, by Cauzzi et al. [518] : a synthetic origin of the copper compounds is proposed by their optical characteristics. Egel and Simon [519], in an investigation of the painting materials in Zhongshan Grottoes (Shaanxi, China) identified in a green paint layer the mineral botallackite as an intentional pigments. A botallackite pigment was proposed also by Hu et al. [520], studying the painting techniques and materials of the murals in the Five Northern Provinces Assembly Hall, Ziyang, China.

Dominguez-Vidal et al. [521], investigating the decorated plasterwork on the stalactite vaults of the Hall of the Kings in the Alhambra (Granada, Spain), evidenced azurite severely degraded to clinoatacamite. Švarcová et al. [522] attempted to differentiate copper pigments in paint layers of works of art by Raman spectroscopy in spite of the large fluorescence. Buzgar et al. [482] reported a series of copper compounds (pigments) in the wall paintings of the Voronet Monastery in Romania (16th c.), including atacamite, posnjakite and conichalcite ($CaCu(AsO_4)(OH)$).

Valadas et al. [523] reported an intentional use of brochantite on 16th c. Portuguese-Flemish paintings attributed to the Master Frei Carlos workshop. Zhang et al. [524] identified atacamite as green pigment in the murals and sculptures in Mogao Grottoes. Wall paintings of Ottoman Fatih Mosque in Istanbul (reconstructed in 1770 and then restored) were studied by Akyuz et al. [525]. For the green colours they found a mixture of celadonite and glauconite, as both celadonite (277 cm^{-1}) and glauconite (265 cm^{-1}) peaks were identified in the Raman spectrum. They suggest also the intentional use of brochantite {$CuSO_4.3Cu(OH)_2$} as pigment.

Aliatis et al. [526] revealed the presence of copper arsenates in a green pigment found in a bowl during Pompei excavations, whereas Baraldi et al. [527] identified agardite, a group of hydrous hydrated arsenates of rare earth elements and copper, in fragments of a fresco painting from San Francesco Basilica, Assisi. Zeng et al. [528] identified as cornwallite $Cu_5(AsO_4)_2(OH)_4 \cdot (H2O)$, and not as a synthetic green pigment, a copper arsenate on the shrine of Kaiping Diaolou (China, 20th c.).

Aurichalcite $(Zn,Cu)_5(CO_3)_2(OH)_6$ is reported as a green pigment by Klisińska-Kopacz [529] in a study on a 17th c. painted silk banner. Rosasite $(Cu,Zn)_2(CO_3)(OH)_2$ has never been reported as pigment, but its discovery in the Darhib Mine, Egypt (Gatto Rotondo et al. [530]) is a good sign that soon it will appear in an artwork, perhaps Egyptian !

Yellow pigments

Jarosite

Jarosite, an iron sulphate $XFe_3(SO_4)_2(OH)_6$, where X is usually a monovalent cation such as Na^+ or K^+, is rarely found as a pigment. Jarosite was probably used in close association with natural iron ochre, but it was also possibly chosen due its distinctive hue. Jarosite has been identified in excavated prehistoric pigments by Dachuk et al. [213] and by Ambers [531] in ancient Egyptian paintings. Buzgar et al. [532] investigated fragments of a wall painting in Graeco-Roman contexts from the Beroe fortress, Romania (4^{th}–6^{th} c.) and identified a yellow-brown pigment as K-jarosite $KFe^{3+}{}_3(OH)_6(SO_4)_2$ and/or Na-jarosite. Sepúlveda et al. [533] studied yellow blocks from the archaeological site Playa Miller 7 (PLM7), on the coast of Atacama Desert in northern Chile, and reported the use of K-jarosite and natrojarosite in prehispanic times (approx. 2500 year BP). Pelosi et al. [534], by micro-Raman analysis, revealed the presence of jarosite in wall paintings in Cappadocia (Turkey).

Crocoite – Phoenicochroite - Hemihedrite

Chrome yellow, $PbCrO_4$, was made available commercially at the beginning of the 19^{th} c. Lead chromate $PbCrO_4$ occurs naturally as the reddish mineral crocoite but it is so rare that it is unlikely to find crocoite on an artwork (Edwards et al. [265]). Synthetic chrome orange, Pb_2CrO_5 or $PbCrO_4.PbO$, has its equivalent in nature in the rare mineral phoenicochroite (Correia et al. [268] [267], Monico et al. [535]). Mugnaini et al. 2006 [536] [537] claim the use of crocoite ($PbCrO_4$) as a natural pigment in the 13^{th} c. wall paintings found under the Siena (Italy) Cathedral. They also report chrysocolla, very unusual for European medieval paintings. Hradil et al. [538] identified natural crocoite by Raman micro-spectroscopy in wall paintings dated around 1300 in Kuřívody, Northern Bohemia, and claimed that it was used intentionally as yellow pigment. Abdel-Ghani and Mahmoud [539] reported a Raman study on the pigments on Sabil-Kuttab Umm 'Abbas ceiling, Mohammed Ali Era in Cairo, Egypt, and identified the chromate mineral hemihedrite ($ZnPb_{10}(CrO_4)_6(SiO_4)_2F_2$) claiming that this unusual pigment was detected for the first time as an artistic pigment. This is a very rare mineral. The Raman spectrum reported corresponds however to the spectrum of phoenicochroite or more probably to the corresponding synthetic pigment chrome orange. A modern retouching could be less unusual. Edwards at al [540] in a study of an important English oil painting of the 18^{th} c. identified the hemihedrite mineral, but the reported Raman spectrum fits again well that of phoenicochroite or chrome orange, suggesting a more probable late retouching. Bellini et al. [541] reported accurate Raman spectra of crocoite, phoenicochroite and hemihedrite crystals, including the low-wavenumber region, usually not reported in literature (Fig.12). The Raman spectra of the three cromate crystals have characteristic features that allow a definite identification of the minerals species. This should avoid incorrect identification of exotic chromate species as hemihedrite for chrome orange. The spectrum of chrome orange is reported also by Zmuda-Trzebiatowska et al. [294] from artist palette of J. Matejko (1838–1893).

FIGURE 12.

Ochres (red-yellow)

Raman microscopy has been extensively used to identify the minerals in ochres, discussing the dependence of the Raman spectra on the laser power and wavelength and the particle size effects on the phase transformations. In particular, the identification of magnetite when hematite is present through the Raman peak at about 660 cm^{-1} is still an open question, evoked in many papers on pigments. Ochres are generally divided in two large groups: red ochres (the main pigment is hematite, anhydrous iron oxide) and yellow ochres (characterized by goethite, a hydrous ferric oxide). Ochres always contain silicates. The colour of the ochre is not only determined by the hematite content, but also by other minerals. Grain (or crystal) size may also influence the colour. Specific Raman investigations on the red-yellow ochres include the following contributions: de Faria et al. [542], Bikiaris et al. [543], Bersani et al. [54], de Oliveira et al. [544], Hradil et al. [545], De Faria and Lopes [59], Chernyshova et al. [546], Legodi and de Waal [547], Hradil et al. [548], Palacios et al. [549]. Froment et al. [550] investigated about 50 natural or treated red to yellow ochre pigments and their secondary phases, discussing on possible provenance criteria. Montagner et al. [551] identified ochres

containing kaolinite matrix and/or sulfate matrix from ochres where only iron oxides and/or hydroxides were detected.

Black pigments

Appolonia [552] analysed Mural Paintings in the Aosta Valley (Italy) and found graphite as black pigment rather than wood or lamp carbon, related to the presence of graphite deposits in the region.

Trentelman and Turner [553], in a manuscript dating to the early 1480s of French artist Jean Bourdichon, found bismuth black (granular elemental bismuth) as a pigment (Fig.13). Metallic bismuth in Bourdichon miniatures was found also by Burgio et al. [242]. Trentelman [554] examined bismuth black pigments comparing the spectra of powdered metallic bismuth, Bi_2S_3 and α-Bi_2O_3 under different excitation wavelengths and laser powers.

FIGURE 13.

Centeno et al. [51] studied, by a multi-technique approach, the surface decorations in selected pottery wares from two Prehispanic archaeological sites in Northwestern (NW) Argentina, dating to the Inca period (AD 900–1530): they found iron manganese spinel jacobsite, $(Mn^{2+},Fe^{2+}, Mg)(Fe^{3+},Mn^{3+})_2O_4$, as the main component of the fired black decorations. Buzgar et al. [555] [556] found mainly pyrolusite (MnO_2) and jacobsite in the black pigment in Cucuteni pottery painting (Neolithic Age, Romania). Jacobsite could form by firing, under oxidizing conditions, manganese and iron-rich clay slips. Some suggestions are given about the provenance of the minerals.

Caggiani and Colomban [91] investigated the best experimental conditions for the identification of the black pigments in glazed ceramics (manganese oxides, cobalt oxides, hematite, magnetite and their mixtures).

Tomasini et al. [87] [557] analysed commercial carbon-based black pigments and tried to find Raman spectral parameters discriminating between them. Tomasini et al. [558] identified, by Raman microscopy, black pigments in four 18th c. Jesuit wooden sculptures. It is very difficult do discriminate the source of carbon-based pigments from their very similar Raman spectra. According to the authors, the combined analysis of Raman spectral parameters (width, position and intensity of G and D bands) allows the identification of bistre, wood charcoal lampblack, and a humic earth pigment. Coccato et al. [89] discuss the carbon Raman signatures of many carbon based pigments, attempting to give some hints for their identification.

Black earths are natural dark earth pigments of varying composition. There are varieties composed of coal, manganese black, stibnite, bismuth, galena and tin-rich bronze powder (Spring et al. [559], Cavallo and Gianoli Barioni [560]). Despite of the historical evidences attesting the use of black earths as painting materials in both a fresco and a secco techniques, there is very little analytical proof of their use as painting material on architectural surfaces and no specific Raman investigation has been reported.

Tomasini et al. [561] identified pyroxene minerals used as black pigments in painted human bones excavated in Northern Patagonia. On the skeleton of a male painted with parallel lines alternating red and black colours, excavated in a secondary burial context in the site of Cima de los Huesos, in the San Matías Gulf (Río Negro, Argentina), Raman and XDR show hematite in the red pigment and ferrosilite ($FeSiO_3$) and enstatite ($MgSiO_3$) pyroxenes along with kanoite ($MnMgSi_2O_6$) for the black colour.

Ay et al. [562] reported on the black pigment material excavated at the cemetery in Müslümantepe, located in Upper Tigris, and dating to the Early Bronze Age. It was most likely used for cosmetic purposes: the major component was found to be pyrolusite, together with calcite and quartz.

Iron oxide minerals and/or structurally disordered graphite consistent with a charred vegetable substance were found by Raman microscopy by van der Weerd [47] as black pigments on prehistoric Southwest American potsherds of the Ancestral Puebloan period.

Darkening and photo-degradation

Cinnabar

Colour degradation of paintworks induced by the action of light is an important issue and attracts the attention of spectroscopysts. The light-induced darkening of vermilion (red mercury (II) sulfide α-HgS, mineral cinnabar in nature) involves historical museum paintings and murals at archaelogical sites worldwide (Noller et al. [563]). Chlorine plays a dominant role in the darkening process of α–HgS, but the exact mechanism is not yet completely clear (Radepont et al. [564], Cotte et al. [565]). The occurrence of secondary compounds ($Hg_3S_2Cl_2$ polymorphs, Hg_2Cl_2 and $HgCl_2$) during the transformation of vermilion is confirmed by X-ray spectroscopy (Hogan and da Pieve [566]).

Lead white and red lead

The darkening of lead-containing pigments, namely red lead and lead white, is a widespread phenomenon in artworks: the degradation products are usually identified (or proposed) as plattnerite (lead (IV) oxide, PbO_2) or galena (lead (II) sulphide, PbS). The "natural" degradation of white lead has been largely investigated by Raman (see for a review, Lussier and Smith [567]) attempting to discriminate between lead(II) sulfide (galena, PbS), plattnerite (PbO_2), or metallic lead (Pb^0).

Burgio et al.[568] and Smith et al. [569] pointed out the problem of laser-induced degradation of lead pigments (lead white and red lead) in art conservation studies. Raman spectroscopy of black degradation products is difficult as dark materials absorb both incident and Raman-scattered light. This strong absorption can induce thermal or photo-oxidative transformation and in the past wrong identifications have been reported. The Raman spectrum from weathered and blackened lead white on the surface of a manuscript at low laser excitation was taken by Smith and Clark [570]. The direct identification by Raman microscopy of PbS as a degradation product of lead white on manuscripts was erroneous as both the samples and the reference were photodegraded to a sulphate species (Clark and Gibbs [571] [572], Burgio et al. [573]). Red lead transforms into plattnerite (β-PbO_2) and also in anglesite $PbSO_4$: the alteration process is controlled by environmental parameters.

The identification of plattnerite is not an easy task (Andalò [574]). Orthorhombic PbO (lead II oxide massicot) is easily photogenerated, presumabily through the sequence plattnerite (PbO_2) → minium (Pb_3O_4) → litharge (tetragonal PbO) → massicot (orthorhombic PbO) and PbO_2 escapes observation (Smith et al. [569], Burgio et al. [568]). Daniilia et al. [575] [576] in a study of wall paintings at the Cypriot Monastery of Christ Antiphonitis reported a detailed identification of pigments. The degradation of red lead from orange Pb_3O_4 to black plattnerite PbO_2 is confirmed by its Raman spectrum. The chromatic alterations (blackening) of lead pigments (red lead and white read) have extensively been investigated by Raman spectroscopy (Aze [577] and Aze et al. [350], Rosado et al. [578]). De Santis et al. [323], investigating fragments of the painted terracotta by Michele Todini, identified indirectly PbO_2 as a black degradation of lead white through its laser degradation to PbO. The degradation of St. Euthymius byzantine wall paintings, in the Cathedral of Thessaloniki, was studied by Sotiropoulou et al. [579]: black tenorite CuO was found as a degradation product of azurite, evidenced by the darkening of the blue shades on the Virgin's mantlet. The alteration of orange minium (Pb_3O_4) gives no plattnerite evidence in the Raman spectrum.

Kotulanová et al. [580] analysed in laboratory the interactions of lead-based pigments (lead white, massicot, red lead) with a number of inorganic salts, degradation agents of wall paintings, and identified $PbMg(CO_3)_2$ in the degradation products. The results should help in the understanding of the degradation of lead white (hydrocerussite) and red lead (minium). On 11th c. frescoes from the church of Saint George in Kostoľany pod Tribečom, the oldest preserved wall paintings in Slovakia, they found plattnerite by XRD, confirming the red lead degradation.

On several samples from mural paintings of Ala di Stura (Piedmont, Italy), Aceto et al. [395] explored the chromatic alteration phenomena of lead pigments. The conversion of lead white $PbCO_3.Pb(OH)_2$ to galena was not observed but they evidenced the conversion of red lead to plattnerite. The formation of PbO_2 from white lead seems to be much more frequent than formation of lead sulfide. The possibility of lead white blackening through Bacteria capable of converting lead white into PbO_2 has been proposed by Petushkova and Lyalikova [581]. Recently, a diffuse presence of plattnerite but not of sulphur bearing compounds was found by Costantini et al. [582]. The study was accomplished on degraded areas originally containing white lead, in a fresco of the castle chapel of St. Stephen in Morter, Italy, called the Sistine Chapel of Val Venosta.

The hypothesis of a lead white blackening through microbiological processes cannot in this case be discarded. The plattnerite spectrum is reported by Costantini et al. [582] up to low Raman wavenumbers. Gutman et al. [583] characterized the pigments in the newly discovered wall painting at the Dominican Monastery in Ptuj (Slovenia) and reported the darkening of the red lead areas into a black or brown plattnerite. The reported "characteristic" Raman band of plattnerite at 521 cm^{-1}, is however too sharp (it is like a pure silicon spectrum !) and does not correspond to any published or reported plattnerite Raman spectrum (Burgio et al. [568], Costantini et al. [582]). A peculiar result was found by Miguel et al. [584] studying the mechanisms of degradation in a medieval Portuguese codex, the Lorvao Apocalypse (1189), by Raman microscopy and micro-X-ray diffraction: the degradation of red lead was attributed to its reaction with orpiment, a lead arsenate compound being the main degradation product.

Inorganic pigments used in three 17th c. hand-coloured maps of Dutch manufacture, two of Portugal and one of the Iberian Peninsula, were studied by Mendes et al. [585]. A "mineral" was found in all the green areas: a copper oxalate, moolooite ($Cu(C_2O_4).nH_2O$ (n<1), presumably a product of the degradation of Verdigris (Fig.14).

FIGURE 14.

Realgar, pararealgar and orpiment

Brightly coloured arsenic-sulphide minerals (realgar As_4S_4, pararealgar and orpiment As_2S_3) ranging from red to orange or yellow have been largely used as pigments. They have been found, on Ancient Egyptian funerary papyri, medieval illuminated manuscripts and Greek icons. Orpiment and realgar are well known for their instability over time and their tendency to be altered by light. Realgar exposed to light degrades first to an orange product (χ-realgar), then to deep yellow pararealgar. The product of complete photodegradation is arsenolite (As_2O_3) which is also the product of the fading of orpiment: the final appearance of the fading of both pigments is colourless or white. The various phases/polymorphs of arsenic sulphides (orange-red natural realgar α-AsS (or α–As_4S_4), the high temperature form β-AsS, now found as mineral bonazziite, the intermediate χ-phase, the yellow- orange light-induced polymorph pararealgar, the yellow orpiment As_2S_3) and their complex photoinduced transformations have been studied by Raman spectroscopy over a period of more than 40 years (see for example, Bonazzi et al. [586] and Bindi et al. [587]). All phases, but β-AsS, have been identified in works of art using Raman spectroscopy (Trentelmann et al. [588], Clark and Gibbs [571], Vandenabeele et al. [589], Edwards et al. [590], David et al. [591], Burgio et al. [592], Vandenabeele and Moens [593], Mazzeo et al. [349], Daniels and Leach [594], Burgio et al. [595], Burgio et al. [513], Murahla et al. [248], Tanevska et al.[255]). It is possible that pararealgar was prepared and used as a pigment. The effect of different light sources on the realgar photo-degradation was investigated by Raman spectroscopy by Macchia et al. [596]. The complex light induced transformations of realgar are discussed in a recent paper by Pratesi and Zoppi [597].

Orpiment, toxic yellow arsenic sulfide mineral, was revealed by Ogalde et al. [598] in an archaeological context from Chorrillos cemetery (Calama, Chile) dating 8th-2nd c. BC. The pigment sample was found in a mollusk shell that was part of the grave goods associated with a female individual. Orpiment was detected also in a 9th c. manuscritpt by Aceto et al. [233], by Campos-Sunol [599] in the portal of a church of the 16th c., in a medieval manuscript by Miguel et al. [584]. El Bakkali [600], in a study of coloring materials in ancient Moroccan Islamic manuscripts, found a mix of orpiment and indigo to produce shades of green (vergaut), a procedure employed in the Islamic world in the 14th c. Vergaut was also hypothesized by Bioletti at al [234] in "The Book of Kells", Trinity College Dublin MS 58, and by Aceto et al. [246] in Byzantine 6th c. manuscripts. Recently, Vermeulen et al. [601] identified an amorphous arsenic sulfide glass (As_xS_x), synthesized from arsenic trioxide and sulfur, in the interior decorations of the Japanese tower in Laeken, Brussels, Belgium. Artificial arsenic sulphide pigments which were identified in artworks have been explored by Grundmann and Richter [602], Grundmann et al. [603], Grundmann and Richter [604].

Unusual mineral pigments

Holakooei and Karimy [605] examined early Islamic pigments used at the Masjid-i Jame of Fahraj, central Iran. They identified a black paint mainly composed of black plattnerite mixed with mimetite $Pb_5(AsO_4)_3Cl$,

hemimorphite $Zn_4(OH)_2Si_2O.7H_2O$ and galena and supposed that black plattnerite was most probably used as a pigment and not formed as a degradation product of lead-based pigments. A cave at about 35 km could have supplied the mineral. More investigations seem however necessary to confirm the intentional use of plattnerite as a pigment.

The white pigment (Melian-earth) of the famous painter Appeles was attributed to a TiO_2 rich Kaolin by Katsaros et al. [606] even if, for a misprinting, the Raman spectrum they reported suggests rutile and not anatase.

Naturally irradiated violet fluorite, called antozonite, is a rare historic pigment. The irradiation is caused by uranium or thorium-rich minerals coexisting with fluorite in certain geological settings. Purple-violet fluorite has been identified on a small number of panel paintings, polychrome wooden sculptures, wall paintings and architectural polychromy of the 1450 to 1520 period in central Europe (Richter et al. [607], Srein [608], Chlumska et al. [609]). The fluorite was probably mined from the area of Wölsendorf in Bavaria. The first Raman spectroscopy identification of violet fluorite pigment was reported by Banerjee et al. [610] in the polychrome colour layers of a sculpture dated the end of the 15th c. Dáňová et al. [611], in a Raman study of the late Gothic polychromy of the Nativity Relief from The Corona Sanctae Mariae Monastery in Třebařov, Moravia, reported the use of purple fluorite in the under-painting beneath the strong azurite layer on the reverse of the cloak of the Virgin Mary.

Two samples of purple fluorite from an altarpiece of the Triptych with St. James the Lesser and St. Philip (dated 1497) located in the chapel of St. Wenceslas and Ladislaus in Italian Court, Kutná Hora, Czech Republic, was compared with sixteen samples of mineral antozonite by Čermáková [612] using five different Raman excitation wavelengths (Fig.15).

FIGURE 15.

Aceto et al. [395] suggested the use of skutterudite $(Co,Ni)_xAs_{3-x}$ as a mineral source for cobalt, to be used for the production of smalt, found in wall paintings in val di Stura, Piedmont, Italy. Skutterudite could have been excavated from Punta Corna mine, in the nearby valley of Viù.

The pigments used in pre-17th c. wall paintings of the Masjid-i Jame of Abarqu, central Iran, were identified by Holakooei and Karimy [613]: atacamite, red lead and smalt for green, red and blue, respectively, mixed with natural ultramarine blue and applied on a white substrate composed of huntite $CaMg_3(CO_3)_4$, reported for the first time in Persian mural paintings, but well known to the Egyptians. Raman spectra seem to indicate glushinskite, a magnesium oxalate $(MgC_2O_4).2H_2O$), identified as a degradation product of the white huntite. In addition, they emphasized not only the use of atacamite as pigment but also claimed that the mineral woodhouseite $(CaAl_3(PO_4,SO_4)_2(OH)_6)$ could be used as a pigment. Glushinskite was reported as a possible white pigment in the paintings of the Church of San Fiorenzo in Bastia Mondovì, Piedmont, Italy by Chiari and Scott [614].

CONCLUSIONS

This work aims to be a review of the most recent contributions of the Raman spectroscopy to the study of minerals and mineral pigments of relevance in Archaeometry and more generally for Cultural Heritage. About six hundred references, mainly in the last decade, demonstrate the large and increasing interest of the scientific community, especially from new geographical areas. In many fields as gemmology or pigments identification, Raman spectroscopy has become a standard technique. A routine use of the Raman technique, however, exacerbated by the spread of "portable" Raman equipments, must be accompanied by the use of the skills and knowledge of physics, chemistry and mineralogy. Works carried out only on the basis of automated Raman databases, without careful comparison with literature and without suitable knowledge of the materials, could lead to wrong identifications, especially when attempting to identify rare or strange phases. Actually, a surprising high number of rare crystalline phases are found in different kind of art and archaeological objects, even if in some cases their presence should be considerend as accidental. Many recent works are pointing the attention on the large amount of data which is possible to harvest in a

short time when analysing museum objects with portable instruments. On the other hand, works carried out with high resolution laboratory spectrometer are showing how it is possible to deepen the knowledge of artistic and archaeologic objects using Raman spectroscopy. The detailed study of the mineral phases is receiving a new impulse by the new generation of software based on DFT approach, allowing a very good simulation of the Raman spectra. The Raman data processing is starting to take advantage from chemiometry, even if multivariate analysis is not so diffuse as other analytical techniques and often limited to Raman map analysis.

REFERENCES

[1] J.M. Madariaga, *J. Raman Spectrosc.* **2010**; *41*, 1389.

[2] D. Bersani, J.M. Madariaga, *J. Raman Spectrosc.* **2012**; *43*, 1523.

[3] P. Ropret, J.M. Madariaga, *J. Raman Spectrosc.* **2014**; *45*, 985.

[4] G.D. Smith, R.J.. H. Clark, *J. Archaeol. Sci.* **2004**; *31*, 1137.

[5] D.C. Smith, *Spectrochim. Acta - Part A Mol. Biomol. Spectrosc.* **2005**; *61*, 2299.

[6] D.C. Smith, *Geol. Soc. London, Spec. Publ.* **2006**; *257*, 9.

[7] C. Fotakis, D. Anglos, V. Zafiropulos, S. Georgiou, V. Tornari, Lasers in the Preservation of Cultural Heritage: Principles and Applications, CRC Press - Taylor & Francis, 2006.

[8] P. Vandenabeele, H.G.M. Edwards, L. Moens, *Chem. Rev.* **2007**; *107*, 675.

[9] D. Bersani, P.P. Lottici, *Anal. Bioanal. Chem.* **2010**; *397*, 2631.

[10] R.J.H. Clark, Chem. New Zeal. **2011**; 75, 13.

[11] P. Colomban, *J. Raman Spectrosc.* **2012**; *43*, 1529.

[12] C.C. Ferrón, S.E.J. Villar, F.M. Soto, J.L. Navarrete, V. Hernández, in *The Conservation of Subterranean Cultural Heritage*, Ed. by C. Saiz-Jimenez, CRC Press, Pages 281–292, Taylor and Francis Group, London, **2014**.

[13] P. Vandenabeele, H.G.M. Edwards, J. Jehlička, *Chem. Soc. Rev.* **2014**; *43*, 2628.

[14] J.M. Madariaga, *Anal. Methods* **2015**; *7*, 4848.

[15] N. Buzgar, G. Bodi, A. Buzatu, A. Ionu, **2013**; *59*, 41.

[16] B. Wopenka, R. Popelka, J.D. Pasteris, S. Rotroff, *Appl. Spectrosc.* **2002**; *56*, 1320.

[17] J. Zuo, C. Xu, C. Wang, Z. Yushi, *J. Raman Spectrosc.* **1999**; *30*, 1053.

[18] M. Sendova, V. Zhelyaskov, M. Scalera, M. Ramsey, *J. Raman Spectrosc.* **2005**; *36*, 829.

[19] R. Alaimo, G. Bultrini, I. Eragalà, R. Giarrusso, I. Iliopoulos, G. Montana, *Appl. Phys. A Mater. Sci. Process.* **2004**; *79*, 221.

[20] I. Cianchetta, J. Maish, D. Saunders, M. Walton, A. Mehta, B. Foran, K. Trentelman, *J. Raman Spectrosc.* **2015**; 46, 996.

[21] L. Medeghini, S. Mignardi, C. De Vito, D. Bersani, P.P. Lottici, M. Turetta, M. Sala, L. Nigro, *Anal. Methods* **2013**; *5*, 6622.

[22] G. Simsek, P. Colomban, S. Wong, B. Zhao, A. Rougeulle, N.Q. Liem, *J. Cult. Herit.* **2015**; *16*, 159.

[23] C. Ricci, I. Borgia, B.G. Brunetti, A. Sgamellotti, B. Fabbri, M.C. Burla, G. Polidori, *Archaeometry* **2005**; *47*, 557.

[24] M. A. Legodi, D. de Waal, *Spectrochim. Acta - Part A Mol. Biomol. Spectrosc.* **2007**; *66*, 135.

[25] D. Bersani, P.P. Lottici, S. Virgenti, A. Sodo, G. Malvestuto, A. Botti, E. Salvioli-Mariani, M. Tribaudino, F. Ospitali, M. Catarsi, *J. Raman Spectrosc.* **2010**; *41*, 1556.

[26] M.J. Ayora-Cañada, A. Domínguez-Arranz, A. Dominguez-Vidal, *J. Raman Spectrosc.* **2012**; *43*, 317.

[27] S. Akyuz, T. Akyuz, S. Basaran, C. Bolcal, A. Gulec, *Vib. Spectrosc.* **2008**; *48*, 276.

[28] P. Comodi, M. Bernardi, A. Bentivoglio, G.D. Gatta, P.F. Zanazzi, *Archaeometry* **2004**; *3*, 405.

[29] P. Colomban, G. Sagon, X. Faurel, *J. Raman Spectrosc.* **2001**; *32*, 351.

[30] D. Tenorio, M.G. Almazán-Torres, F. Monroy-Guzmán, N.L. Rodríguez-García, L.C. Longoria, *J. Radioanal. Nucl. Chem.* **2005**; *266*, 471.

[31] L. Medeghini, S. Mignardi, C. De Vito, D. Bersani, P.P. Lottici, M. Turetta, J. Costantini, E. Bacchini, M. Sala, L. Nigro, *Eur. J. Mineral.* **2013**; *25*, 881.

[32] L. Medeghini, P.P. Lottici, C. De Vito, S. Mignardi, D. Bersani, *J. Raman Spectrosc.* **2014**; *45*, 1244.

[33] C. Lofrumento, A. Zoppi, E.M. Castellucci, *J. Raman Spectrosc.* **2004**; *35*, 650.

[34] J. Striova, C. Lofrumento, A. Zoppi, E.M. Castellucci, *J. Raman Spectrosc.* **2006**; *37*, 1139.

[35] P. Ballirano, C. De Vito, L. Medeghini, S. Mignardi, V. Ferrini, P. Matthiae, D. Bersani, P.P. Lottici, *Ceram. Int.* **2014**; *40*, 16409.

[36] A. Raškovska, B. Minčeva-Šukarova, O. Grupče, P. Colomban, *J. Raman Spectrosc.* **2010**; *41*, 431.

[37] S. Kiruba, S. Ganesan, *Spectrochim. Acta - Part A Mol. Biomol. Spectrosc.* **2015**; *145*, 594.

[38] P. Ricciardi, P. Colomban, B. Fabbri, V. Milande, *E-Preservation Sci.* **2009**; *6*, 22.

[39] V. Tanevska, P. Colomban, B. Minčeva-Šukarova, O. Grupče, *J. Raman Spectrosc.* **2009**; *40*, 1240.

[40] E. Cantisani, M. Cavalieri, C. Lofrumento, E. Pecchioni, M. Ricci, *Archaeol. Anthropol. Sci.* **2012**; *4*, 29.

[41] C. De Vito, L. Medeghini, S. Mignardi, D. Orlandi, L. Nigro, F. Spagnoli, P.P. Lottici, D. Bersani, *Appl. Clay Sci.* **2014**; *88-89*, 202.

[42] P. Colomban, *Arts* **2013**; *2*, 77.

[43] P. Sciau, P. Goudeau, *Eur. Phys. J. B* **2015**; *88*, 132.

[44] A. Issi, A. Kara, A.O. Alp, *Ceram. Int.* **2011**; *37*, 2575.

[45] S. Akyuz, T. Akyuz, S. Basaran, C. Bolcal, A. Gulec, *J. Mol. Struct.* **2007**; *834-836*, 150.

[46] S. Cîntă Pînzaru, D. Pop, L. Nemeth, *Stud. Univ. Babes-Bolyai, Geol.* **2008**; *53*, 31.

[47] J. van der Weerd, G.D. Smith, S. Firth, R.J.H. Clark, *J. Archaeol. Sci.* **2004**; *31*, 1429.

[48] A.S. Cavalheri, A. M.O.A. Balan, R. Künzli, C.J.L. Constantino, *Vib. Spectrosc.* **2010**; *54*, 164.

[49] I.M. Catalano, A. Genga, C. Laganara, R. Laviano, a. Mangone, D. Marano, a. Traini, *J. Archaeol. Sci.* **2007**; *34*, 503.

[50] F. Rosi, V. Manuali, C. Miliani, B.G. Brunetti, A. Sgamellotti, T. Grygar, D. Hradil, *J. Raman Spectrosc.* **2009**; *40*, 107.

[51] S.A. Centeno, V.I. Williams, N.C. Little, R.J. Speakman, *Vib. Spectrosc.* **2012**; *58*, 119.

[52] J.M. Pérez, R. Esteve-Tébar, *Archaeometry* **2004**; *46*, 607.

[53] L. Wang, J. Zhu, Y. Yan, Y. Xie, C. Wang, *J. Raman Spectrosc.* **2009**; *40*, 998.

[54] D. Bersani, P.P. Lottici, A. Montenero, *J. Raman Spectrosc.* **1999**; *30*, 355.

[55] Y.S. Liou, Y. Chang Liu, H.Y. Huang, *J. Raman Spectrosc.* **2011**; *42*, 1062.

[56] D. Bersani, P.P. Lottici, A. Montenero, *J. Mater. Sci.* **2000**; *35*, 4301.

[57] M. Olivares, M.C. Zuluaga, L. A. Ortega, X. Murelaga, A. Alonso-Olazabal, M. Urteaga, L. Amundaray, I. Alonso-Martin, N. Etxebarria, *J. Raman Spectrosc.* **2010**; *41*, 1543.

[58] K.F. McCarty, D.R. Boehme, *J. Solid State Chem.* **1989**; *79*, 19.

[59] D.L.A. de Faria, F.N. Lopes, *Vib. Spectrosc.* **2007**; *45*, 117.

[60] I. Chourpa, L. Douziech-Eyrolles, L. Ngaboni-Okassa, J.-F. Fouquenet, S. Cohen-Jonathan, M. Souce, H. Marchais, P. Dubois, *Analyst* **2005**; *130*, 1395.

[61] P. Colomban, R. De Laveaucoupet, V. Milande, *J. Raman Spectrosc.* **2005**; *36*, 857.

[62] G. Simsek, P. Colomban, V. Milande, *J. Raman Spectrosc.* **2010**; *41*, 529.

[63] A.P. Middleton, H.G.M. Edwards, P.S. Middleton, J. Ambers, *J. Raman Spectrosc.* **2005**; *36*, 984.

[64] R.J.H. Clark, Q. Wang, A. Correia, *J. Archaeol. Sci.* **2007**; *34*, 1787.

[65] F.C. Gennari, D.M. Pasquevich, *J. Am. Ceram. Soc.* **1999**; *82*, 1915.

[66] D. Bersani, G. Antonioli, P.P. Lottici, T. Lopez, *J. Non. Cryst. Solids* **1998**; *232-234*, 175.

[67] I. Krivtsov, M. Ilkaeva, V. Avdin, Z. Amghouz, S.A. Khainakov, J.R. Garcia, E. Diaz, S. Ordonez, *RSC Adv.* **2015**; *5*, 36634.

[68] L.C. Prinsloo, **2009**; available at: http://repository.up.ac.za/handle/2263/24936.

[69] W.H. Jay, J.D. Cashion, B. Blenkinship, *J. Raman Spectrosc.* **2015**; doi: 10.1002/jrs.4750

[70] E. Murad, *Clays Clay Miner.* **2003**; *51*, 689.

[71] A. Di Paola, M. Bellardita, L. Palmisano, *Catalysts* **2013**; *3*, 36.

[72] S. Shoval, E. Yadin, G. Panczer, *J. Therm. Anal. Calorim.* **2015**; 104, 515.

[73] J.Z. W. A. Deer, R. A. Howie, An Introduction to Rock-Forming Minerals, 2nd Ed., The Geological Society, Bath, 2001.

[74] R.F. Geller, A.S. Creamer, *J. Am. Ceram. Soc.* **1931**; *14*, 30.

[75] V. Bendel, B.C. Schmidt, *Eur. J. Mineral.* **2008**; *20*, 1055.

[76] J.J. Freeman, A. Wang, K.E. Kuebler, B.L. Jolliff, L. A. Haskin, *Can. Mineral.* **2008**; *46*, 1477.

[77] B. Minčeva-Šukarova, A. Issi, A. Raškovska, O. Grupče, V. Tanevska, M. Yaygingöl, A. Kara, P. Colomban, *J. Raman Spectrosc.* **2012**; *43*, 792.

[78] J. V. Smith, Feldspar Minerals I, Springer-Verlag, Heidelberg, 1974.

[79] P.H. Ribbe, Feldspar Mineral. (Reviews Mineral. 2), Mineralogical Society of America, Washington, 1983.

[80] J. V. Smith, W.L. Brown, Feldspar Minerals. 1. Crystal Structures, Physical, Chemical and Microtextural Properties, Springer-Verlag, Berlin, 1988.

[81] P. Colomban, F. Treppoz, *J. Raman Spectrosc.* **2001**; *32*, 93.

[82] P.J. Jin, Z.Q. Yao, M.L. Zhang, Y.H. Li, H.P. Xing, *J. Raman Spectrosc.* **2010**; *41*, 222.

[83] P. Colomban, *J. Raman Spectrosc.* **2003**; *34*, 420.

[84] M.C. Caggiani, N. Ditaranto, M.R. Guascito, P. Acquafredda, R. Laviano, L.C. Giannossa, S. Mutino, A. Mangone, *X-Ray Spectrom.* **2015**; *44*, 191.

[85] M.C. Caggiani, P. Acquafredda, P. Colomban, A. Mangone, *J. Raman Spectrosc.* **2014**; *45*, 1251.

[86] G. Barone, D. Bersani, V. Crupi, F. Longo, U. Longobardo, P.P. Lottici, I. Aliatis, D. Majolino, P. Mazzoleni, S. Raneri, V. Venuti, *J. Raman Spectrosc.* **2014**; *45*, 1309.

[87] E.P. Tomasini, E.B. Halac, M. Reinoso, E.J. Di Liscia, M.S. Maier, *J. Raman Spectrosc.* **2012**; *43*, 1671.

[88] T. Jawhari, A. Roid, J. Casado, *Carbon N. Y.* **1995**; *33*, 1561.

[89] A. Coccato, J. Jehlicka, L. Moens, P. Vandenabeele, *J. Raman Spectrosc.* **2015**; 46, 1003.

[90] D. Parras, P. Vandenabeele, A. Sanchez, M. Montejo, L. Moens, N. Ramos, *J. Raman Spectrosc.* **2010**; *41*, 68.

[91] M.C. Caggiani, P. Colomban, *J. Raman Spectrosc.* **2011**; *42*, 839.

[92] P. Colomban, *J. Cult. Herit.* **2008**; *9*, e55.

[93] P. Colomban, V. Milande, *J. Raman Spectrosc.* **2006**; *37*, 606.

[94] P. Colomban, *Appl. Phys. A Mater. Sci. Process.* **2004**; *79*, 167.

[95] P. Colomban, *J. Non. Cryst. Solids* **2003**; *323*, 180.

[96] P. Colomban, M.P. Etcheverry, M. Asquier, M. Bounichou, A. Tournié, *J. Raman Spectrosc.* **2006**; *37*, 614.

[97] P. Colomban, A. Tournie, L. Bellot-Gurlet, *J. Raman Spectrosc.* **2006**; *37*, 841.

[98] P. Colomban, O. Paulsen, *J. Am. Ceram. Soc.* **2005**; *88*, 390.

[99] P. Colomban, *Eur. J. Mineral.* **2014**; *25*, 863.

[100] J. Miao, B. Yang D. Mu, *Archaeometry* **2010**; *52*, 146.

[101] B. Kirmizi, E.H. Göktürk, P. Colomban, *Archaeometry* **2015**; *57*, 476.

[102] L.F. Vieira Ferreira, D.S. Conceição, D.P. Ferreira, L.F. Santos, T.M. Casimiro, I. Ferreira Machado, *J. Raman Spectrosc.* **2014**; *45*, 838.

[103] L.F. Vieira Ferreira, D.P. Ferreira, D.S. Conceição, L.F. Santos, M.F.C. Pereira, T.M. Casimiro, I. Ferreira Machado, *Spectrochim. Acta - Part A Mol. Biomol. Spectrosc.* **2015**; *149*, 285.

[104] P. Colomban, V. Milande, H. Lucas, *J. Raman Spectrosc.* **2004**; *35*, 68.

[105] B. Kirmizi, P. Colomban, M. Blanc, *J. Raman Spectrosc.* **2010**; *41*, 1240.

[106] E. Marengo, M. Aceto, E. Robotti, M.C. Liparota, M. Bobba, G. Pantò, *Anal. Chim. Acta* **2005**; *537*, 359.

[107] E. Widjaja, G.H. Lim, Q. Lim, A. Bin Mashadi, M. Garland, *J. Raman Spectrosc.* **2011**; *42*, 377.

[108] G. Barone, V. Crupi, F. Longo, D. Majolino, P. Mazzoleni, S. Raneri, V. Venuti, *X-Ray Spectrom.* **2014**; *43*, 83.

[109] F. Antonelli, P. Santi, A. Renzulli, A. Bonazza, *Geol. Soc. London, Spec. Publ.* **2006**; *257*, 229.

[110] P. Santi, F. Antonelli, A. Renzulli, *Archaeometry* **2005**; *47*, 253.

[111] F. Antonelli, L. Lazzarini, *Archaeometry* **2012**; *54*, 1.

[112] C. Baita, P.P. Lottici, E. Salvioli-Mariani, P. Vandenabeele, M. Librenti, F. Antonelli, D. Bersani, *J. Raman Spectrosc.* **2014**; *45*, 114.

[113] D. Bersani, S. Andò, P. Vignola, G. Moltifiori, I.G. Marino, P.P. Lottici, V. Diella, *Spectrochim. Acta - Part A Mol. Biomol. Spectrosc.* **2009**; *73*, 484.

[114] T. Cerasoli, A. Coccato, D. Bersani, P.P. Lottici, R. Conversi, 6th International Congress on the Application of Raman Spectroscopy in Art and Archaeology (RAA 2011) 5-8 September 2011, Parma, Italy, Timeo ed. Bologna, p. 129-130 - ISBN: 9788897162209

[115] K.E. Kuebler, B.L. Jolliff, A. Wang, L. A. Haskin, *Geochim. Cosmochim. Acta* **2006**; *70*, 6201.

[116] H.J. Schubnel, M. Pinet, D.C. Smith, B. Lasnier, *La Microsonde Raman En Gemmologie*, Association française de gemmologie, Paris, 1992.

[117] M. L. Dele, P. Dhamelincourt, J. P. Poirot, J. M. Dereppe, C. Moreaux, *J. Raman Spectrosc.* **1997**; *28*, 673.

[118] M.-L. Delé Dubois, P. Dhamelincourt, H.-J. Schubnel, *Rev. Fr. Gemmol.* **1980**; *63*, 11.

[119] M.-L. Delé Dubois, P. Dhamelincourt, H.-J. Schubnel, *Rev. Fr. Gemmol.* **1980**; 64, 13.

[120] L. Kiefert, J.P. Chalain, S. Haberli, in:, H.G.M. Edwards, J.M. Chalmers (Eds.), Raman Spectrosc. Archaeol. Art Hist., Royal society of chemistry, 2005.

[121] L. Kiefert, S. Karampelas, *Spectrochim. Acta - Part A Mol. Biomol. Spectrosc.* **2011**; *80*, 119.

[122] L. Kiefert, M. Epelboym, H.-P. Kan-Nyunt, S. Paralusz, in *Infrared Raman Spectroscopy in Forensic Science, p.455, eds. J.M. Chalmers, H.G.M. Edwards, M.D. Hargreaves,* Wiley, **2012**

[123] S. Domínguez-Bella, *Archaeomineralogy of Prehistoric Artifacts and Gemstones*, J.M. Herrero, M. Vendrell (Eds.), Archaeometry and Cultural Heritage: the Contribution of Mineralogy. Seminarios SEM, Vol. 9 Sociedad Española de Mineralogía, Madrid (2012) 112 p. ISSN 1698-5478, pp. 5-28.

[124] S. Karampelas, M. Wörle, K. Hunger, H. Lanz, *J. Raman Spectrosc.* **2012**; *43*, 1833.

[125] S. Karampelas, M. Wörle, K. Hunger, H. Lanz, D. Bersani, S. Gübelin, *Gems Gemol.* **2010**; *46*, 292.

[126] M. Jeršek, S. Kramar, *J. Raman Spectrosc.* **2014**; *45*, 1000.

[127] R.T. Liddicoat, *Handbook of Gem Identification*, Gemological Institute of America, Santa Monica, 1993.

[128] L.L. Reiche I., Pages-Camagna S., *J. Raman Spectrosc.* **2004**; *35*, 719.

[129] Z. Petrová, J. Jehlička, T. Čapoun, R. Hanus, T. Trojek, V. Goliáš, *J. Raman Spectrosc.* **2012**; *43*, 1275.

[130] G. Barone, D. Bersani, J. Jehlička, P.P. Lottici, P. Mazzoleni, S. Raneri, P. Vandenabeele, C. Di Giacomo, G. Larinà, *J. Raman Spectrosc.* **2015**; 46, 989.

[131] G. Barone, P. Mazzoleni, S. Raneri, D. Bersani, J. Jehlička, P.P. Lottici, P. Vandenabeele, G. Lamagna, A.M. Manenti, *Applied Spectrosc* **2015**; *in press*.

[132] D. Bersani, G. Azzi, E. Lambruschi, G. Barone, P. Mazzoleni, S. Raneri, U. Longobardo, P.P. Lottici, *J. Raman Spectrosc.* **2014**; 45, 1293.

[133] J. Dong, Y. Han, J. Ye, Q. Li, S. Liu, D. Gu, *J. Raman Spectrosc.* **2014**; *45*, 596.

[134] P. Gołyźniak, L. Natkaniec-Nowak, M. Dumańska-Słowik, B. Naglik, *Archaeometry* **2015**; doi: 10.1111/arcm.12174

[135] J. Götze, L. Nasdala, R. Kleeberg, M. Wenzel, *Contrib. to Mineral. Petrol.* **1998**; *133*, 96.

[136] L. Paral, J. Garcia Guinea, R. Kibar, A. Cetin, N. Can, *J. Lumin.* **2011**; *131*, 2317.

[137] D. Pop, C. Constantina, D. Tătar, W. Kiefer, *Stud. UBB, Geol.* **2012**; *49*, 41.

[138] J. Whalley, Studies Conservation **2012**; 57 , S313.

[139] E. Gliozzo, N. Grassi, P. Bonanni, C. Meneghini, M.A. Tomei, *Archaeometry* **2011**; *53*, 469.

[140] C. Capel Ferrón, L. León Reina, S. Jorge-Villar, J.M. Compaña, M.A.G. Aranda, J.T. López Navarrete, V. Hernández, F.J. Medianero, J. Ramos, G.C. Weniger, S. Domínguez-Bella, J. Linstaedter, P. Cantalejo, M.Y. Espejo, J.J. Durán Valsero, *Archaeol. Anthropol. Sci.* **2015**; 235.

[141] A. Wesełucha-Birczyńska, L. Natkaniec-Nowak, *Vib. Spectrosc.* **2011**; *57*, 248.

[142] B. Kolesov, *Phys. Chem. Miner.* **2008**; *35*, 271.

[143] L.T.-T. Huong, W. Hofmeister, T. Häger, S. Karampelas, N.D.-T. Kien, *Gems Gemol.* **2014**; *50*, 287.

[144] L.T.-T. Huong, T. Hager, W. Hofmeister, *Gems Gemol.* **2010**; *46*, 36.

[145] Y. Ruzeng, Y. Song, *J. Gems Gemmol.* **2014**; *1*, 9.

[146] E. Lambruschi, G.D. Gatta, I. Adamo, D. Bersani, E. Salvioli-Mariani, P.P. Lottici, *J. Raman Spectrosc.* **2014**; *45*, 993.

[147] B.M. Laurs, W.B. Simmons, G.R. Rossman, E.P. Quinn, S.F. McClure, A. Peretti, T. Armbruster, F.C. Hawthorne, A.U. Falster, D. Günther, others, *Gems Gemol.* **2003**; *39*, 284.

[148] G.D. Gatta, I. Adamo, M. Meven, E. Lambruschi, *Phys. Chem. Miner.* **2012**; *39*, 829.

[149] M. Giarola, G. Mariotto, M. Barberio, D. Ajò, *J. Raman Spectrosc.* **2012**; *43*, 1828.

[150] M. Superchi, F. Pezzotta, E. Gambini, E. Castaman, *Gems Gemol.* **2010**; *46*, 274.

[151] F. Pezzotta, I. Adamo, V. Diella, *Gems Gemol.* **2011**; *47*, 2.

[152] A.-K. Malsy, S. Karampelas, D. Schwarz, L. Klemm, T. Armbruster, D.A. Tuan, The Journal of Gemmology, **2012**; 33, 19.

[153] L.T.-T. Huong, T. Häger, W. Hofmeister, C. Hauzenberger, D. Schwarz, P. Van Long, U. Wehmeister, N.N. Khoi, N.T. Nhung, *Gems Gemol.* **2012**; *48*, 158.

[154] M. Giarola, G. Mariotto, D. Ajò, *J. Raman Spectrosc.* **2012**; *43*, 556.

[155] M. Ayvackli, J. Garcia-Guinea, A. Jorge, I. Akaln, Z. Kotan, N. Can, *J. Lumin.* **2012**; *132*, 1750.

[156] M. Dumańska-Słowik, A. Wesełucha-Birczyńska, L. Natkaniec-Nowak, *Spectrochim. Acta - Part A Mol. Biomol. Spectrosc.* **2013**; *109*, 97.

[157] N. Noguchi, A. Abduriyim, I. Shimizu, N. Kamegata, S. Odake, H. Kagi, *J. Raman Spectrosc.* **2013**; *44*, 147.

[158] B.I. Łydzba-Kopczyńska, B. Gediga, J. Chojcan, M. Sachanbiński, *J. Raman Spectrosc.* **2012**; *43*, 1839.

[159] R.H. Brody, H.G.M. Edwards, A. M. Pollard, *Spectrochim. Acta - Part A Mol. Biomol. Spectrosc.* **2001**; *57*, 1325.

[160] J. Jehlička, S.E. Jorge Villar, H.G.M. Edwards, *J. Raman Spectrosc.* **2004**; *35*, 761.

[161] W. Winkler, M. Musso, E.C. Kirchner, *J. Raman Spectrosc.* **2003**; *34*, 157.

[162] Z. Rao, K. Dong, X. Yang, J. Lin, X. Cui, R. Zhou, Q. Deng, *Sci. China Physics, Mech. Astron.* **2013**; *56*, 1598.

[163] E.D. Zu, S.Q. Li, Y. Zou, X.G. Zhao, Y.D. Sun, Y.F. Lin, H. Li, Key Eng. Mater.**2011**; 492, 341.

[164] M. Sachanbiński, R. Girulski, D. Bobak, B. Łydzba-Kopczyńska, J. Raman Spectrosc. **2008**; 39, 1012.

[165] L. Kiefert, H. a Hanni, J.P. Chalain, *Opt. Devices Diagnostics Mater. Sci.* **2000**; *4098*, 241.

[166] S.F. Mcclure, R.E. Kane, N. Sturman, *Gems Gemol.* **2010**; *46*, 218.

[167] M. Hall, T.M. Moses, *Gems Gemol.* **2001**; *37*, 214.

[168] K.S. Moe, T.M. Moses, P. Johnson, *Gems Gemol.* **2007**; *43*, 149.

[169] D. De Ghionno, P. Owens, *Gems Gemol.* **2003**; *39*, 214.

[170] G.B. Andreozzi, F. Princivalle, H. Skogby, A. Della Giusta, *Am. Mineral.* **2000**; *85*, 1164.

[171] L. Nasdala, O. Beyssac, J.W. Schopf, B. Bleisteiner, Raman Imaging, Springer SDeries in Optical Sciences vol. 168, Springer, **2012**, pp. 145–187.

[172] E. Gaillou, J. E. Post, A. Steele, J. E. Butler, *AGU Fall Meeting Abstracts* **2013**; A2350.

[173] Y. Tuncer Arslanlar, J. Garcia-Guinea, R. Kibar, A. Çetin, M. Ayvacikli, N. Can, *Appl. Radiat. Isot.* **2011**; *69*, 1299.

[174] R. Wang, W.S. Zhang, *J. Raman Spectrosc.* **2011**; *42*, 1324.

[175] F. Casadio, J.G. Douglas, K.T. Faber, *Anal. Bioanal. Chem.* **2007**; *387*, 791.

[176] D. Bersani, S. Andò, L. Scrocco, P. Gentile, E. Salvioli-Mariani, P.P. Lottici, in:, 11th Int. GeoRaman Conf. St. Louis, Missouri, USA, Lunar and Planetary Institute, St. Louis, 2014.

[177] J.R. Petriglieri, E. Salvioli-Mariani, L. Mantovani, M. Tribaudino, P.P. Lottici, C. Laporte-Magoni, D. Bersani, *J. Raman Spectrosc.* **2015**; 46, 953.

[178] Y.Y. Wang, F.X. Gan, H.X. Zhao, *Vib. Spectrosc.* **2013**; *66*, 19.

[179] A.A.D. Robles, J. Luis, R. Sil, P. Claes, M.D.M. Ortega, E.C. González, M. Ángel, M. Rojas, M.C. García, S.G. Castillo, *Herit. Sci.* **2015**; 1.

[180] J.R. Barnett, S. Miller, E. Pearce, *Opt. Laser Technol.* **2006**; *38*, 445.

[181] D.A. Scott, *Stud. Conserv.* **2015**; doi: 10.1179/2047058414Y.0000000162.

[182] N. Eastaugh, V. Walsh, T. Chaplin, R. Siddall, The Pigment Compendium: A Dictionary of Historical Pigments., Elsevier - Butterworth Heinemen, 2004.

[183] L.C. Prinsloo, W. Barnard, I. Meiklejohn, K. Hall, *J. Raman Spectrosc.* **2008**; *39*, 646.

[184] A. Hernanz, J.M. Gavira-Vallejo, J.F. Ruiz-López, H.G.M. Edwards, *J. Raman Spectrosc.* **2008**; *39*, 972.

[185] A. Hernanz, J.F. Ruiz-López, J.M. Gavira-Vallejo, S. Martin, E. Gavrilenko, *J. Raman Spectrosc.* **2010**; *41*, 1394.

[186] L. Darchuk, Z. Tsybrii, A. Worobiec, C. Vázquez, O.M. Palacios, E. A. Stefaniak, G. Gatto Rotondo, F. Sizov, R. Van Grieken, *Spectrochim. Acta - Part A Mol. Biomol. Spectrosc.* **2010**; *75*, 1398.

[187] S. Gialanella, R. Belli, G. Dalmeri, I. Lonardelli, M. Mattarelli, M. Montagna, L. Toniutti, *Archaeometry* **2011**; *53*, 950.

[188] S. Lahlil, M. Lebon, L. Beck, H. Rousselière, C. Vignaud, I. Reiche, M. Menu, P. Paillet, F. Plassard, *J. Raman Spectrosc.* **2012**; *43*, 1637.

[189] L. Beck, D. Genty, S. Lahlil, M. Lebon, F. Tereygeol, C. Vignaud, I. Reiche, E. Lambert, H. Valladas, E. Kaltnecker, F. Plassard, M. Menu, P. Paillet, *Radiocarbon* **2013**; *55*, 436.

[190] D.L. a De Faria, F.N. Lopes, L.A.C. Souza, H.D. De Oliveira Castello Branco, *Quim. Nova* **2011**; *34*, 1358.

[191] A. Tournié, L.C. Prinsloo, C. Paris, P. Colomban, B. Smith, *J. Raman Spectrosc.* **2011**; *42*, 399.

[192] C. Lofrumento, M. Ricci, L. Bachechi, D. De Feo, E.M. Castellucci, *J. Raman Spectrosc.* **2012**; *43*, 809.

[193] L. Darchuk, G.G. Rotondo, M. Swaenen, A. Worobiec, Z. Tsybrii, Y. Makarovska, R. Van Grieken, *Spectrochim. Acta - Part A Mol. Biomol. Spectrosc.* **2011**; *83*, 34.

[194] P. Jezequel, G. Wille, C. Beny, F. Delorme, V. Jean-Prost, R. Cottier, J. Breton, F. Dure, J. Despriee, *J. Archaeol. Sci.* **2011**; *38*, 1165.

[195] B. Erdogu, A. Ulubey, *Oxford J. Archaeol.* **2011**; *30*, 1.

[196] A. Bonneau, D.G. Pearce, A. M. Pollard, *J. Archaeol. Sci.* **2012**; *39*, 287.

[197] A. Bonneau, D.G. Pearce, P.J. Mitchell, C. Arthur, T. Higham, M. Lamothe, *Proc. 39th Int. Symp. Archaeom. Leuven* **2012**; 319.

[198] P.M. Martin-Sanchez, S. Sanchez-Cortes, E. Lopez-Tobar, V. Jurado, F. Bastian, C. Alabouvette, C. Saiz-Jimenez, *J. Raman Spectrosc.* **2012**; *43*, 464.

[199] A. Hernanz, J.M. Gavira-Vallejo, J.F. Ruiz-Lõpez, S. Martin, Á. Maroto-Valiente, R. De Balbín-Behrmann, M. Menéndez, J.J. Alcolea-González, *J. Raman Spectrosc.* **2012**; *43*, 1644.

[200] A. Hernanz, J.F. Ruiz-López, J.M. Madariaga, E. Gavrilenko, M. Maguregui, S. Fdez-Ortiz de Vallejuelo, I. Martínez-Arkarazo, R. Alloza-Izquierdo, V. Baldellou-Martínez, R. Viñas-Vallverdú, A. Rubio i Mora, À. Pitarch, A. Giakoumaki, *J. Raman Spectrosc.* **2014**; *45*, 1236.

[201] T.R. Ravindran, A. K. Arora, M. Singh, S.B. Ota, *J. Raman Spectrosc.* **2013**; *44*, 108.

[202] M. Mas, A. Jorge, B. Gavilán, M. Solís, E. Parra, P.P. Pérez, *J. Archaeol. Sci.* **2013**; *40*, 4635.

[203] M. Olivares, K. Castro, M.S. Corchón, D. Gárate, X. Murelaga, A. Sarmiento, N. Etxebarria, *J. Archaeol. Sci.* **2013**; *40*, 1354.

[204] À. Pitarch, J.F. Ruiz, S. Fdez-Ortiz de Vallejuelo, A. Hernanz, M. Maguregui, J.M. Madariaga, *Anal. Methods* **2014**; *6*, 6641.

[205] H. Gomes, H. Collado, A. Martins, G.H. Nash, P. Rosina, C. Vaccaro, *Mediterr. Archaeol. Archaeom.* **2015**; *15*, 163.

[206] L. Dayet, P.J. Texier, F. Daniel, G. Porraz, *J. Archaeol. Sci.* **2013**; *40*, 3492.

[207] L. Dayet, F. d'Errico, R. Garcia-Moreno, *J. Archaeol. Sci.* **2014**; *44*, 180.

[208] M. Iriarte, A. Hernanz, J.F. Ruiz-Lõpez, S. Martín, *J. Raman Spectrosc.* **2013**; *44*, 1557.

[209] M. Maguregui, U. Knuutinen, K. Castro, J.M. Madariaga, *J. Raman Spectrosc.* **2010**; *41*, 1400.

[210] H. Gomes, P. Rosina, P. Holakooei, T. Solomon, C. Vaccaro, *J. Archaeol. Sci.* **2013**; *40*, 4073.

[211] E. López-Montalvo, V. Villaverde, C. Roldán, S. Murcia, E. Badal, *J. Archaeol. Sci.* **2014**; *52*, 535.

[212] D. Bonjean, Y. Vanbrabant, G. Abrams, S. Pirson, C. Burlet, K. Di Modica, M. Otte, J. Vander Auwera, M. Golitko, R. McMillan, E. Goemaere, *J. Archaeol. Sci.* **2015**; *55*, 253.

[213] L. Darchuk, E. a Stefaniak, C. Vázquez, O.M. Palacios, A. Worobiec, R. Van Grieken, *E-Preservation Sci.* **2009**; *6*, 112.

[214] M.Á. Rogerio-Candelera, L.K. Herrera, A.Z. Miller, L. García Sanjuán, C. Mora Molina, D.W. Wheatley, Á. Justo, C. Saiz-Jimenez, *J. Archaeol. Sci.* **2013**; *40*, 279.

[215] R.S. Román, C.B. Bañón, M.D. Landete Ruiz, *J. Archaeol. Sci.* **2015**; *60*, 84.

[216] J. Zilhão, D.E. Angelucci, E. Badal-García, F. d'Errico, F. Daniel, L. Dayet, K. Douka, T.F.G. Higham, M.J. Martínez-Sánchez, R. Montes-Bernárdez, S. Murcia-Mascarós, C. Pérez-Sirvent, C. Roldán-García, M. Vanhaeren, V. Villaverde, R. Wood, J. Zapata, J. Zilhao, D.E. Angelucci, E. Badal-Garcia, F. d'Errico, F. Daniel, L. Dayet, K. Douka, T.F.G. Higham, M.J. Martinez-Sanchez, R. Montes-Bernardez, S. Murcia-Mascaros, C. Perez-Sirvent, C. Roldan-Garcia, M. Vanhaeren, V. Villaverde, R. Wood, J. Zapata, J. Zilhão, D.E. Angelucci, E. Badal-García, F. d'Errico, F. Daniel, L. Dayet, K. Douka, T.F.G. Higham, M.J. Martínez-Sánchez, R. Montes-Bernárdez, S. Murcia-Mascarós, C. Pérez-Sirvent, C. Roldán-García, M. Vanhaeren, V. Villaverde, R. Wood, J. Zapata, *Proc. Natl. Acad. Sci. U. S. A.* **2010**; *107*, 1023.

[217] C.S. Henshilwood, F. d'Errico, K.L. van Niekerk, Y. Coquinot, Z. Jacobs, S.-E. Lauritzen, M. Menu, R. Garcia-Moreno, *Science (80-.).* **2011**; *334*, 219.

[218] P. Villa, L. Pollarolo, I. Degano, L. Birolo, M. Pasero, C. Biagioni, K. Douka, R. Vinciguerra, J.J. Lucejko, L. Wadley, *PLoS One* **2015**; *10*, e0131273.

[219] A. Rousaki, C. Bellelli, M. Carballido Calatayud, V. Aldazabal, G. Custo, L. Moens, P. Vandenabeele, C. Vázquez, *J. Raman Spectrosc.* **2015**; *46, 1016*.

[220] S. di Lernia, S. Bruni, I. Cislaghi, M. Cremaschi, M. Gallinaro, V. Gugliemi, A.M. Mercuri, G. Poggi, A. Zerboni, *Archaeol. Anthropol. Sci.* **2015**; *486*, 2012.

[221] J. Huntley, M. Aubert, J. Ross, H.E. A. Brand, M.J. Morwood, *Archaeometry* **2015**; *57*, 77.

[222] B. Guineau, *Stud. Conserv.* **1984**; *29*, 35.

[223] B. Guineau, *J. Forensic Sci.* **1984**; *29*, 15.

[224] K. Brown, M. Brown, D. Jacobs, *Stud. Conserv.* **2002**; *47*, 4.

[225] M. Clarke, *Stud. Conserv.* **2004**; *49*, 231.

[226] R.J.H. Clark, *Comptes Rendus Chim.* **2002**; *5*, 7.

[227] M. Clarke, *Rev. Conserv.* **2013**; *2*, 3.

[228] S. Pessanha, M. Manso, M.L. Carvalho, *Spectrochim. Acta - Part B At. Spectrosc.* **2012**; *71-72*, 54.

[229] M.V. Orna, in:, Archaeol. Chem. VIII, 2013, pp. 3–18.

[230] T.D. Chaplin, R.J.H. Clark, A. McKay, S. Pugh, *J. Raman Spectrosc.* **2006**; *37*, 865.

[231] T.D. Chaplin, R.J.H. Clark, D. Jacobs, K. Jensen, G.D. Smith, *Anal. Chem.* **2005**; *77*, 3611.

[232] D. Bersani, P.P. Lottici, F. Vignali, G. Zanichelli, *J. Raman Spectrosc.* **2006**; *37*, 1012.

[233] M. Aceto, A. Agostino, E. Boccaleri, F. Crivello, A.C. Garlanda, *J. Raman Spectrosc.* **2006**; *37*, 1160.

[234] S. Bioletti, R. Leahy, J. Fields, B. Meehan, W. Blau, *J. Raman Spectrosc.* **2009**; *40*, 1043.

[235] G. Van der Snickt, W. De Nolf, B. Vekemans, K. Janssens, *Appl. Phys. A* **2008**; *92*, 59.

[236] P. Baraldi, G. Moscardi, P. Bensi, M. Aceto, L. Tassi, *E-Preservation Sci.* **2009**; *6*, 163.

[237] T.D. Chaplin, R.J.H. Clark, M. Martinón-Torres, *J. Mol. Struct.* **2010**; *976*, 350.

[238] M. Aceto, A. Agostino, E. Boccaleri, F. Crivello, A. Cerutti Garlanda, *J. Raman Spectrosc.* **2010**; *41*, 1434.

[239] P. Zannini, P. Baraldi, M. Aceto, A. Agostino, G. Fenoglio, D. Bersani, E. Canobbio, E. Schiavon, G. Zanichelli, A. De Pasquale, *J. Raman Spectrosc.* **2012**; *43*, 1722.

[240] L. Burgio, R.J.H. Clark, R.R. Hark, *Proc. Natl. Acad. Sci. U. S. A.* **2010**; *107*, 5726.

[241] S. Daniilia, K.S. Andrikopoulos, *J. Raman Spectrosc.* **2007**; *38*, 332.

[242] L. Burgio, R.J.H. Clark, R.R. Hark, M.S. Rumsey, C. Zannini, *Appl. Spectrosc.* **2009**; *63*, 611.

[243] A. Duran, M.L. Franquelo, M. A. Centeno, T. Espejo, J.L. Perez-Rodriguez, *J. Raman Spectrosc.* **2011**; *42*, 48.

[244] A. Deneckere, M. De Reu, M.P.J. Martens, K. De Coene, B. Vekemans, L. Vincze, P. De Maeyer, P. Vandenabeele, L. Moens, *Spectrochim. Acta - Part A Mol. Biomol. Spectrosc.* **2011**; *80*, 125.

[245] A. Deneckere, M. Leeflang, M. Bloem, C.A. A. Chavannes-Mazel, B. Vekemans, L. Vincze, P. Vandenabeele, L. Moens, *Spectrochim. Acta - Part A Mol. Biomol. Spectrosc.* **2011**; *83*, 194.

[246] M. Aceto, A. Agostino, G. Fenoglio, P. Baraldi, P. Zannini, C. Hofmann, E. Gamillscheg, *Spectrochim. Acta - Part A Mol. Biomol. Spectrosc.* **2012**; *95*, 235.

[247] V.S.F. Muralha, C. Miguel, M.J. Melo, *J. Raman Spectrosc.* **2012**; *43*, 1737.

[248] V.S.F. Muralha, L. Burgio, R.J.H. Clark, *Spectrochim. Acta - Part A Mol. Biomol. Spectrosc.* **2012**; *92*, 21.

[249] M. Aceto, A. Agostino, G. Fenoglio, M. Gulmini, V. Bianco, E. Pellizzi, *Spectrochim. Acta - Part A Mol. Biomol. Spectrosc.* **2012**; *91*, 352.

[250] K.L. Rasmussen, A.L. Tenorio, I. Bonaduce, M.P. Colombini, L. Birolo, E. Galano, A. Amoresano, G. Doudna, A.D. Bond, V. Palleschi, G. Lorenzetti, S. Legnaioli, J. van der Plicht, J. Gunneweg, *J. Archaeol. Sci.* **2012**; *39*, 2956.

[251] A. El Bakkali, T. Lamhasni, S. Ait Lyazidi, M. Haddad, F. Rosi, C. Miliani, S. Sánchez-Cortés, M. El Rhaiti, *Vib. Spectrosc.* **2014**; *74*, 47.

[252] I. Nastova, O. Grupče, B. Minčeva-Šukarova, S. Turan, M. Yaygingol, M. Ozcatal, V. Martinovska, Z. Jakovlevska-Spirovska, *J. Raman Spectrosc.* **2012**; *43*, 1729.

[253] I. Nastova, O. Grupče, B. Minčeva-Šukarova, M. Kostadinovska, M. Ozcatal, *Vib. Spectrosc.* **2015**; *78*, 39.

[254] I. Nastova, O. Grupče, B. Minčeva-Šukarova, M. Ozcatal, L. Mojsoska, *Vib. Spectrosc.* **2013**; *68*, 11.

[255] V. Tanevska, I. Nastova, B. Minčeva-Šukarova, O. Grupče, M. Ozcatal, M. Kavčić, Z. Jakovlevska-Spirovska, *Vib. Spectrosc.* **2014**; *73*, 127.

[256] D. Lauwers, V. Cattersel, L. Vandamme, A. Van Eester, K. De Langhe, L. Moens, P. Vandenabeele, *J. Raman Spectrosc.* **2014**; *45*, 1266.

[257] A. Le Gac, S. Pessanha, S. Longelin, M. Guerra, J.C. Frade, F. Lourenço, M.C. Serrano, M. Manso, M.L. Carvalho, *Appl. Radiat. Isot.* **2013**; *82*, 242.

[258] I. Lukačević, I. Ergotić, M. Vinaj, *Museum* **2013**; *385*, 1.

[259] M. Manso, A. Le Gac, S. Longelin, S. Pessanha, J.C. Frade, M. Guerra, A.J. Candeias, M.L. Carvalho, *Spectrochim. Acta - Part A Mol. Biomol. Spectrosc.* **2013**; *105*, 288.

[260] M. Kostadinovska, Z. Jakovleska-Spirovska, B. Minčeva-Šukarova, in: Adv. Res. Sci. Areas, EDIS - Publishing Institution of the University of Zilina, **2013**, pp. 311–316.

[261] A. Duran, A. López-Montes, J. Castaing, T. Espejo, *J. Archaeol. Sci.* **2014**; *45*, 52.

[262] A. Zoleo, L. Nodari, M. Rampazzo, F. Piccinelli, U. Russo, C. Federici, M. Brustolon, *Archaeometry* **2014**; *56*, 496.

[263] J.T.J. Yardley, A. Hagadorn, *Harv. Theol. Rev.* **2014**; *107*, 1.

[264] D. Buti, D. Domenici, C. Miliani, C. García Sáiz, T. Gómez Espinoza, F. Jímenez Villalba, A. Verde Casanova, A. Sabía de la Mata, A. Romani, F. Presciutti, B. Doherty, B.G. Brunetti, A. Sgamellotti, *J. Archaeol. Sci.* **2014**; *42*, 166.

[265] H.G.M. Edwards, S.E. Jorge Villar, K. A. Eremin, *J. Raman Spectrosc.* **2004**; *35*, 786.

[266] A. Kamińska, M. Sawczak, M. Oujja, C. Domingo, M. Castillejo, G. Śliwiński, *J. Raman Spectrosc.* **2006**; *37*, 1125.

[267] A.M. Correia, R.J.H. Clark, M.I.M. Ribeiro, M.L.T.S. Duarte, *J. Raman Spectrosc.* **2007**; *38*, 1390.

[268] A.M. Correia, M.J. V Oliveira, R.J.H. Clark, M.I. Ribeiro, M.L. Duarte, *Anal. Chem.* **2008**; *80*, 1482.

[269] H.G.M. Edwards, T.J. Benoy, *Anal. Bioanal. Chem.* **2007**; *387*, 837.

[270] S. Daniilia, K.S. Andrikopoulos, S. Sotiropoulou, I. Karapanagiotis, *Appl. Phys. A Mater. Sci. Process.* **2008**; *90*, 565.

[271] D. Lau, C. Villis, S. Furman, M. Livett, *Anal. Chim. Acta* **2008**; *610*, 15.

[272] I.D. van der Werf, R. Gnisci, D. Marano, G.E. De Benedetto, R. Laviano, D. Pellerano, F. Vona, F. Pellegrino, E. Andriani, I.M. Catalano, A.F. Pellerano, L. Sabbatini, *J. Cult. Herit.* **2008**; *9*, 162.

[273] P. Vandenabeele, M.C. Christensen, L. Moens, *J. Raman Spectrosc.* **2008**; *39*, 1030.

[274] M.-J. Benquerença, N.F.C. Mendes, E. Castellucci, V.M.F. Gaspar, F.P.S.C. Gil, *J. Raman Spectrosc.* **2009**; *40*, 2135.

[275] J. Bredal-Jørgensen, J. Sanyova, V. Rask, M.L. Sargent, R.H. Therkildsen, *Anal. Bioanal. Chem.* **2011**; *401*, 1433.

[276] T. Li, Y.F. Xie, Y.M. Yang, C.S. Wang, X.Y. Fang, J.L. Shi, Q.J. He, *J. Raman Spectrosc.* **2009**; *40*, 1911.

[277] S. Pessanha, M.L. Carvalho, M.I. Cabaço, S. Valadas, J.L. Bruneel, M. Besnard, M.I. Ribeiro, *J. Raman Spectrosc.* **2010**; *41*, 1510.

[278] S. Pessanha, A. Le Gac, T.I. Madeira, J.L. Bruneel, S. Longelin, M.L. Carvalho, *J. Raman Spectrosc.* **2012**; *43*, 1699.

[279] A. Duran, M.B. Siguenza, M.L. Franquelo, M.C.J. De Haro, A. Justo, J.L. Perez-Rodriguez, *Anal. Chim. Acta* **2010**; *671*, 1.

[280] T.R. Ravindran, A. K. Arora, S. Ramya, R. V. Subba Rao, B. Raj, *J. Raman Spectrosc.* **2011**; *42*, 803.

[281] M. Odlyha, D. Thickett, L. Sheldon, *J. Therm. Anal. Calorim.* **2011**; *105*, 875.

[282] N. Marchettini, a Atrei, F. Benetti, N. Proietti, V. Di Tullio, M. Mascalchi, I. Osticioli, S. Siano, I.T. Memmi, *Surf. Eng.* **2012**; *29*, 153.

[283] D. Mancini, A. Tournié, M.C. Caggiani, P. Colomban, *J. Raman Spectrosc.* **2012**; *43*, 294.

[284] S. Akyuz, T. Akyuz, G. Emre, A. Gulec, S. Basaran, *Spectrochim. Acta - Part A Mol. Biomol. Spectrosc.* **2012**; *89*, 74.

[285] Ľ. Vančo, M. Kadlečíková, J. Breza, Ľ. Čaplovič, M. Gregor, *Appl. Surf. Sci.* **2013**; *264*, 692.

[286] E. Pięta, E. Proniewicz, B. Szmelter-Fausek, J. Olszewska-Świetlik, L.M. Proniewicz, *J. Raman Spectrosc.* **2014**; *45*, 1019.

[287] P.C. Gutiérrez-Neira, F. Agulló-Rueda, A. Climent-Font, C. Garrido, *Vib. Spectrosc.* **2013**; *69*, 13.

[288] L. Van De Voorde, J. Van Pevenage, K. De Langhe, R. De Wolf, B. Vekemans, L. Vincze, P. Vandenabeele, M.P.J. Martens, *Spectrochim. Acta - Part B At. Spectrosc.* **2014**; *97*, 1.

[289] F. Marte, V.P. Careaga, N. Mastrangelo, D.L. A. de Faria, M.S. Maier, *J. Raman Spectrosc.* **2014**; *45*, 1046.

[290] M.V. Quattrini, M. Ioele, A. Sodo, G.F. Priori, D. Radeglia, *Stud. Conserv.* **2014**; *59*, 328.

[291] V. Antunes, A. Candeias, M.J. Oliveira, S. Longelin, V. Serrão, A.I. Seruya, J. Coroado, L. Dias, J. Mirão, M.L. Carvalho, *J. Raman Spectrosc.* **2014**; *45*, 1026.

[292] H.G.M. Edwards, P. Vandenabeele, T.J. Benoy, *Spectrochim. Acta - Part A Mol. Biomol. Spectrosc.* **2015**; *137*, 45.

[293] A. Veiga, D.M. Teixeira, A.J. Candeias, J. Mirão, A. Manhita, C. Miguel, P. Rodrigues, J.G. Teixeira, *Microchem. J.* **2015**; *123*, 51.

[294] I. Żmuda-Trzebiatowska, M. Wachowiak, A. Klisińska-Kopacz, G. Trykowski, G. Śliwiński, *Spectrochim. Acta - Part A Mol. Biomol. Spectrosc.* **2015**; *136*, 793.

[295] E. Pięta, E. Proniewicz, B. Szmelter-Fausek, J. Olszewska-Świetlik, L.M. Proniewicz, *Spectrochim. Acta - Part A Mol. Biomol. Spectrosc.* **2015**; *136*, 594.

[296] L. Damjanović, M. Gajić-Kvaščev, J. Đurđević, V. Andrić, M. Marić-Stojanović, T. Lazić, S. Nikolić, *Radiat. Phys. Chem.* **2015**; *115*, 135.

[297] K.S. Andrikopoulos, S. Daniilia, B. Roussel, K. Janssens, *J. Raman Spectrosc.* **2006**; *37*, 1026.

[298] E. Kouloumpi, P. Vandenabeele, G. Lawson, V. Pavlidis, L. Moens, *Anal. Chim. Acta* **2007**; *598*, 169.

[299] M. Abdel-Ghani, H.G.M. Edwards, R. Janaway, B. Stern, *Vib. Spectrosc.* **2008**; *48*, 69.

[300] M. Abdel-Ghani, B. Stern, H.G.M. Edwards, R. Janaway, *Vib. Spectrosc.* **2012**; *62*, 98.

[301] A. Iordanidis, J. Garcia-Guinea, A. Strati, A. Gkimourtzina, *Anal. Lett.* **2013**;

[302] S. Sotiropoulou, S. Daniilia, *Acc. Chem. Res.* **2010**; *43*, 877.

[303] I. Karapanagiotis, D. Lampakis, A. Konstanta, H. Farmakalidis, *J. Archaeol. Sci.* **2013**; *40*, 1471.

[304] S. Lahlil, E. Martin, *J. Cult. Herit.* **2012**; *13*, 332.

[305] M. Abdel-Ghani, H.G.M. Edwards, B. Stern, R. Janaway, *Spectrochim. Acta - Part A Mol. Biomol. Spectrosc.* **2009**; *73*, 566.

[306] M. Abdel-Ghani, *Mediterr. Archaeol. Archaeom.* **2015**; *15*, xx.

[307] L. Damjanovic, O. Marjanovic, M. Maric-Stojanovic, V. Andric, U. Mioc, *J. Serbian Chem. Soc.* **2015**; *80*, 805.

[308] A. Daveri, B. Doherty, P. Moretti, C. Grazia, A. Romani, E. Fiorin, B.G. Brunetti, M. Vagnini, *Spectrochim. Acta - Part A Mol. Biomol. Spectrosc.* **2015**; *135*, 398.

[309] H.G.M. Edwards, D.W. Farwell, E.M. Newton, F.R. Perez, S.J. Villar, *J. Raman Spectrosc.* **2000**; *31*, 407.

[310] I.C.A. Sandu, M.H. de Sá, M.C. Pereira, *Surf. Interface Anal.* **2011**; *43*, 1134.

[311] A.C. Prieto, A. Guedes, A. Dória, F. Noronha, **2005**;

[312] H.G.M. Edwards, E.M. Newton, S. O'Connor, D. Evans, *Anal. Bioanal. Chem.* **2010**; *397*, 2685.

[313] L. He, N. Wang, X. Zhao, T. Zhou, Y. Xia, J. Liang, B. Rong, *J. Archaeol. Sci.* **2012**; *39*, 1809.

[314] K. Castro, A. Sarmiento, M. Maguregui, I. Martínez-Arkarazo, N. Etxebarria, M. Angulo, M.U. Barrutia, J.M. González-Cembellín, J.M. Madariaga, *Anal. Bioanal. Chem.* **2008**; *392*, 755.

[315] P.J. Jin, W. Huang, Jianhua-Wang, G. Zhao, X.L. Wang, *J. Mol. Struct.* **2010**; *983*, 22.

[316] N. Wang, L. He, E. Egel, S. Simon, B. Rong, *Microchem. J.* **2014**; *114*, 125.

[317] P. Baraldi, A. Lo Monaco, F. Ortenzi, C. Pelosi, F. Quarato, L. Rossi, *Archaeometry* **2014**; *56*, 313.

[318] H.G.M. Edwards, E. Beale, N.C. Garrington, J. –M. Alia, *J. Raman Spectrosc.* **2007**; *38*, 316.

[319] I. Aliatis, D. Bersani, P. Paolo, I. Gabriel, P.P. Lottici, I.G. Marino, *ArcheoSciences* **2012**; *36*, 7.

[320] M.L. Franquelo, A. Duran, J. Castaing, D. Arquillo, J.L. Perez-Rodriguez, *Talanta* **2012**; *89*, 462.

[321] A. Lo Monaco, E. Mattei, C. Pelosi, M. Santancini, *J. Cult. Herit.* **2013**; *14*, 537.

[322] S. Kuckova, I.C.A. Sandu, M. Crhova, R. Hynek, I. Fogas, V.S. Muralha, A.V. Sandu, *Microchem. J.* **2013**; *110*, 538.

[323] A. De Santis, E. Mattei, C. Pelosi, *J. Raman Spectrosc.* **2007**; *38*, 1368.

[324] L.D. Kock, D. De Waal, *Spectrochim. Acta - Part A Mol. Biomol. Spectrosc.* **2008**; *71*, 1348.

[325] M.S. Walton, K. TRENTELMAN, *Archaeometry* **2009**; *51*, 845.

[326] L. Bonizzoni, S. Bruni, V. Guglielmi, M. Milazzo, O. Neri, *Archaeometry* **2011**; *53*, 1212.

[327] M.L. Franquelo, A. Duran, L.K. Herrera, M.C. Jimenez de Haro, J.L. Perez-Rodriguez, *J. Mol. Struct.* **2009**; *924-926*, 404.

[328] C. Canevali, P. Gentile, M. Orlandi, F. Modugno, J.J. Lucejko, M.P. Colombini, L. Brambilla, S. Goidanich, C. Riedo, O. Chiantore, P. Baraldi, C. Baraldi, M.C. Gamberini, *Anal. Bioanal. Chem.* **2011**; *401*, 1801.

[329] Z. Tóth, J. Mihály, A.J. Tóth, G. Ilon, *Archeometriai Műhely* **2013**; *X*, 103.

[330] Z. Liu, Y. Han, L. Han, Y. Cheng, Y. Ma, L. Fang, *Spectrochim. Acta - Part A Mol. Biomol. Spectrosc.* **2013**; *109*, 42.

[331] M.M.V. Campos, T.A. Aguayo, *Herit. Sci.* **2015**; *3*, 18.

[332] A. Fostiridou, I. Karapanagiotis, S. Vivdenko, D. Lampakis, D. Mantzouris, L. Achilara, P. Manoudis, *Archaeometry* **2015**; doi: 10.1111/arcm.12177n/a.

[333] V. Košařová, D. Hradil, I. Němec, P. Bezdička, V. Kanický, *J. Raman Spectrosc.* **2013**; *44*, 1570.

[334] M. Oujja, M. Sanz, E. Rebollar, J.F. Marco, C. Domingo, P. Pouli, S. Kogou, C. Fotakis, M. Castillejo, *Spectrochim. Acta - Part A Mol. Biomol. Spectrosc.* **2013**; *102*, 7.

[335] N. Navas, J. Romero-Pastor, E. Manzano, C. Cardell, *J. Raman Spectrosc.* **2010**; *41*, 1486.

[336] E. Siotto, M. Dellepiane, M. Callieri, R. Scopigno, C. Gratziu, A. Moscato, L. Burgio, S. Legnaioli, G. Lorenzetti, V. Palleschi, *J. Cult. Herit.* **2014**; *16*, 307.

[337] C. Conti, C. Colombo, M. Realini, P. Matousek, *J. Raman Spectrosc.* **2015**; *46*, 476.

[338] D. Barilaro, V. Crupi, D. Majolino, G. Barone, R. Ponterio, *J. Appl. Phys.* **2005**; *97*, 044907.

[339] F. Rosi, C. Miliani, I. Borgia, B. Brunetti, a Sgamellotti, *J. Raman Spectrosc.* **2004**; *35*, 610.

[340] O. López-Cruz, A. García-Bueno, V.J. Medina-Flórez, A. Sánchez-Navas, N. Velilla, *Mater. Construcción* **2015**; *65*, e054.

[341] P. Baraldi, A. Bonazzi, N. Giordani, F. Paccagnella, P. Zannini, *Archaeometry* **2006**; *48*, 481.

[342] R. Mazzeo, E. Joseph, V. Minguzzi, G. Grillini, P. Baraldi, D. Prandstraller, *J. Raman Spectrosc.* **2006**; *37*, 1086.

[343] D. Parras-Guijarro, M. Montejo-Gámez, N. Ramos-Martos, A. Sánchez, *Spectrochim. Acta - Part A Mol. Biomol. Spectrosc.* **2006**; *64*, 1133.

[344] L. Lepot, S. Denoël, B. Gilbert, *J. Raman Spectrosc.* **2006**; *37*, 1098.

[345] T. Zorba, K.S. Andrikopoulos, K.M. Paraskevopoulos, E. Pavlidou, K. Popkonstantinov, R. Kostova, V. Platnyov, S. Daniilia, *Ann. Chim.* **2007**; *97*, 491.

[346] G.A. Mazzocchin, D. Rudello, E. Murgia, *Ann. Chim.* **2007**; *97*, 807.

[347] S. Daniilia, S. Sotiropoulou, D. Bikiaris, C. Salpistis, G. Karagiannis, Y. Chryssoulakis, B. A. Price, J.H. Carlson, *J. Cult. Herit.* **2000**; *1*, 91.

[348] P. Baraldi, C. Baraldi, R. Curina, L. Tassi, P. Zannini, *Vib. Spectrosc.* **2007**; *43*, 420.

[349] R. Mazzeo, P. Baraldi, R. Lujàn, C. Fagnano, *J. Raman Spectrosc.* **2004**; *35*, 678.

[350] S. Aze, J.-M. Vallet, A. Baronnet, O. Grauby, *Eur. J. Mineral.* **2006**; *18*, 835.

[351] M. Pérez-Alonso, K. Castro, I. Martinez-Arkarazo, M. Angulo, M. A. Olazabal, J.M. Madariaga, *Anal. Bioanal. Chem.* **2004**; *379*, 42.

[352] M. Pérez-Alonso, K. Castro, M. Álvarez, J.M. Madariaga, *Anal. Chim. Acta* **2004**; *524*, 379.

[353] G.A. Mazzocchin, E.F. Orsega, P. Baraldi, P. Zannini, *Ann. Chim.* **2006**; *96*, 377.

[354] R. A. Goodall, J. Hall, H.G.M. Edwards, R.J. Sharer, R. Viel, P.M. Fredericks, *J. Archaeol. Sci.* **2007**; *34*, 666.

[355] F. Bordignon, P. Postorino, A. Nucara, P. Dore, G. Trojsi, V. Bellelli, *J. Cult. Herit.* **2008**; *9*, 23.

[356] S. Daniilia, E. Minopoulou, K.S. Andrikopoulos, A. Tsakalof, K. Bairachtari, *J. Archaeol. Sci.* **2008**; *35*, 2474.

[357] M. Castriota, E. Meduri, T. Barone, G. De Santo, E. Cazzanelli, *J. Raman Spectrosc.* **2008**; *39*, 284.

[358] A. Zucchiatti, *Surf. Eng.* **2008**; *24*, 162.

[359] M. Sawczak, A. Kamińska, G. Rabczuk, M. Ferretti, R. Jendrzejewski, G. Śliwiński, *Appl. Surf. Sci.* **2009**; *255*, 5542.

[360] H.G.M. Edwards, P.S. Middleton, M.D. Hargreaves, *Spectrochim. Acta - Part A Mol. Biomol. Spectrosc.* **2009**; *73*, 553.

[361] B. Minceva-Sukarova, O. Grupce, V. Tanevska, L. Robeva-Cukovska, S. Mamucevska-Miljkovic, *Maced. J. Chem. Chem. Eng.* **2007**; *26*, 103.

[362] A. Sodo, D. Artioli, A. Botti, G. De Palma, A. Giovagnoli, M. Mariottini, A. Paradisi, C. Polidoro, M.A. Ricci, *J. Raman Spectrosc.* **2008**; *39*, 1035.

[363] A. Nevin, J.L. Melia, I. Osticioli, G. Gautier, M.P. Colombini, *J. Cult. Herit.* **2008**; *9*, 154.

[364] A. Hernanz, I. Bratu, O.F. Marutoiu, C. Marutoiu, J.M. Gavira-Vallejo, H.G.M. Edwards, *Anal. Bioanal. Chem.* **2008**; *392*, 263.

[365] L. Boselli, S. Ciattini, M. Galeotti, M.R. Lanfranchi, C. Lofrumento, M. Picollo, A. Zoppi, *E-Preservation Sci.* **2009**; *6*, 38.

[366] P. Vandenabeele, R. Garcia-Moreno, F. Mathis, K. Leterme, E. Van Elslande, F.-P.P. Hocquet, S. Rakkaa, D. Laboury, L. Moens, D. Strivay, M. Hartwig, *Spectrochim. Acta - Part A Mol. Biomol. Spectrosc.* **2009**; *73*, 546.

[367] Q.G. Zeng, G.X. Zhang, C.W. Leung, J. Zuo, *Microchem. J.* **2010**; *96*, 330.

[368] A. Sansonetti, J. Striova, D. Biondelli, E.M. Castellucci, *Anal. Bioanal. Chem.* **2010**; *397*, 2667.

[369] A. Duran, M.C. Jimenez De Haro, J.L. Perez-Rodriguez, M.L. Franquelo, L.K. Herrera, A. Justo, *Archaeometry* **2010**; *52*, 286.

[370] A. Deneckere, W. Schudel, M. Van Bos, H. Wouters, A. Bergmans, P. Vandenabeele, L. Moens, *Spectrochim. Acta - Part A Mol. Biomol. Spectrosc.* **2010**; *75*, 511.

[371] R.J.H. Clark, R.R. Hark, N. Salvadó, S. Butí, T. Pradell, *J. Raman Spectrosc.* **2010**; *41*, 1418.

[372] T. Aguayo, E. Clavijo, F. Eisner, C. Ossa-Izquierdo, M.M. Campos-Vallette, *J. Raman Spectrosc.* **2011**; *42*, 2143.

[373] I. Garofano, A. Duran, J.L. Perez-Rodriguez, M.D. Robador, in:, Spectrosc. Lett., CSIC, Spain, Madrid, 2011, pp. 560–565.

[374] M.K. Donais, D. George, B. Duncan, S.M. Wojtas, A. M. Daigle, *Anal. Methods* **2011**; *3*, 1061.

[375] D. Comelli, A. Nevin, G. Valentini, I. Osticioli, E.M. Castellucci, L. Toniolo, D. Gulotta, R. Cubeddu, *J. Cult. Herit.* **2011**; *12*, 11.

[376] H.H.M. Mahmoud, *Mediterr. Archaeol. Archaeom.* **2011**; *11*, 99.

[377] A. Duran, J.L. Perez-Rodriguez, M.C. Jimenez de Haro, M.L. Franquelo, M.D. Robador, *J. Archaeol. Sci.* **2011**; *38*, 2366.

[378] C. Clementi, V. Ciocan, M. Vagnini, B. Doherty, M.L. Tabasso, C. Conti, B.G. Brunetti, C. Miliani, *Anal. Bioanal. Chem.* **2011**; *401*, 1815.

[379] M. Maguregui, U. Knuutinen, I. Martínez-Arkarazo, K. Castro, J.M. Madariaga, *Anal. Chem.* **2011**; *83*, 3319.

[380] J. Romero-Pastor, A. Duran, A.B. Rodríguez-Navarro, R. Van Grieken, C. Cardell, *Anal. Chem.* **2011**; *83*, 8420.

[381] M. Gil, M.L. Carvalho, S. Longelin, I. Ribeiro, S. Valadas, J. Mirão, A.E. Candeias, *Appl. Spectrosc.* **2011**; *65*, 782.

[382] A. Iordanidis, J. Garcia-Guinea, A. Strati, A. Gkimourtzina, A. Papoulidou, *Spectrochim. Acta - Part A Mol. Biomol. Spectrosc.* **2011**; *78*, 874.

[383] E. Gliozzo, F. Cavari, D. Damiani, I. Memmi, *Archaeometry* **2012**; *54*, 278.

[384] H.H.M. Mahmoud, *Archeometriai Műhely* **2012**; 3, 205.

[385] G. Nord, K. Tronner, **2014**; *109*, 118.

[386] M.T. Doménech-Carbó, H.G.M. Edwards, A. Doménech-Carbó, J.M. Del Hoyo-Meléndez, J. De La Cruz-Canizares, *J. Raman Spectrosc.* **2012**; *43*, 1250.

[387] M. Irazola, M. Olivares, K. Castro, M. Maguregui, I. Martínez-Arkarazo, J.M. Madariaga, *J. Raman Spectrosc.* **2012**; *43*, 1676.

[388] A. Paradisi, A. Sodo, D. Artioli, A. Botti, D. Cavezzali, A. Giovagnoli, C. Polidoro, M. A. Ricci, *Archaeometry* **2012**; *54*, 1060.

[389] A. Sánchez, J. Tuñón, M. Montejo, D. Parras, *J. Raman Spectrosc.* **2012**; *43*, 1788.

[390] H.H.M. Mahmoud, N. Kantiranis, J. Stratis, *Mediterr. Archaeol. Archaeom.* **2012**; *12*, 81.

[391] E. Conz, L. Appolonia, P. Galinetto, M.P. Riccardi, S. Tarantino, M. Zema, *Procedia Chem.* **2013**; *8*, 78.

[392] F. Toschi, A. Paladini, F. Colosi, P. Cafarelli, V. Valentini, M. Falconieri, S. Gagliardi, P. Santoro, *Appl. Surf. Sci.* **2013**; *284*, 291.

[393] M. Gil, C. Araujo, M.L. Carvalho, S. Longelin, L. Dias, S. Valadas, C. Souto, J. Frade, I. Ribeiro, J. Mirão, A. Candeias, *X-Ray Spectrom.* **2013**; *42*, 242.

[394] H.H.M. Mahmoud, *Acta Phys. Pol. A* **2013**; *123*, 782.

[395] M. Aceto, G. Gatti, A. Agostino, G. Fenoglio, V. Giordano, M. Varetto, G. Castagneri, *J. Raman Spectrosc.* **2012**; *43*, 1754.

[396] D. Bersani, P.P. Lottici, A. Casoli, M. Ferrari, S. Lottini, D. Cauzzi, *Lasers Conserv. Artworks Lacona VI Proceedings, Vienna, Austria, Sept. 21-25, 2005* **2007**; 383.

[397] M. Maguregui, U. Knuutinen, I. Martínez-Arkarazo, A. Giakoumaki, K. Castro, J.M. Madariaga, *J. Raman Spectrosc.* **2012**; *43*, 1747.

[398] M. Maguregui, U. Knuutinen, J. Trebolazabala, H. Morillas, K. Castro, I. Martinez-Arkarazo, J.M. Madariaga, *Anal. Bioanal. Chem.* **2012**; *402*, 1529.

[399] A. Zoppi, C. Lofrumento, M. Ricci, E. Cantisani, T. Fratini, E.M. Castellucci, *J. Raman Spectrosc.* **2012**; *43*, 1663.

[400] L.R. Čukovska, B. Minčeva - Šukarova, A. Lluveras-Tenorio, A. Andreotti, M.P. Colombini, I. Nastova, *J. Raman Spectrosc.* **2012**; *43*, 1685.

[401] G.E. De Benedetto, A. Savino, D. Fico, D. Rizzo, A. Pennetta, A. Cassiano, B. Minerva, *Open J. Archaeom.* **2013**; *1*, 12.

[402] T. Zhu, J. Chen, R. Hui, *Anal. Lett.* **2013**; *46*, 37.

[403] A. Iordanidis, J. Garcia-Guinea, A. Strati, A. Gkimourtzina, *Anal. Lett.* **2014**; *47*, 2708.

[404] Z. Li, L. Wang, Q. Ma, J. Mei, *Herit. Sci.* **2014**; *2*, 21.

[405] D. Damiani, E. Gliozzo, I. Memmi Turbanti, *Archaeol. Anthropol. Sci.* **2014**; *6*, 363.

[406] D. Bersani, M. Berzioli, S. Caglio, A. Casoli, P.P. Lottici, L. Medeghini, G. Poldi, P. Zannini, *Microchem. J.* **2014**; *114*, 80.

[407] M. Gil, V. Serrão, M.L. Carvalho, S. Longelin, L. Dias, A. Cardoso, A. T. Caldeira, T. Rosado, J. Mirão, A. E. Candeias, *Color Res. Appl.* **2014**; *39*, 288.

[408] O. Syta, K. Rozum, M. Choińska, D. Zielińska, G.Z. Żukowska, A. Kijowska, B. Wagner, *Spectrochim. Acta - Part B At. Spectrosc.* **2014**; *101*, 140.

[409] J.M. Madariaga, M. Maguregui, S.F.-O. De Vallejuelo, U. Knuutinen, K. Castro, I. Martinez-Arkarazo, A. Giakoumaki, A. Pitarch, *J. Raman Spectrosc.* **2014**; *45*, 1059.

[410] H.H.M. Mahmoud, *Herit. Sci.* **2014**; *2*, 18.

[411] J.L. Perez-Rodriguez, M.D. Robador, M.A. Centeno, B. Siguenza, A. Duran, *Spectrochim. Acta - Part A Mol. Biomol. Spectrosc.* **2014**; *120*, 602.

[412] M. Gelzo, M. Grimaldi, A. Vergara, V. Severino, A. Chambery, A. Dello Russo, C. Piccioli, G. Corso, P. Arcari, *Chem. Cent. J.* **2014**; *8*, 1.

[413] M.J. de la Torre-López, A. Dominguez-Vidal, M.J. Campos-Suñol, R. Rubio-Domene, U. Schade, M.J. Ayora-Cañada, *J. Raman Spectrosc.* **2014**; *45*, 1052.

[414] C. Araya, J. Jaque, N. Naranjo, M. Icaza, R.E. Clavijo, T. Aguayo, M.M. Campos-Vallette, *Spectrosc. Lett.* **2014**; *47*, 177.

[415] E. Cheilakou, M. Troullinos, M. Koui, *J. Archaeol. Sci.* **2014**; *41*, 541.

[416] A. Paladini, F. Toschi, F. Colosi, G. Rubino, P. Santoro, *Appl. Phys. A* **2014**; *118*, 131.

[417] E. Aquilia, A. Giuffrida, C. Ingoglia, P. Mazzoleni, S. Raneri, *Rend. Fis. Acc. Lincei* **2015**; 26, 475.

[418] M.L. Amadori, S. Barcelli, G. Poldi, F. Ferrucci, A. Andreotti, P. Baraldi, M.P. Colombini, *Microchem. J.* **2015**; *118*, 183.

[419] L.D. Mateos, D. Cosano, M. Mora, I. Muñiz, R. Carmona, C. Jiménez-Sanchidrián, J.R. Ruiz, *Spectrochim. Acta - Part A Mol. Biomol. Spectrosc.* **2015**; *151*, 16.

[420] N. Salvadó, S. Butí, M. A. G. Aranda, T. Pradell, *Anal. Methods* **2014**; *6*, 3610.

[421] M. Veneranda, M. Irazola, A. Pitarch, M. Olivares, A. Iturregui, K. Castro, J.M. Madariaga, *J. Raman Spectrosc.* **2014**; *45*, 228.

[422] M. Veneranda, M. Irazola, M. Díez, A. Iturregui, J. Aramendia, K. Castro, J.M. Madariaga, *J. Raman Spectrosc.* **2014**; *45*, 1110.

[423] M. Maguregui, K. Castro, H. Morillas, J. Trebolazabala, U. Knuutinen, R. Wiesinger, M. Schreiner, J.M. Madariaga, *Anal. Methods* **2014**; *6*, 372.

[424] I. Kakoulli, S. V. Prikhodko, A. King, C. Fischer, *J. Archaeol. Sci.* **2014**; *44*, 148.

[425] R. Piovesan, L. Maritan, J. Neguer, *J. Archaeol. Sci.* **2014**; *46*, 68.

[426] M.S. Gill, C.P. Rendo, S. Menon, *Stud. Conserv.* **2014**; *59*, 300.

[427] L. Yong, W. Shiwei, *Stud. Conserv.* **2014**; *59*, 314.

[428] B.A. Schmidt, M.A. Ziemann, S. Pentzien, T. Gabsch, W. Koch, J. Krüger, *Stud. Conserv.* **2015**; doi: 10.1179/2047058414Y.0000000152

[429] M. Gutman, B. Zupanek, M. Lesar Kikelj, S. Kramar, *Archaeometry* **2015**; doi: 10.1111/arcm.12167.

[430] V. Crupi, G. Galli, M.F. La Russa, F. Longo, G. Maisano, D. Majolino, M. Malagodi, A. Pezzino, M. Ricca, B. Rossi, S.A. Ruffolo, V. Venuti, *Appl. Surf. Sci.* **2015**; *349*, 924.

[431] H. Berke, *Chem. Soc. Rev.* **2007**; *36*, 15.

[432] E. Mattei, G. De Vivo, A. De Santis, C. Gaetani, C. Pelosi, U. Santamaria, *J. Raman Spectrosc.* **2008**; *39*, 302.

[433] F. Daniel, A. Mounier, J. Aramendia, L. Gómez, K. Castro, S. Fdez-Ortiz de Vallejuelo, M. Schlicht, *J. Raman Spectrosc.* **2015**; doi: 10.1002/jrs.4770

[434] M. Aru, L. Burgio, M.S. Rumsey, *J. Raman Spectrosc.* **2014**; *45*, 1013.

[435] G. Chiari, R. Giustetto, G. Ricchiardi, *Eur. J. Mineral.* **2003**; *15*, 21.

[436] R. Giustetto, F.X. Llabrés i Xamena, G. Ricchiardi, S. Bordiga, A. Damin, R. Gobetto, M.R. Chierotti, *J. Phys. Chem. B* **2005**; *109*, 19360.

[437] R. Giustetto, K. Seenivasan, F. Bonino, G. Ricchiardi, S. Bordiga, M.R. Chierotti, R. Gobetto, *J. Phys. Chem. C* **2011**; *115*, 16764.

[438] P. Vandenabeele, S. Bodé, A. Alonso, L. Moens, *Spectrochim. Acta - Part A Mol. Biomol. Spectrosc.* **2005**; *61*, 2349.

[439] M. Sánchez Del Río, M. Picquart, E. Haro-Poniatowski, E. Van Elslande, V.H. Uc, *J. Raman Spectrosc.* **2006**; *37*, 1046.

[440] F.S. Manciu, L. Reza, L. A. Polette, B. Torres, R.R. Chianelli, *J. Raman Spectrosc.* **2007**; *38*, 1193.

[441] H.G. Wiedemann, K.-W.W. Brzezinka, K. Witke, I. Lamprecht, *Thermochim. Acta* **2007**; *456*, 56.

[442] M.S. del Río, L. A. T. Montes, *Thermochim. Acta* **2007**; *466*, 75.

[443] G. Garcia Moreno, D. Strivay, B. Gilbert, *J. Raman Spectrosc.* **2008**; *39*, 1050.

[444] F.S. Manciu, A. Ramirez, W. Durrer, J. Govani, R.R. Chianelli, *J. Raman Spectrosc.* **2008**; *39*, 1257.

[445] A. Doménech, M.T. Doménech-Carbó, H.G.M. Edwards, *J. Raman Spectrosc.* **2011**; *42*, 86.

[446] C. Tsiantos, M. Tsampodimou, G.H. Kacandes, M. Sánchez del Río, V. Gionis, G.D. Chryssikos, *J. Mater. Sci.* **2012**; *47*, 3415.

[447] C. Dejoie, P. Martinetto, E. Dooryhée, P. Strobel, S. Blanc, P. Bordat, R. Brown, F. Porcher, M. Sanchez Del Rio, M. Anne, *ACS Appl. Mater. Interfaces* **2010**; *2*, 2308.

[448] Y. Zhang, L. Fan, H. Chen, J. Zhang, Y. Zhang, A. Wang, *Microporous Mesoporous Mater.* **2015**; *211*, 124.

[449] T. Chivers, P.J.W. Elder, *Chem. Soc. Rev.* **2013**; *42*, 5996.

[450] R.J.H. Clark, T.J. Dines, M. Kurnoo, *Inorg. Chem.* **1983**; *22*, 2766.

[451] N. Gobeltz, A. Demortier, J.P. Lelieur, C. Duhayon, *J. Chem. Soc. Faraday Trans.* **1998**; *94*, 677.

[452] M. Bicchieri, M. Nardone, P.A. Russo, A. Sodo, M. Corsi, G. Cristoforetti, V. Palleschi, A. Salvetti, E. Tognoni, *Spectrochim. Acta - Part B At. Spectrosc.* **2001**; *56*, 915.

[453] M. Ostroumov, E. Fritsch, E. Faulques, O. Cauvet, *Can. Mineral.* **2002**; *40*, 1.

[454] N. Gobeltz-Hautecoeur, A. Demortier, B. Lede, J.P. Lelieur, C. Duhayon, *Inorg. Chem.* **2002**; *41*, 2848.

[455] V. Desnica, K. Furic, M. Schreiner, *E-Preservation Sci.* **2004**; *1*, 15.

[456] E. Del Federico, W. Shöfberger, J. Schelvis, S. Kapetanaki, L. Tyne, A. Jerschow, *Inorg. Chem.* **2006**; *45*, 1270.

[457] P. Ballirano, A. Maras, *Am. Mineral.* **2006**; *91*, 997.

[458] E.M. a Ali, H.G.M. Edwards, *Spectrochim. Acta - Part A Mol. Biomol. Spectrosc.* **2014**; *121*, 415.

[459] M.M. Barsan, I.S. Butler, D.F.R. Gilson, *Spectrochim. Acta - Part A Mol. Biomol. Spectrosc.* **2012**; *98*, 457.

[460] R. Clark, M. Curri, C. Laganara, *Spectrochim. Acta - Part A Mol. Biomol. Spectrosc.* **1997**; *53*, 597.

[461] R. Clark, M. Curri, G. Henshaw, C. Laganara, *J. Raman Spectrosc.* **1997**; *28*, 105.

[462] P. Colomban, *Revue Annuelle de la Société Française d'étude de la céramique Orientale* **2005**; *4*, 145.

[463] S. Greiff, J. Schuster, *J. Cult. Herit.* **2008**; *9*, e27.

[464] A. Mangone, G.E. De Benedetto, D. Fico, L.C. Giannossa, R. Laviano, L. Sabbatini, I.D. van der Werf, A. Traini, *New J. Chem.* **2011**; *35*, 2860.

[465] A. Tournié, L.C. Prinsloo, P. Colomban, *J. Raman Spectrosc.* **2012**; *43*, 532.

[466] L.C. Prinsloo, A. Tournié, P. Colomban, *J. Archaeol. Sci.* **2011**; *38*, 3264.

[467] P. Colomban, A. Tournié, M.C. Caggiani, C. Paris, *J. Raman Spectrosc.* **2012**; *43*, 1975.

[468] M. Sendova, B. Kaiser, M. Scalera, V. Zhelyaskov, *J. Raman Spectrosc.* **2010**; *41*, 469.

[469] M. Derrick, D. Stulik, J. Landry, Infrared Spectroscopy in Conservation Science, The Getty , Los Angeles, **2000**.

[470] C. Miliani, A. Daveri, B.G. Brunetti, A. Sgamellotti, *Chem. Phys. Lett.* **2008**; *466*, 148.

[471] M. Bacci, C. Cucci, E. Del Federico, A. Ienco, A. Jerschow, J.M. Newman, M. Picollo, *Vib. Spectrosc.* **2009**; *49*, 80.

[472] M. Favaro, A. Guastoni, F. Marini, S. Bianchin, A. Gambirasi, *Anal. Bioanal. Chem.* **2012**; *402*, 2195.

[473] I. Osticioli, N.F.C. Mendes, A. Nevin, F.P.S.C. Gil, M. Becucci, E. Castellucci, *Spectrochim. Acta - Part A Mol. Biomol. Spectrosc.* **2009**; *73*, 525.

[474] I. Osticioli, N.F.C. Mendes, A. Nevin, A. Zoppi, C. Lofrumento, M. Becucci, E.M. Castellucci, *Rev. Sci. Instrum.* **2009**; *80*, 78.

[475] C.M. Schmidt, M.S. Walton, K. Trentelman, *Anal. Chem.* **2009**; *81*, 8513.

[476] A. R. De Torres, S. Ruiz-Moreno, A. López-Gil, P. Ferrer, M.C. Chillón, *J. Raman Spectrosc.* **2014**; *45*, 1279.

[477] A. Dominguez-Vidal, M. Jose de la Torre-Lopez, R. Rubio-Domene, M.J. Ayora-Cañada, *Analyst* **2012**; *137*, 5763.

[478] A. Veiga, J. Mirão, A.J. Candeias, P. Simões Rodrigues, D. Martins Teixeira, V.S.F. Muralha, J. Ginja Teixeira, *J. Raman Spectrosc.* **2014**; *45*, 947.

[479] A. Palet Casas, J.D. Andrés Llopis, *Stud. Conserv.* **1992**; *37*, 132.

[480] F. Daniel, A. Mounier, B. Laborde, É. Coulon, in: Proceedings of V Congr. Naz. Di Archeometria, Syracuse, Italy, **2008**, pp 307-316

[481] F. Daniel, B. Laborde, A. Mounier, É. Coulon, *ArcheoSciences Rev. D'archéometrie* **2008**; *32*, 83.

[482] N. Buzgar, A. Buzatu, A.-I. Apopei, V. Cotiugă, *Vib. Spectrosc.* **2014**; *72*, 142.

[483] J. Pérez-Arantegui, C. Pardos, J.-L. Abad, J.-R. García, *Microsc. Microanal.* **2013**; *19*, 1645.

[484] R. Garcia Moreno, F. Mathis, V. Mazel, M. Dubus, T. Calligaro, D. Strivay, *Archaeometry* **2008**; *50*, 658.

[485] D. A. Scott, G. Eggert, *Rev. Conserv.* **2007**; *52 Suppl.1*, 3.

[486] Z. Čermáková, J. Hradilová, J. Jehlička, K. Osterrothová, A. Massanek, P. Bezdička, D. Hradil, *Archaeometry* **2014**; *56*, 148.

[487] Z. Čermáková, S. Švarcová, J. Hradilová, P. Bezdička, A. Lančok, V. Vašutová, J. Blažek, D. Hradil, *Spectrochim. Acta - Part A Mol. Biomol. Spectrosc.* **2015**; *140*, 101.

[488] J.T. Kloprogge, D. Visser, W.N. Martens, L.V. Duong, R.L. Frost, *Netherlands J. Geosci. En Mijnbouw.* **2003**; *82*, 209.

[489] S.E. Filippakis, B. Perdikatsis, T. Paradellis, *Stud. Conserv.* **1976**; *21*, 143.

[490] A. Brysbaert, *J. Archaeol. Sci.* **2008**; *35*, 2761.

[491] P. Westlake, P. Siozos, A. Philippidis, C. Apostolaki, B. Derham, A. Terlixi, V. Perdikatsis, R. Jones, D. Anglos, *Anal. Bioanal. Chem.* **2012**; *402*, 1413.

[492] A.G. Vlachopoulos, S. Sotiropoulou, *Talanta* **2012**; *44*, 245.

[493] S. Sotiropoulou, V. Perdikatsis, K. Birtacha, C. Apostolaki, A. Devetzi, *Archaeol. Anthropol. Sci.* **2012**; *4*, 263.

[494] K. Castro, A. Sarmiento, I. Martínez-Arkarazo, J.M. Madariaga, L.A. Fernández, I. Martínez-Arkarazo, J.M. Madariaga, L.A. Fernández, *Anal. Chem.* **2008**; *80*, 4103.

[495] B.S. Yu, J.N. Fang, E.P. Huang, *J. Raman Spectrosc.* **2013**; *44*, 630.

[496] I. Aliatis, D. Bersani, E. Campani, A. Casoli, P.P. Lottici, S. Mantovan, I.G. Marino, F. Ospitali, *Spectrochim. Acta - Part A Mol. Biomol. Spectrosc.* **2009**; *73*, 532.

[497] L.M. Moretto, E.F. Orsega, G.A. Mazzocchin, *J. Cult. Herit.* **2011**; *12*, 384.

[498] C. Genestar, C. Pons, *Anal. Bioanal. Chem.* **2005**; *382*, 269.

[499] S. Daniilia, D. Bikiaris, L. Burgio, P. Gavala, R.J.H. Clark, Y. Chryssoulakis, *J. Raman Spectrosc.* **2002**; *33*, 807.

[500] R. A. Goodall, J. Hall, R. Viel, F.R. Agurcia, H.G.M. Edwards, P.M. Fredericks, *J. Raman Spectrosc.* **2006**; *37*, 1072.

[501] F. Ospitali, D. Bersani, G. Di Lonardo, P.P. Lottici, *J. Raman Spectrosc.* **2008**; *39*, 1066.

[502] O. Cristini, C. Kinowski, S. Turrell, *J. Raman Spectrosc.* **2010**; *41*, 1410.

[503] J.L. Perez-Rodriguez, M.D.C.J. de Haro, B. Siguenza, J.M. Martinez-Blanes, *Appl. Clay Sci.* **2015**; 116-117, 211.

[504] K.F. Gebremariam, L. Kvittingen, F.-G. Banica, *Archaeometry* **2015**. doi: 10.1111/arcm.12163

[505] C. Pelosi, G. Agresti, M. Andaloro, P. Baraldi, P. Pogliani, U. Santamaria, M.F. La Russa, S. A. Ruffolo, N. Rovella, *Archaeometry* **2015**; doi: 10.1111/arcm.12184

[506] D. Scott, *Stud. Conserv.* **2000**; *45*, 39.

[507] D.A. Scott, *Copper and Bronze in Art : Corrosion, Colorants, Conservation*, Getty Conservation Institute, **2002**.

[508] B. Gilbert, S. Denoël, G. Weber, D. Allart, *Analyst* **2003**; *128*, 1213.

[509] K. Castro, S. Pessanha, N. Proietti, E. Princi, D. Capitani, M.L. Carvalho, J.M. Madariaga, *Anal. Bioanal. Chem.* **2008**; *391*, 433.

[510] G. Bertolotti, D. Bersani, P.P. Lottici, M. Alesiani, T. Malcherek, J. Schlüter, *Anal. Bioanal. Chem.* **2012**; *402*, 1451.

[511] K. Eremin, J. Stenger, M. Li Green, *J. Raman Spectrosc.* **2006**; *37*, 1119.

[512] E. Bidaud, E. Halwax, E. Pantos, B. Sipek, *Stud. Conserv.* **2008**; *53*, 81.

[513] L. Burgio, R.J.H. Clark, V.S.F. Muralha, T. Stanley, *J. Raman Spectrosc.* **2008**; *39*, 1482.

[514] M.J. Campos-Suñol, M.J. De la torre-Lopez, M.J. Ayora-Cañada, A. Dominguez-Vidal, *J. Raman Spectrosc.* **2009**; *40*, 2104.

[515] Q.M. S. Wei, M. Schreiner, H. Guo, *Int. J. Conserv. Sci.* **2010**; *1*, 99.

[516] E.P. Tomasini, C.R. Landa, G. Siracusano, M.S. Maier, *J. Raman Spectrosc.* **2013**; *44*, 637.

[517] L. Yong, *Stud. Conserv.* **2012**; *57*, 106.

[518] D. Cauzzi, G. Chiavari, S. Montalbani, D. Melucci, D. Cam, H. Ling, *J. Cult. Herit.* **2013**; *14*, 70.

[519] E. Egel, S. Simon, *Herit. Sci.* **2013**; *1*, 29.

[520] K. Hu, *Herit. Sci.* **2013**; *1*, 1.

[521] A. Dominguez-Vidal, M.J. de la Torre-López, M.J. Campos-Suñol, R. Rubio-Domene, M.J. Ayora-Cañada, *J. Raman Spectrosc.* **2014**; *45*, 1006.

[522] S. Švarcová, Z. Čermáková, J. Hradilová, P. Bezdička, D. Hradil, *Spectrochim. Acta - Part A Mol. Biomol. Spectrosc.* **2014**; *132*, 514.

[523] S. Valadas, R. V. Freire, A. Cardoso, J. Mirão, C.B. Dias, P. Vandenabeele, A. Candeias, *Microsc. Microanal.* **2015**; *21*, 518.

[524] Y. Zhang, J. Wang, H. Liu, X. Wang, S. Zhang, *Anal. Lett.* **2015**; *48*, 2400.

[525] T. Akyuz, S. Akyuz, A. Gulec, *Spectrochim. Acta - Part A Mol. Biomol. Spectrosc.* **2015**; *149*, 744.

[526] I. Aliatis, D. Bersani, E. Campani, A. Casoli, P.P. Lottici, S. Mantovan, I.G. Marino, *J. Raman Spectrosc.* **2010**; *41*, 1537.

[527] P. Baraldi, P. Moioli, P. Santopadre, C. Seccaroni, *Boll. ICR* **2009**; *18-19*, 23.

[528] Q.G. Zeng, G.X. Zhang, J.H. Tan, C.W. Leung, J. Zuo, *J. Raman Spectrosc.* **2011**; *42*, 1311.

[529] A. Klisińska-Kopacz, *J. Raman Spectrosc.* **2015**; *46*, 317.

[530] G. Gatto Rotondo, L. Darchuk, M. Swaenen, R. Van Grieken *J. Anal. Sci. Methods Instrum.* **2012**; *2*, 42.

[531] J. Ambers, *J. Raman Spectrosc.* **2004**; *35*, 768.

[532] N. Buzgar, A. Buzatu, A.I. Apopei, D. Aștefanei, F. Topoleanu, *Analele Stiint. Ale Univ. " Al. I. Cuza" Din Iasi , Geol.* **2011**; *57*, 15.

[533] M. Sepúlveda, S. Gutierrez, M. Campos-Vallette, E. Clavijo, P. Walter, J.J. Cárcamo, *J. Chil. Chem. Soc.* **2013**; *58*, 1836.

[534] C. Pelosi, G. Agresti, M. Andaloro, P. Baraldi, P. Pogliani, U. Santamaria, *E-Preservation Sci.* **2013**; *10*, 99.

[535] L. Monico, K. Janssens, E. Hendriks, B.G. Brunetti, C. Miliani, *J. Raman Spectrosc.* **2014**; *45*, 1034.

[536] Mugnaini, S, A. Bagnoli, P. Bensi, F. Droghini, A. Scala, G. Guasparri, *J. Cult. Herit.* **2006**; *7*, 355.

[537] G. Guasparri, *J. Cult. Herit.* **2006**; *7*, 355.

[538] D. Hradil, J. Hradilová, P. Bezdička, S. Švarcová, Z. Čermáková, V. Košařová, I. Němec, *J. Raman Spectrosc.* **2014**; *45*, 848.

[539] M. Abdel-Ghani, H.H.M. Mahmoud, *J. Archaeol. Restor. Stud.* **2013**; *3*, 95.

[540] H.G.M. Edwards, P. Vandenabeele, J. Jehlicka, T.J. Benoy, *Spectrochim. Acta - Part A Mol. Biomol. Spectrosc.* **2014**; *118*, 598.

[541] F. Bellini, D. Bersani, H.G.M. Edwards, J. Jehlicka, P. Vandenabeele, P. P. Lottici, 8th Congress on the Application of Raman Spectroscopy in Art and Archaeology - RAA 2015, Wroclaw, 1-5 September 2015, M. Czarnecka and B. Lydzba-Kopczynska eds., Faculty of Chemistry, University of Wroclaw - ISBN:978-83-60043-27-1

[542] D.L.A. de Faria, S.V. Silva, M.T. de Oliveira, *J. Raman Spectrosc.* **1997**; *28*, 873.

[543] D. Bikiaris, S. Daniilia, S. Sotiropoulou, O. Katsimbiri, E. Pavlidou, A.P.P. Moutsatsou, Y. Chryssoulakis, *Spectrochim. Acta - Part A Mol. Biomol. Spectrosc.* **2000**; *56*, 3.

[544] L.F.C. de Oliveira, H.G.M. Edwards, R.L. Frost, J.T. Kloprogge, P.S. Middleton, *Analyst* **2002**; *127*, 536.

[545] D. Hradil, T. Grygar, J. Hradilová, P. Bezdička, *Appl. Clay Sci.* **2003**; *22*, 223.

[546] I. V Chernyshova, M.F. Hochella, a S. Madden, *Phys. Chem. Chem. Phys.* **2007**; *9*, 1736.

[547] M. A. Legodi, D. de Waal, *Dye. Pigment.* **2006**; *74*, 161.

[548] D. Hradil, J. Hradilová, P. Bezdicka, in: D. Hradil, J. Hradilova (Eds.), Acta Artis Acad. 2010 Príbeh Umení Promen. Výtvarného Díla v Case Sborník 3. Mezioborové Konf. ALMA = Story Art Artwork Chang. Time Proc. 3rd Interdiscip. Conf. ALMA, Acad Mat Res Lab Painted Artworks, 2010, pp. 123–136.

[549] P.R. Palacios, A. Bustamante, P. Romero-Gómez, J.C. González, *Hyperfine Interact.* **2011**; *203*, 113.

[550] F. Froment, A. Tournié, P. Colomban, *J. Raman Spectrosc.* **2008**; *39*, 560.

[551] C. Montagner, D. Sanches, J. Pedroso, M.J. Melo, M. Vilarigues, *Spectrochim. Acta - Part A Mol. Biomol. Spectrosc.* **2013**; *103*, 409.

[552] L. Appolonia, D. Vaudan, V. Chatel, M. Aceto, P. Mirti, *Anal. Bioanal. Chem.* **2009**; *395*, 2005.

[553] K. Trentelman, N. Turner, *J. Raman Spectrosc.* **2009**; *40*, 577.

[554] K. Trentelman, *J. Raman Spectrosc.* **2009**; *40*, 585.

[555] N. Buzgar, A.I. Apopei, A. Buzatu, *J. Archaeol. Sci.* **2013**; *40*, 2128.

[556] N. Buzgar, G. Bodi, A. Buzatu, A.-I. Apopei, D. Aştefanei, *Analele Stiint. Ale Univ. " Al. I. Cuza" Din Iasi, Geol.* **2010**; *56*, 95.

[557] E. P. Tomasini, G. Siracusano, M.S. Maier, *Microchem. J.* **2012**; *102*, 28.

[558] E.P. Tomasini, B. Gómez, E.B. Halac, M. Reinoso, E.J. Di Liscia, G. Siracusano, M.S. Maier, *Herit. Sci.* **2015**; *3*, 19.

[559] M. Spring, R. Grout, R. White, *Natl. Gall. Tech. Bull.* **2003**; *24*, 96.

[560] G. Cavallo, K. Gianoli Barioni, *Herit. Sci.* **2015**; *3*, 5.

[561] E.P. Tomasini, C.M. Favier Dubois, N.C. Little, S. A. Centeno, M.S. Maier, *Microchem. J.* **2015**; *121*, 157.

[562] E. Ay, M. Kibaroğlu, C. Berthold, *Archaeol. Anthropol. Sci.* **2014**; *6*, 125.

[563] R. Nöller, *Stud. Conserv*. **2015**; *60*, 79.

[564] M. Radepont, Y. Coquinot, K. Janssens, J.-J. Ezrati, W. de Nolf, M. Cotte, *J. Anal. At. Spectrom.* **2015**; *30*, 599.

[565] M. Cotte, J. Susini, N. Metrich, A. Moscato, C. Gratziu, A. Bertagnini, M. Pagano, *Anal. Chem.* **2006**; *78*, 7484.

[566] C. Hogan, F. Da Pieve, *J. Anal. At. Spectrom.* **2015**; *30*, 588.

[567] S.M. Lussier, G.D. Smith, *Rev. Conserv.* **2007**; *52*, 41.

[568] L. Burgio, R.J.H. Clark, S. Firth, *Analyst* **2001**; *126*, 222.

[569] G.D. Smith, L. Burgio, S. Firth, R.J.H. Clark, *Anal. Chim. Acta* **2001**; *440*, 185.

[570] G. D. Smith, R. J. H. Clark, *Journal of Cultural Heritage* **2002**; 3, 101.

[571] R.J.H. Clark, P.J. Gibbs, *Chem. Commun.* **1997**; 11, 1003.

[572] R.J.H. Clark, P.J. Gibbs, *Anal. Chem.* **1998**; *70*, 99A.

[573] L. Burgio, R. J. H. Clark, P. J. Gibbs, J. Raman Spectrosc. **1999**; 30,*181*.

[574] C. Andalò, M. Bicchieri, P. Bocchini, G. Casu, G.C. Galletti, P. a Mandò, M. Nardone, A. Sodo, M. {Plossi Zappala}, M. Zappalà, C. Andalo, P. a Mando, M. Plossi Zappala, *Anal. Chim. Acta* **2001**; *429*, 279.

[575] S. Daniilia, E. Minopoulou, F.D. Demosthenous, G. Karagiannis, *J. Archaeol. Sci.* **2008**; *35*, 1695.

[576] S. Daniilia, E. Minopoulou, *Appl. Phys. A Mater. Sci. Process.* **2009**; *96*, 701.

[577] S. Aze, Alterations chromatiques des pigments au plomb dans les œuvres du patrimoine - Etude expérimentale des altérations observées sur les peintures murales. PhD Thesis, **2005**, https://tel.archives-ouvertes.fr/tel-00079251.

[578] M. G. T. Rosado, A. Candeias, A.T Caldeira, J. Mirao, in *Science, Technology and Cultural Heritage*, M. A. Rogerio-Candelera, Ed. (CRC Press, **2014**), pp. 217 - 222.

[579] S. Sotiropoulou, S. Daniilia, C. Miliani, F. Rosi, L. Cartechini, D. Papanikola-Bakirtzis, *Appl. Phys. A* **2008**; *92*, 143.

[580] E. Kotulanová, P. Bezdička, D. Hradil, J. Hradilová, S. Švarcová, T. Grygar, *J. Cult. Herit.* **2009**; *10*, 367.

[581] J.P. Petushkova, N.N. Lyalikova, *Stud. Conserv.* **2008**; *31*, 65.

[582] I. Costantini, A. Casoli, D. Pontiroli, D. Bersani, P.P. Lottici, in: P. Ropret, N. Ocepek (Eds.), 7th Int. Congr. Appl. Raman Spectrosc. Art Archaeol. RAA2013, ICPH of Slovenia, Ljubljana, 2013, pp. 6–7.

[583] M. Gutman, M. Lesar-Kikelj, A. Mladenovič, V. Čobal-Sedmak, A. Križnar, S. Kramar, *J. Raman Spectrosc.* **2014**; *45*, 1103.

[584] C. Miguel, A. Claro, A.P. Gonçalves, V.S.F. Muralha, M.J. Melo, *J. Raman Spectrosc.* **2009**; *40*, 1966.

[585] N. Mendes, C. Lofrumento, A. Migliori, E.M. Castellucci, *J. Raman Spectrosc.* **2008**; *39*, 289.

[586] P. Bonazzi, S. Menchetti, G. Pratesi, M. Muniz-Miranda, G.. Sbrana, *Am. Mineral.* **1996**; *81*, 874.

[587] L. Bindi, G. Pratesi, M. Muniz-Miranda, M. Zoppi, L. Chelazzi, G.O. Lepore, S. Menchetti, *Mineral. Mag.* **2015**; *79*, 121.

[588] K. Trentelman, L. Stodulski, M. Pavlosky, *Anal. Chem.* **1996**; *68*, 1755.

[589] P. Vandenabeele, A. von Bohlen, L. Moens, R. Klockenkämper, F. Joukes, G. Dewispelaere, *Anal. Lett.* **2000**; *33*, 3315.

[590] H.G.M. Edwards, F. Rull, P. Vandenabeele, E.M. Newton, L. Moens, J. Medina, C. Garcia, *Appl. Spectrosc.* **2001**; *55*, 71.

[591] R. David, H.G.M. Edwards, D.W. Farwell, D.L. A. De Faria, *Archaeometry* **2001**; *43*, 461.

[592] L. Burgio, R.J.H. Clark, K. Theodoraki, *Spectrochim. Acta - Part A Mol. Biomol. Spectrosc.* **2003**; *59*, 2371.

[593] P. Vandenabeele, L. Moens, in:, K. Janssens, R. van Grieken (Eds.), Compr. Anal. Chem., Elsevier, Amsterdam, **2004**, pp. 635–662.

[594] V. Daniels, B. Leach, *Stud. Conserv.* **2004**; *49*, 73.

[595] L. Burgio, R.J.H. Clark, M. Rosser-Owen, *J. Archaeol. Sci.* **2007**; *34*, 756.

[596] A. Macchia, S.N. Cesaro, L. Campanella, A. Maras, M. Rocchia, G. Roscioli, *J. Appl. Spectrosc.* **2013**; *80*, 1.

[597] G. Pratesi, M. Zoppi, *Am. Mineral.* **2015**; *100*, 1222.

[598] J.P. Ogalde, C.O. Salas, N. Lara, P. Leyton, C. Paipa, M. Campos-vallette, B. Arriaza, *J. Chil. Chem. Soc.* **2014**; *59*, 2571.

[599] M.J. Campos- Suñol, M.J. De la Torre-Lopez, M.J. Ayora- Cañada, A. Dominguez-Vidal, *J. Raman Spectrosc.* **2009**; *40*, 2104.

[600] A. El Bakkali, T. Lamhasni, M. Haddad, S. Ait Lyazidi, S. Sanchez-Cortes, E. Del Puerto Nevado, *J. Raman Spectrosc.* **2013**; *44*, 114.

[601] M. Vermeulen, J. Sanyova, K. Janssens, *Herit. Sci.* **2015**; *3*, 9.

[602] G. Grundmann, M. Richter, *Fatto D'archimia Los Pigment. Artif. En Las Técnicas Pictóricas* **2012**; 119.

[603] G. Grundmann, N. Ivleva, M. Richter, H. Stege, C. Haisch, *Stud. Old Master Paint. Technol. Pract. Natl. Gall. Tech. Bull. 30th Anniv. Conf. Postprints* **2011**; 269.

[604] G. Grundmann, M. Richter, *Chim. Int. J. Chem.* **2008**; *62*, 903.

[605] P. Holakooei, A.-H. Karimy, *J. Archaeol. Sci.* **2015**; *54*, 217.

[606] T. Katsaros, I. Liritzis, N. Laskaris, *Mediterr. Archaeol. Archaeom.* **2009**; *9*, 29.

[607] M. Richter, O. Hahn, R. Fuchs, *Stud. Conserv.* **2014**; *46*, 1.

[608] V. Šrein, B. Šreinová, J. Hradilová, in: D. Hradil, J. Hradilová (Eds.), Acta Artis Acad. 2010 Príbeh Umení Promen. Výtvarného Díla v Case Sborník 3. Mezioborové Konf. ALMA = Story Art Artwork Chang. Time Proc. 3rd Interdiscip. Conf. ALMA, Acad Mat Res Lab Painted Artworks, 2010, pp. 299–302.

[609] Š. Chlumská, D. Pechová, R. Šefcu, A. Treštíková, in: D. Hradil, J. Hradilová (Eds.), Acta Artis Acad. 2010 Príbeh Umení Promen. Výtvarného Díla v Case Sborník 3. Mezioborové Konf. ALMA = Story Art Artwork Chang. Time Proc. 3rd Interdiscip. Conf. ALMA, Acad Mat Res Lab Painted Artworks, 2010, pp. 179–188.

[610] A. Banerjee, L. Nasdala, A. Wähning, *Arbeitsblätter Für Restaur.* **2000**; *32*, 243.

[611] H. Dáňová, R. Šefců, A. Třeštíková, P. V., in:, Art'14. 11th Intern. Conf., Madrid, 2014, pp. 1–9.

[612] Z. Čermáková, P. Bezdička, I. Němec, J. Hradilová, V. Šrein, J. Blažek, D. Hradil, *J. Raman Spectrosc.* **2015**; *46*, 236.

[613] P. Holakooei, A. Karimy, *Spectrochim. Acta - Part A Mol. Biomol. Spectrosc.* **2015**; *134*, 419.

[614] G. Chiari, D. Scott, *Period. Mineral.* **2004**; *73*, 227.

CAPTION FOR FIGURES

Fig. 1 - Raman spectra of minerals identified in the ceramics body of glazed pottery finds from Skopsko Kale (Republic of Macedonia). (left) Main components: (a) hematite and magnetite; (b) maghemite; (c) quartz; (d) anatase; (e) rutile; (f) titanite; (g) albite; (h) microcline; (i) calcite; (j) carbon black; (k) graphite; (l) apatite. (right) Other minerals detected: (m) barite and sphalerite; (n) phlogopite; (o) epidote; (p) augite; (q) olivine; (r) fayalite; (s) hornblende;(t) diopside; (u) siderite; (v) dolomite; (w) spessartine (by Raškovska et al. [36]).

Fig. 2 - Raman micro-map of the orientation of the chlorite laminas in an archaeological sample of pietra ollare. A) 50x microscope image. B) Grey-scale map of the ratio between the areas of the bands at 681 cm^{-1} and 200 cm^{-1}. White = nearly horizontal laminas (laser polarization parallel to c axis). Black = nearly vertical laminas (by Baita et al. [112]).

Fig. 3 – Raman spectrum of a mounted gem on a Messinian goldsmith's artifact of XVIII c. (Messina Regional Museum, inv. A104). An indigo painted background was used to correct the hue of a diamond (reworked figure, by Barone et al. [130]).

Fig. 4 - Raman spectra, in the OH stretching region, of three gems with different origin. The band below 3600 cm^{-1} is attributed to water type II (in presence of alkali ions), and the band over 3600 cm^{-1} to water type I (reworked figure, by Bersani et al. [132]).

Fig. 5 - Maps of the shift of the six Raman bands – A_{1g} (a, b) and E_g (c–f) – around a zircon inclusion in a sapphire crystal. The maps show anisotropic patterns and vary with the Raman band. They include the regions of negative shifts, indicating contributions of nonhydrostatic stress components, induced by the zircon inclusion (by Noguchi et al. [157]).

Fig. 6 - Raman spectra of representative points of the specimens of red pigment from the Tito Bustillo and El Buxu caves (Spain): (a) wüstite (wü); (b) hematite (h); (c) hematite with a small amount of hydroxyapatite (ha) (by Hernanz et al. [199]).

Fig. 7 - Raman spectra of a bluish black pigment from prehistoric paintings in the Abrigo Remacha rock shelter (Villaseca, Segovia, Spain): (a) representative spectrum of light violet microparticles and (b) representative spectrum of black microparticles. ac, amorphous carbon; ca, calcite; pq, paracoquimbite; w, whewellite; wd, weddellite (by Iriarte et al. [208]). In Fig. 7a a strong ripple is visible, maybe caused by etaloning. Some kind of spectral pre-processing could be useful in this case, but it's not always possible to obtain clean spectra without modifications of the Raman bands.

Fig.8 - Micro-SORS spectra of a blue layered sample: (a) fragment image (the white square indicates the area analysed with micro-spatially offset Raman spectroscopy); (b) optical image and scheme of the stratigraphy; (c) the defocused spectra are shown for different distances from the 'imaged' plane indicated next to each spectrum (0 = 'imaged' position); (d) Raman intensity ratio (Prussian blue/lazurite) of the spectra acquired at different defocusing distances Δz (by Conti et al. [337]).

Fig. 9 - Representative Raman signatures recorded on blue beads excavated at Mapungubwe hill (South Africa) (by Tournié et al. [465]).

Fig. 10 - Raman spectrum of the faint blue layer on a Chinese funerary lacquer ware of West Han Dynasty, showing the band of CuS (by Jin et al. [82]).

Fig. 11 - Raman spectrum of a copper arsenate from a green area in a mural painting of Ala di Stura (Piedmont, Italy) (by Aceto et al. [395]).

Fig. 12 – The unpolarized Raman spectra of different lead chromates: crocoite, phoenicochroite, hemihedrite (by Bellini et al. [541]).

Fig. 13 - Raman spectrum of bismuth black (powdered bismuth metal) from *The Annunciation to the Shepherds*, Katherine Hours, obtained by 1064 nm excitation. Inset: photomicrograph of a bismuth particle (by Trentelman and Turner [553]).

Fig. 14 - The Raman spectrum of moolooite $Cu(C_2O_4)nH_2O$ (n<1) present in 17th c. coloured maps (by Mendes et al. [585]).

Fig. 15 - Raman spectra of fragment of a crystal from naturally irradiated fluorite (photograph in the inset), indicating the increase of the bands below 500 cm^{-1} with increasing violet colour saturation (colourless—spectrum at the bottom, very deep violet—spectrum at the top): a) 532 nm laser, b) 780 nm laser. The bands above 500 cm $^{-1}$ most probably relate to the different REE content in different positions (by Čermáková et al. [612]).

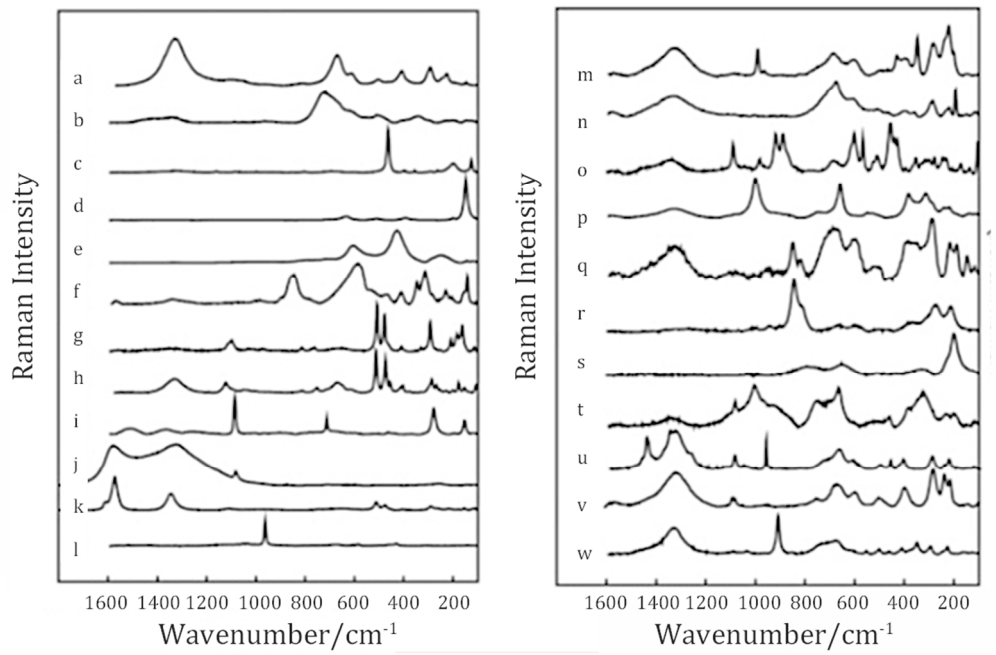

Fig. 1 - Raman spectra of minerals identified in the ceramics body of glazed pottery finds from Skopsko Kale (Republic of Macedonia). (left) Main components: (a) hematite and magnetite; (b) maghemite; (c) quartz; (d) anatase; (e) rutile; (f) titanite; (g) albite; (h) microcline; (i) calcite; (j) carbon black; (k) graphite; (l) apatite. (right) Other minerals detected: (m) barite and sphalerite; (n) phlogopite; (o) epidote; (p) augite; (q) olivine; (r) fayalite; (s) hornblende;(t) diopside; (u) siderite; (v) dolomite; (w) spessartine (by Raškovska et al. [36]).
427x280mm (72 x 72 DPI)

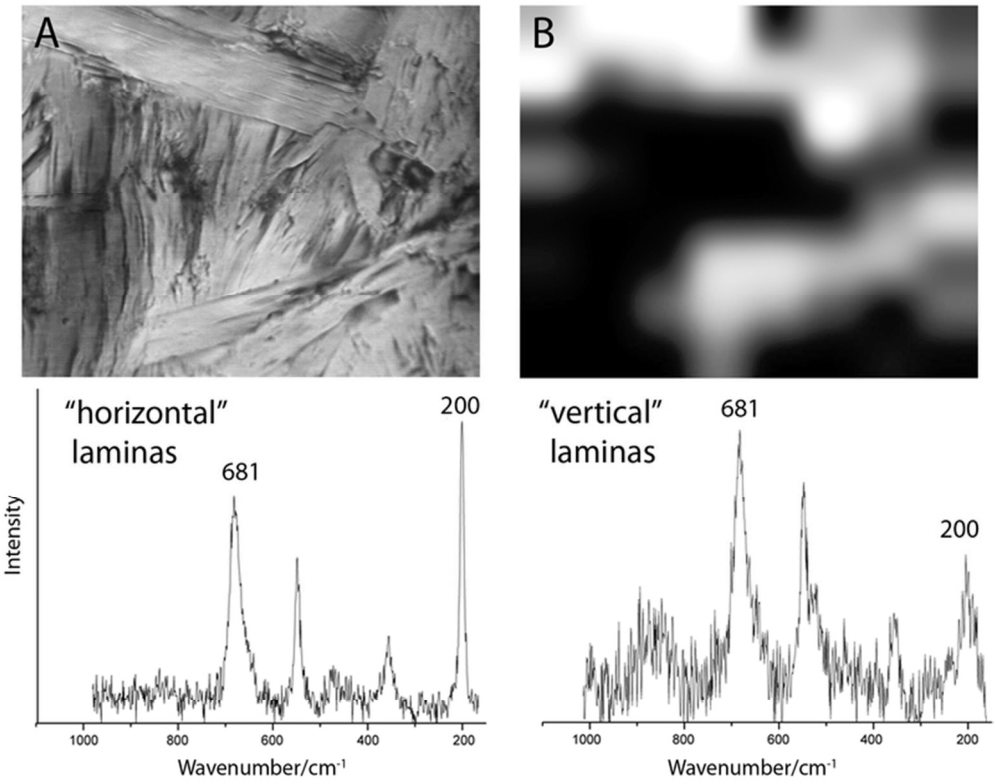

Fig. 2 - Raman micro-map of the orientation of the chlorite laminas in an archaeological sample of pietra ollare. A) 50x microscope image. B) Grey-scale map of the ratio between the areas of the bands at 681 cm^{-1} and 200 cm^{-1}. White = nearly horizontal laminas (laser polarization parallel to c axis). Black = nearly vertical laminas (by Baita et al. [112]).
68x55mm (300 x 300 DPI)

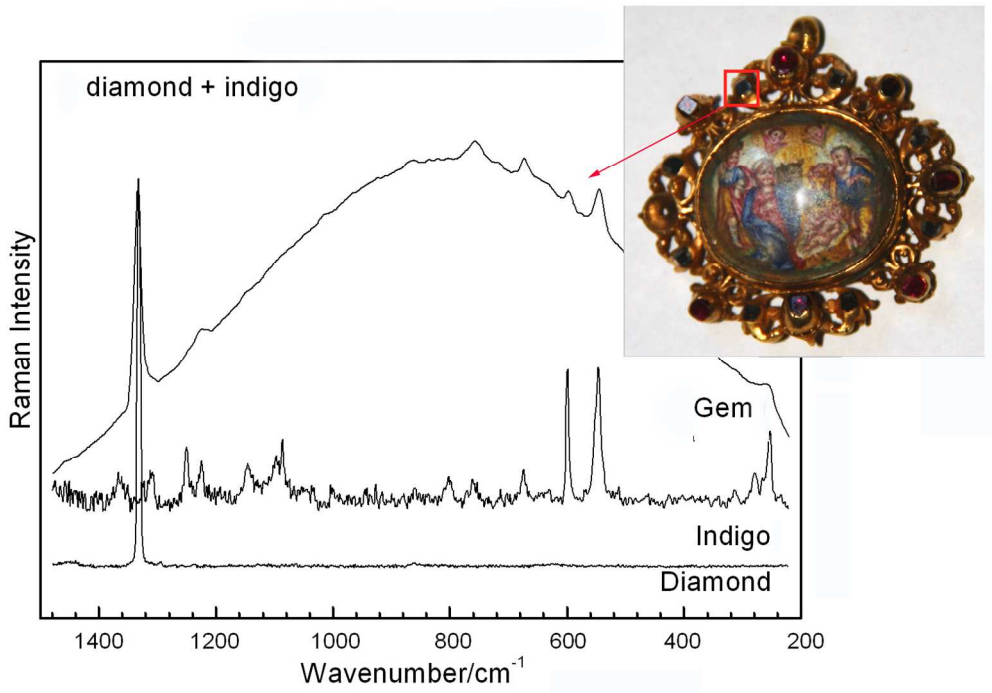

Fig. 3 – Raman spectrum of a mounted gem on a Messinian goldsmith's artifact of XVIII c. (Messina Regional Museum, inv. A104). An indigo painted background was used to correct the hue of a diamond (by Barone et al. [130]).
135x104mm (299 x 299 DPI)

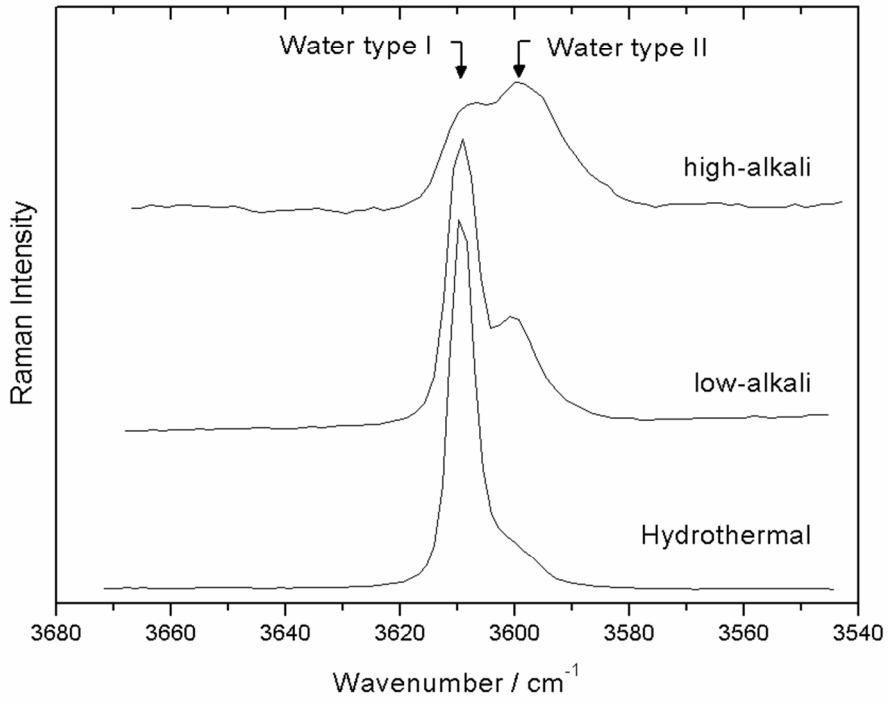

Fig. 4 - Raman spectra, in the OH stretching region, of three gems with different origin. The band below 3600 cm^{-1} is attributed to water type II (in presence of alkali ions), and the band over 3600 cm^{-1} to water type I (by Bersani et al. [132]).
79x64mm (300 x 300 DPI)

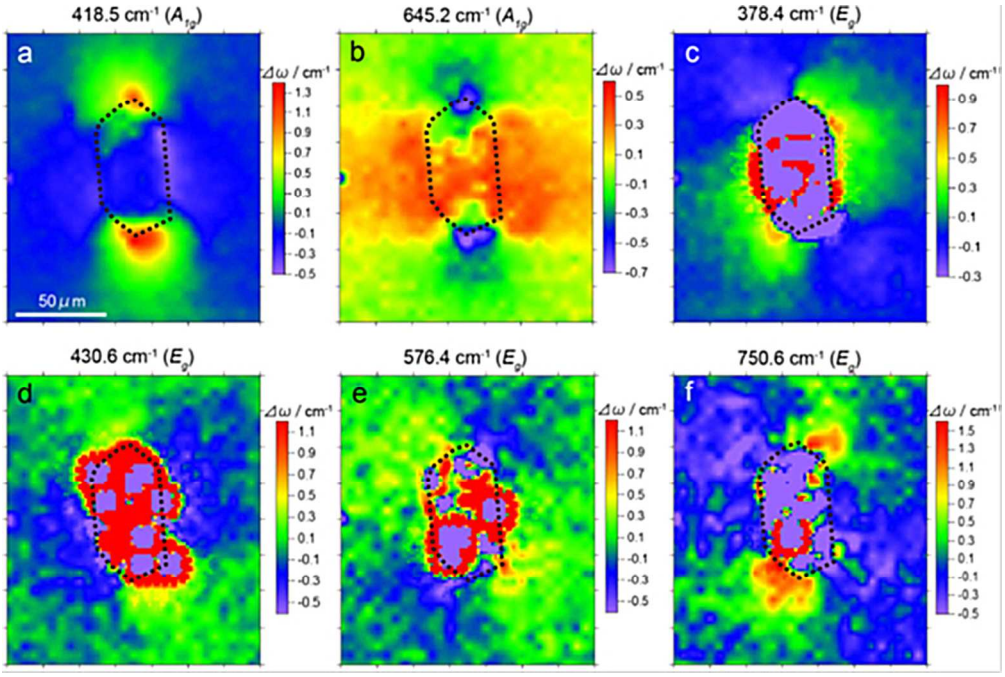

Fig. 5 - Maps of the shift of the six Raman bands – A_{1g} (a, b) and E_g (c–f) – around a zircon inclusion in a sapphire crystal. The maps show anisotropic patterns and vary with the Raman band. They include the regions of negative shifts, indicating contributions of nonhydrostatic stress components, induced by the zircon inclusion (by Noguchi et al. [157]).
453x302mm (72 x 72 DPI)

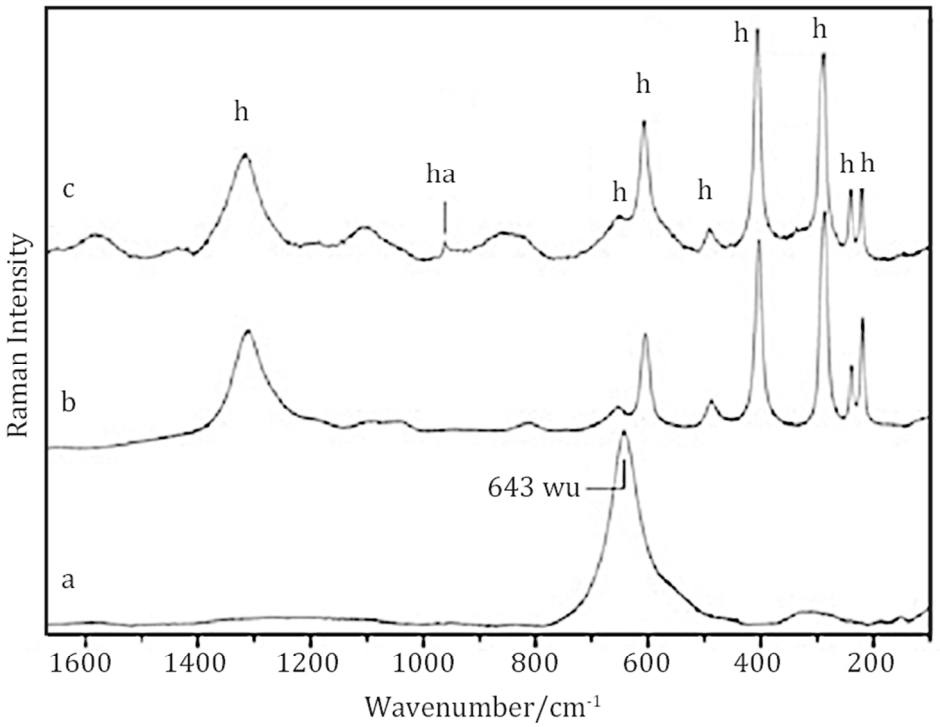

Fig. 6 - Raman spectra of representative points of the specimens of red pigment from the Tito Bustillo and El Buxu caves (Spain): (a) wüstite (wü); (b) hematite (h); (c) hematite with a small amount of hydroxyapatite (ha) (by Hernanz et al. [199]).
360x280mm (72 x 72 DPI)

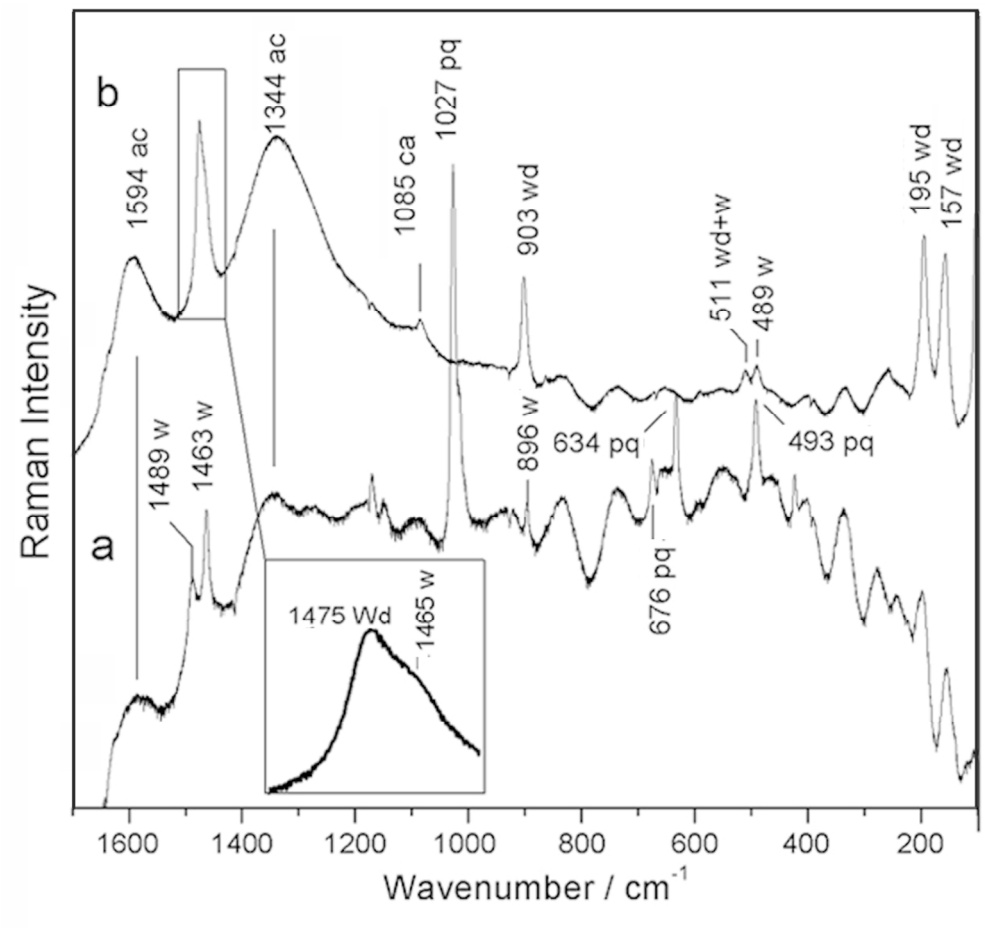

Fig. 7 - Raman spectra of a bluish black pigment from prehistoric paintings in the Abrigo Remacha rock shelter (Villaseca, Segovia, Spain): (a) representative spectrum of light violet microparticles and (b) representative spectrum of black microparticles. ac, amorphous carbon; ca, calcite; pq, paracoquimbite; w, whewellite; wd, weddellite (by Iriarte et al. [208]). In Fig. 7a a strong ripple is visible, maybe caused by etaloning. Some kind of spectral pre-processing could be useful in this case, but it's not always possible to obtain clean spectra without modifications of the Raman bands.
440x407mm (72 x 72 DPI)

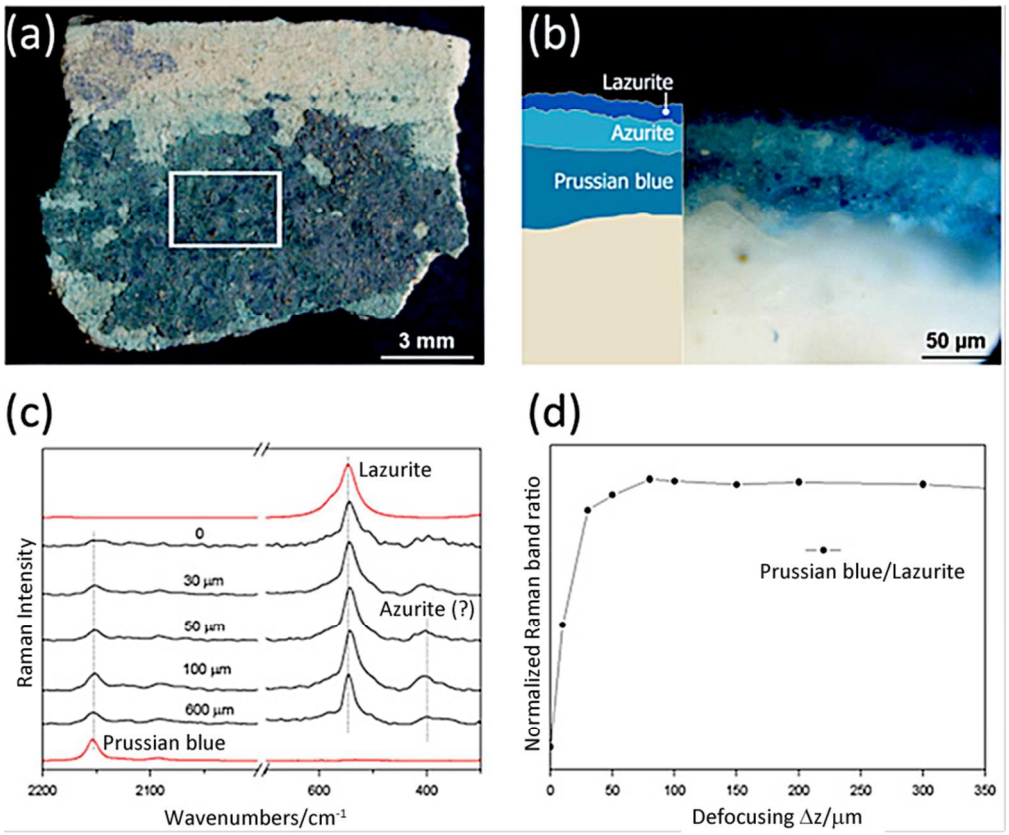

Fig.8 - Micro-SORS spectra of a blue layered sample: (a) fragment image (the white square indicates the area analysed with micro-spatially offset Raman spectroscopy); (b) optical image and scheme of the stratigraphy; (c) the defocused spectra are shown for different distances from the 'imaged' plane indicated next to each spectrum (0 = 'imaged' position); (d) Raman intensity ratio (Prussian blue/lazurite) of the spectra acquired at different defocusing distances Δz (by Conti et al. [337]).
341x282mm (72 x 72 DPI)

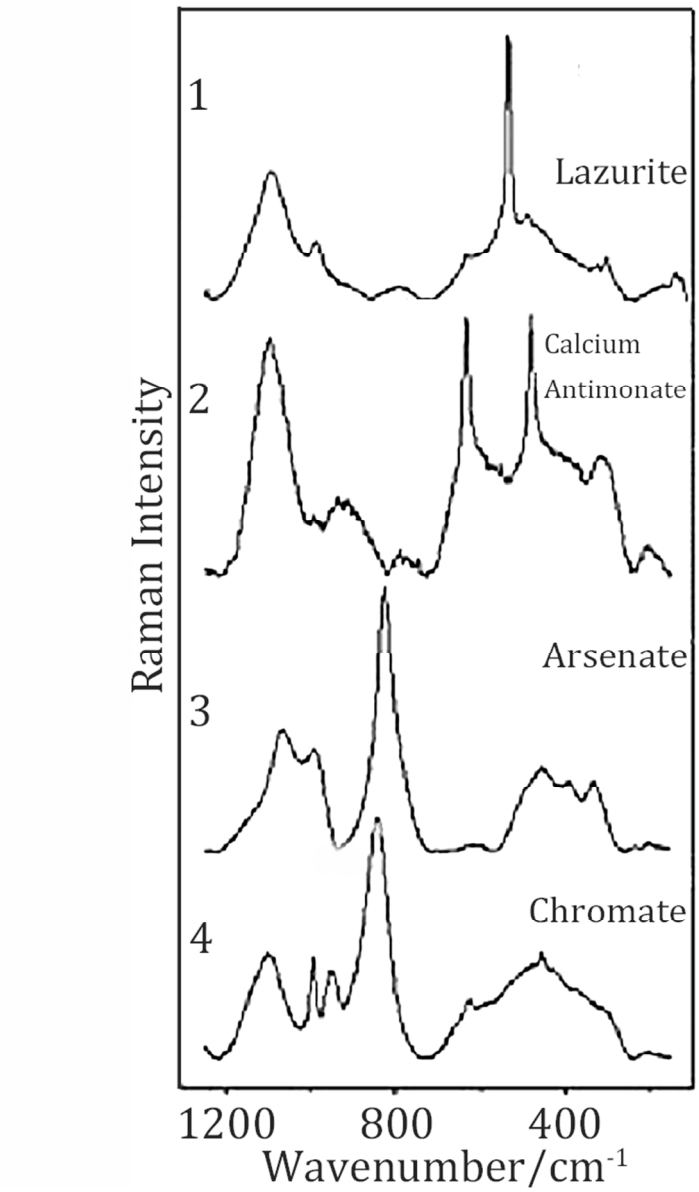

Fig. 9 - Representative Raman signatures recorded on blue beads excavated at Mapungubwe hill (South Africa) (by Tournié et al. [465]).
280x446mm (72 x 72 DPI)

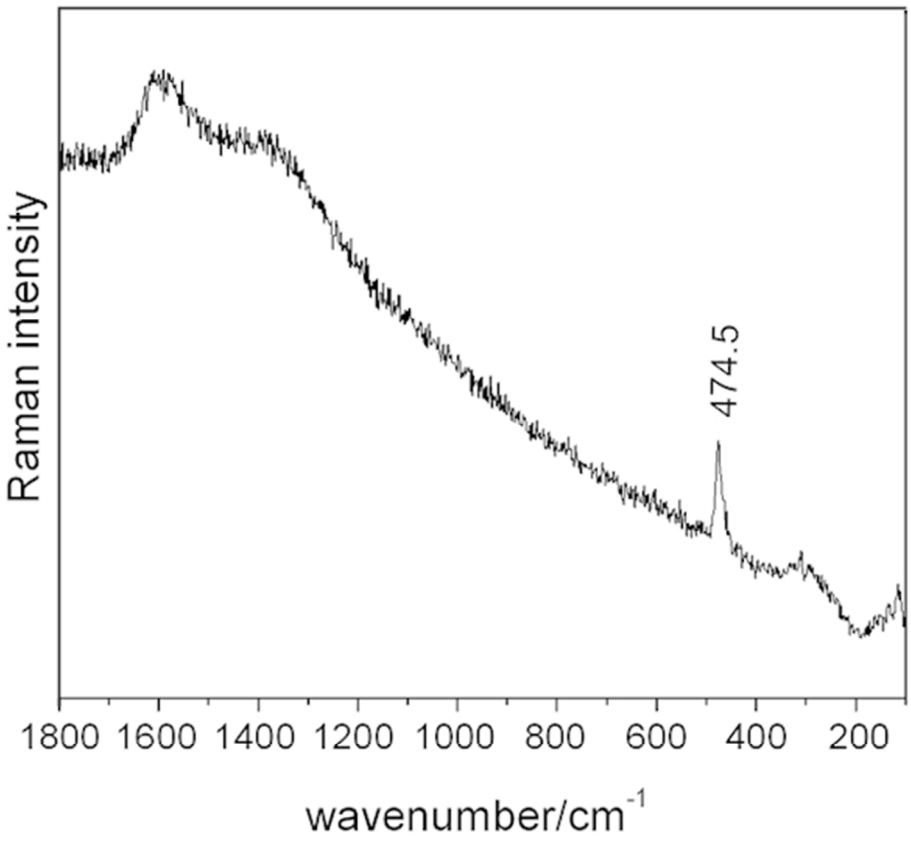

Fig. 10 - Raman spectrum of the faint blue layer on a Chinese funerary lacquer ware of West Han Dynasty, showing the band of CuS (by Jin et al. [82]).
226x192mm (72 x 72 DPI)

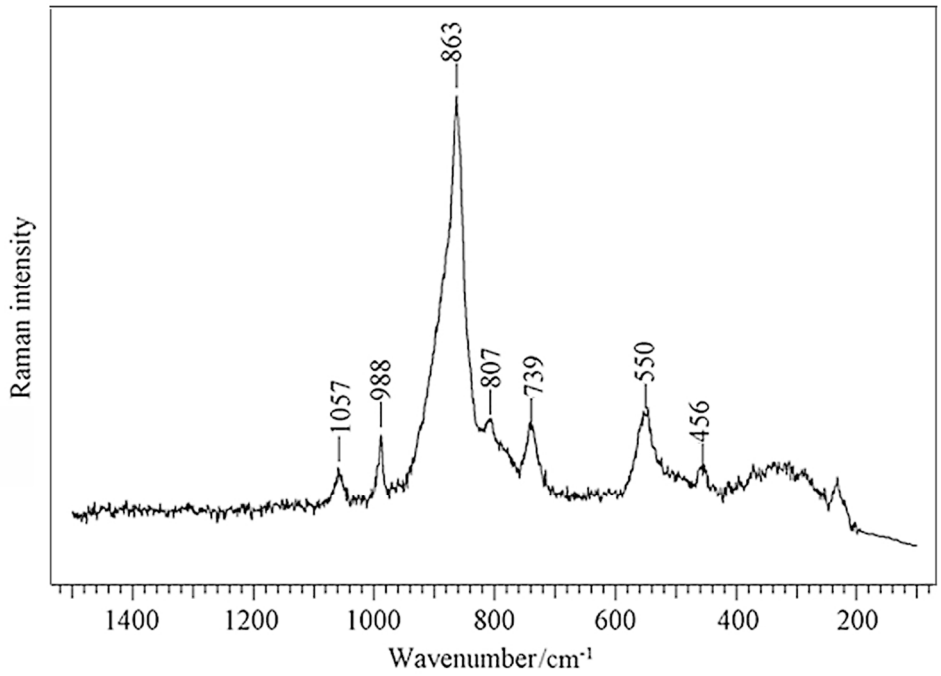

Fig. 11 - Raman spectrum of a copper arsenate from a green area in a mural painting of Ala di Stura (Piedmont, Italy) (by Aceto et al. [395]).
412x301mm (72 x 72 DPI)

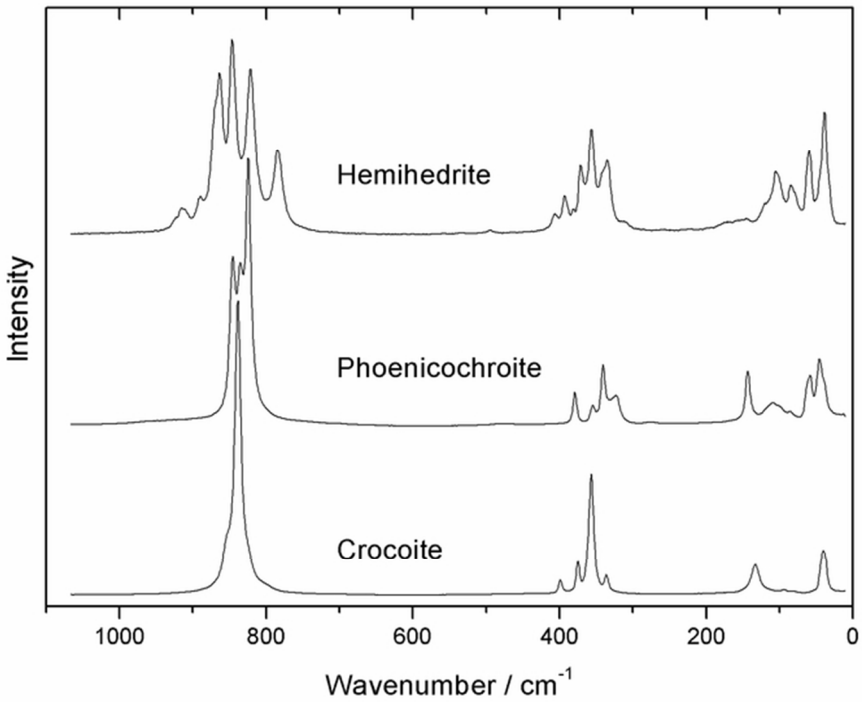

Fig. 12 – The unpolarized Raman spectra of different lead chromates: crocoite, phoenicochroite, hemihedrite (by Bellini et al. [541]).
65x53mm (300 x 300 DPI)

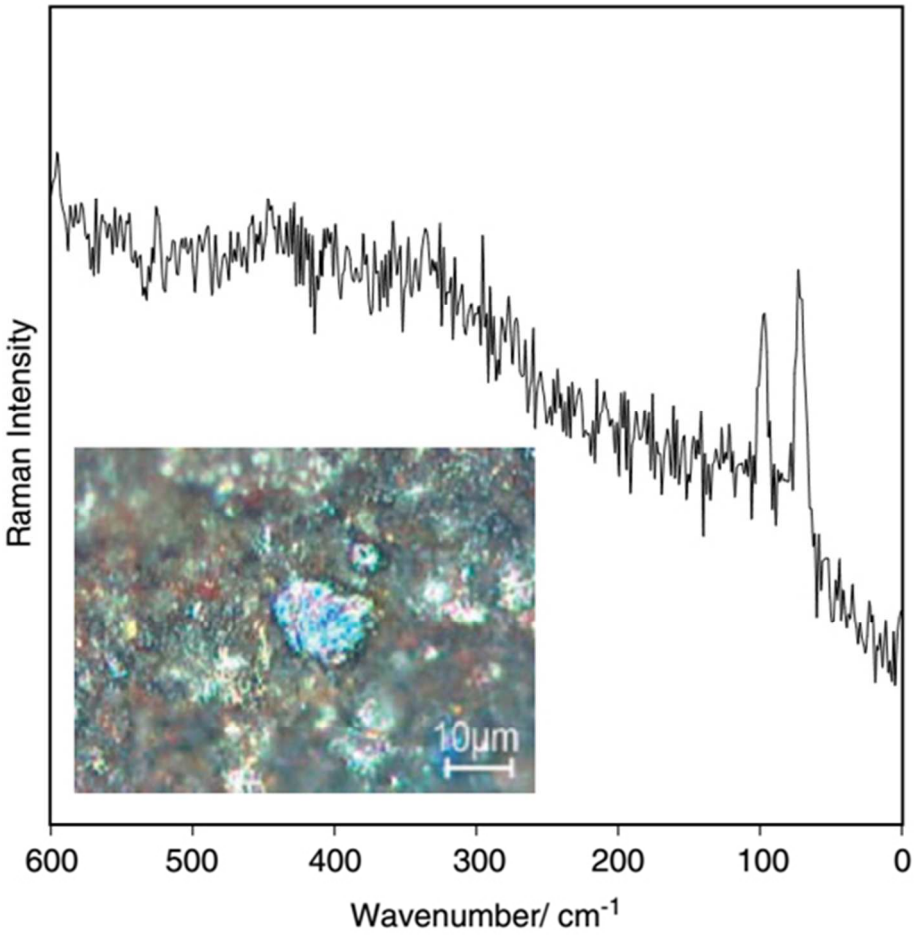

Fig. 13 - Raman spectrum of bismuth black (powdered bismuth metal) from The Annunciation to the Shepherds, Katherine Hours, obtained by 1064 nm excitation. Inset: photomicrograph of a bismuth particle (by Trentelman and Turner [553]).
226x215mm (72 x 72 DPI)

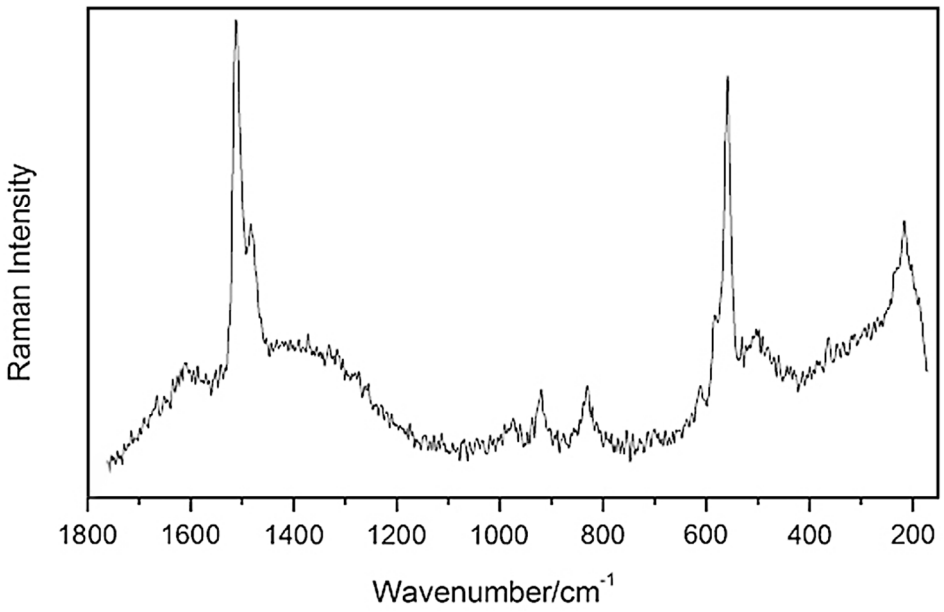

Fig. 14 - The Raman spectrum of moolooite $Cu(C_2O_4)nH_2O$ (n<1) present in 17th c. coloured maps (by Mendes et al. [585]).
407x251mm (72 x 72 DPI)

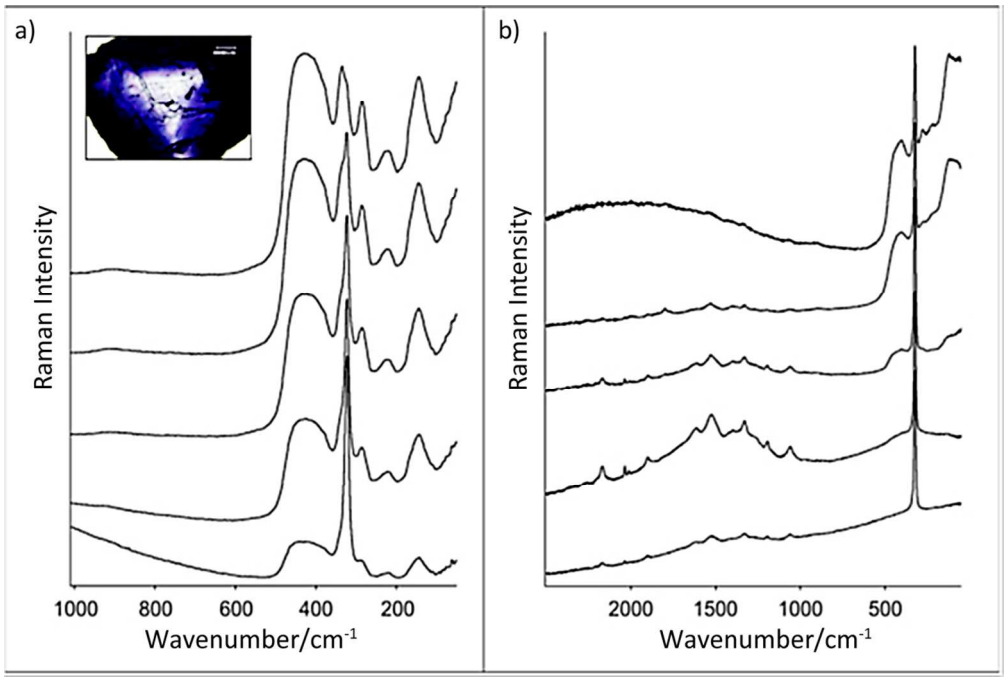

Fig. 15 - Raman spectra of fragment of a crystal from naturally irradiated fluorite (photograph in the inset), indicating the increase of the bands below 500 cm^{-1} with increasing violet colour saturation (colourless—spectrum at the bottom, very deep violet—spectrum at the top): a) 532 nm laser, b) 780 nm laser. The bands above 500 cm^{-1} most probably relate to the different REE content in different positions (by Čermáková et al. [612]).
453x304mm (72 x 72 DPI)

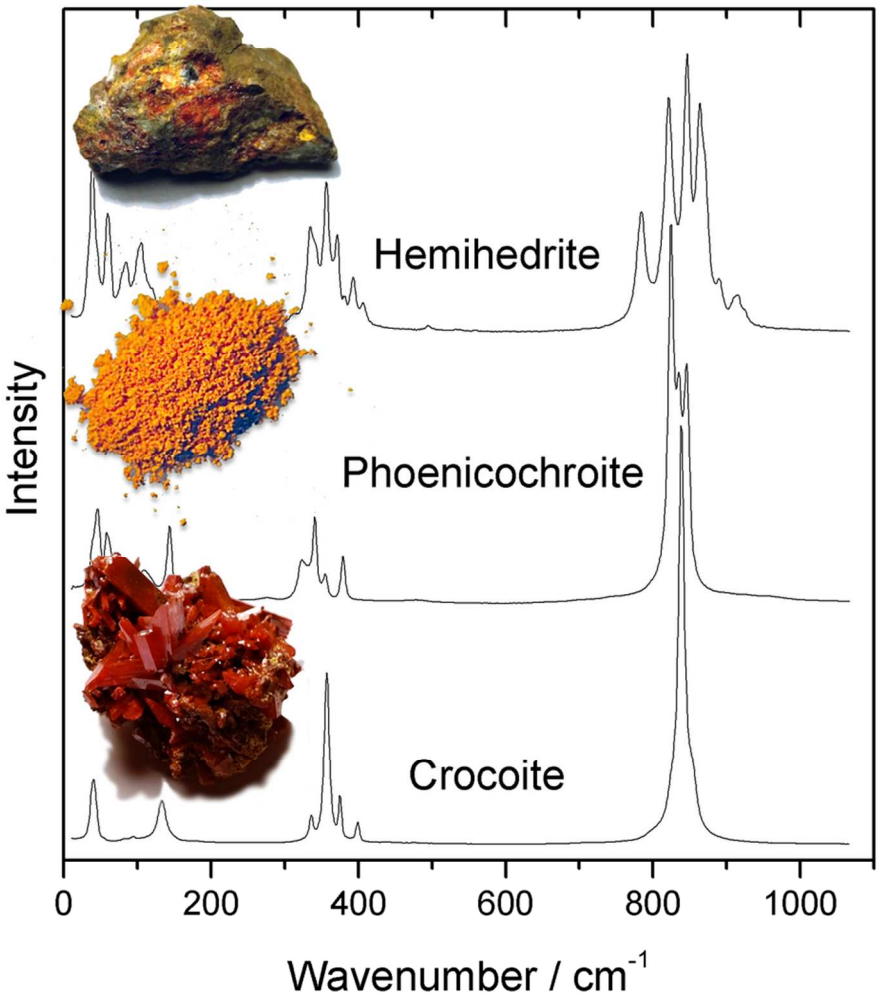

89x99mm (300 x 300 DPI)